

TRACK STITCHING AND UN-SWITCHING ALGORITHMS FOR MULTIPLE TARGET TRACKING

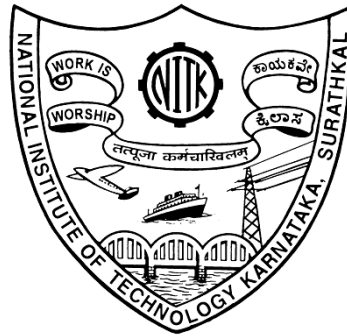
Thesis

Submitted in partial fulfillment of the requirements for the degree of

DOCTOR OF PHILOSOPHY

by

RAGHU J



DEPARTMENT OF ELECTRONICS AND COMMUNICATION ENGINEERING

NATIONAL INSTITUTE OF TECHNOLOGY KARNATAKA

SURATHKAL, MANGALURU - 575025

SEPTEMBER, 2018

To my family: Avva, Appa, Anna, Akka and Mama

DECLARATION

by the Ph.D. Research Scholar

I hereby declare that the Research Thesis entitled **TRACK STITCHING AND UN-SWITCHING ALGORITHMS FOR MULTIPLE TARGET TRACKING** which is being submitted to the **National Institute of Technology Karnataka, Surathkal**, in partial fulfilment of the requirements for the award of the Degree of **Doctor of Philosophy in Electronics and Communication Engineering** is a *bonafide report of the research work carried-out by me*. The material contained in this Research Thesis has not been submitted to any University or Institution for the award of any degree.

Raghu J

Reg. Number: 145069EC14F08

Department of Electronics and
Communication Engineering

NITK Surathkal

Place: NITK, Surathkal.

Date: September 21, 2018

CERTIFICATE

This is to *certify* that the Research Thesis entitled **TRACK STITCHING AND UN-SWITCHING ALGORITHMS FOR MULTIPLE TARGET TRACKING**, (Reg. Number: 145069EC14F08) as the record of the research work carried-out by him, is *accepted as the Research Thesis submission* in partial fulfilment of the requirements for the award of Degree of **Doctor of Philosophy**.

Dr. Pathipati Srihari
Research Guide, Asst. Professor
Dept. of E & C Engg.,
NITK Surathkal

Dr. T. Laxminidhi
Chairman - DRPC, Head & Professor
Dept. of E & C Engg.,
NITK Surathkal
(Signature with Date and Seal)

Acknowledgment

My Ph.D study had involved many people in its journey. Foremost I would like to express my sincere gratitude to my research guide **Dr. Pathipati Srihari**, Assistant Professor, Department of Electronics and Communication Engineering (ECE), NITK, Surathkal, who gave me an opportunity to pursue Ph.D. I greatly acknowledge his invaluable guidance, support and encouragement received throughout my research work. I deeply realize that for me, he is not only research guide who always reminds me to keep on right track, but also a person from whom I learnt a lot about working.

I express heartfelt thanks to my Research Progress Assessment Committee (RPAC) members **Dr. U. Shripathi Acharya**, Professor & Former Head, Department of ECE, and **Dr. Jaidhar C. D.**, Assistant Professor, Department of Information Technology, for their valuable suggestions and constant encouragement to improve my research work.

I convey my special thanks to Doctoral Thesis Assessment Committee (DTAC) Members

1. **Dr. T. Srinivas**, Indian Examiner, Associate Professor, Department of Electronics and Communication Engineering, Indian Institute of Science, Bengaluru-560012.
2. **Dr. Raviraj Adve**, Foreign Examiner, Professor, Department of Electrical and Computer Engineering, University of Toronto, Canada.
3. **Dr. T. Laxminidhi**, Chairman-DRPC, Professor & Head, Department of Electronics and Communication Engineering, NITK Surathkal.
4. **Dr. Subhaschandra Kattimani**, Associate Professor, Department of Mechanical Engineering, NITK Surathkal.

5. **Dr. Muralidhar Kulkarni**, Professor and Former Head, Department of Electronics and Communication Engineering, NITK Surathkal.
6. **Dr. Pathipati Srihari**, Thesis Supervisor & Assistant Professor, Department of Electronics and Communication Engineering, NITK, Surathkal.

who have spent valuable time out of their extremely busy schedule to review my thesis and to give comments and suggestions that helped me in improving the quality of the thesis further. I also thank them for appreciating and commending the thesis work.

I would like to express my sincere gratitude to **Dr. T. Kirubarajan**, Distinguished Engineering Professor, Electrical and Computer Engineering (ECE) Department, McMaster University, Canada, who gave me an opportunity to work as a visiting Ph.D research scholar under his guidance and to be part of his research team at the Estimation, Tracking and Fusion Research Laboratory (ETFLab), McMaster University, Canada, in 2016. I greatly acknowledge all his invaluable suggestions, comments and guidance I received, without which I would not have been what I am today. I also want to thank **Dr. R. Tharmarasa**, Research associate, ECE Department, McMaster University, Canada, who wholeheartedly, enthusiastically and immediately accepted for research discussion every time I demand and gave valuable suggestions that put me on the right track.

My appreciation goes to all my research group members **Dr. Gnane Swarnadh Satapathi**, **Mr. B. Pardhasaradhi**, **Mr. Gunnary Srinath** and **Mr. Purushottama T. L.**, Assistant Professor, SIT Tumakur, for their stimulated discussion throughout my stay at NITK.

I sincerely thank **Dr. M. S. Bhat**, Professor and former head, Department of ECE, for accepting and approving my request to do an internship at McMaster University, Canada. I extend my sincere thanks to all teaching staffs of the Department of ECE for their encouragement during my research work.

I appreciate Mrs. Sowmya, Mrs. Vagdevi Prabha, Mr. Rathish, Mr. Guruthilak Shriyan, Mr. Sheik Mohammed, Mrs. Amitha P. Amin, Mrs. Asha and her son Mr. Malathesh, Mr. Narayana Naik, Mrs. Pushpalatha, Mr. Sanjeeva Poojary, Mr. Subrahmanya Karanth, Mr. Vasudeva Shettigar B. and other non-teaching staffs of the Department of ECE for their help during my research work.

I also would like to thank **Dr. Amba Shetty**, Treasurer, Alumni Association, **Dr. B. K. Krishnamurthy**, President, Alumni Association, **Dr. Sumam David S.**, former Dean (Academic), **Dr. Katta Venkataramana**, former Dean (Academic), **Dr. M. B. Saidutta**, Dean (Academic), **Dr. Swapan Battacharya**, former Director, **Dr. K Umamaheshwar Rao**, Director, NITK, and other administrative staffs of NITK.

Thanks to all my friends Mr. Girish G. N., Mr. Bheemappa H. Halvar, Dr. Nagaraj Yamanakkanavar, Mr. Chandra Shaker Balure, Mr. Chetan L. Srinidhi, Mr. Ragesh Rajan M., Mr. Karthik R., Dr. Gowtham Simha G. D., Mr. Barathan Rajaguru, Dr. Haragovind Soni, and all other friends from following departments: ECE, CSE, EEE, Civil, MACS, IT, AMD, Mechanical, Physics and all other deratments, who helped me in relishing homely environment during my stay at NITK. I also appreciate Smt. Poojitha M. for her friendship, encouragement and moral support.

I sincerely thank **Dr. T. V. Rama Murthy**, Retired Scientist, NAL, Bengaluru, **Dr. Ragavendra V Kulkarni**, Professor and Head, Department of CSE, M. S. Ramaiah University of Applied Sceinces, Bengaluru, and **Prof. N. C. Patil**, Associate Professor and Head, Department of ECE, Auden Technology and Management Academy (ATMA), Bengaluru, for their motivation and encouragement.

I extend my sincere thanks to **Dr. Bharathi S. H.**, Deputy Director, Reva University, **Dr. Prasad S. N.**, Assistant Director, Reva University, **Dr. Sunilku-mar S. Manvi**, Principal/Director, Reva University, all the faculty members of ECE department, Reva University, **Dr. Aravinda H. S.**, Professor and Head, Department of ECE, JSS Academy of Technical Education, Bengaluru, **Prof. Puttamade Gowda**, Asst. Professor, Department of ECE, ATMA, Bengaluru, all other faculty members of department of ECE, ATMA, Bengaluru, for their support.

When I think of my gurus (teachers) of schooldays, more than hundreds of names strike my mind. All teachers of Bharathi PU college, K. M. Doddi, Government High School, Kyathagatta, Higher Primary School, Kallimeledoddi, Lower Primary School, Arethippuru (Aarathipura), Lower Primary School, Thorechakanahally, you all filled enough confidence in me and motivated me. These things dragged me all the way and hence I express my heartfelt thanks to each one of you.

I appreciate and acknowledge all the continuous helps, support and cooperation

I received during my studies from my mama **Sri. Shivalingegowda C. B.**, T. C. Halli, doddamma **Smt. Channamma**, cousins **Sri. Muthuraju P.**, **Smt. Renuka Y. P.**, and **Sri. Srinivas R.**, Bengaluru, and grand parents **Smt. Kempamma** and Late. **Sri. Boregowda (Kapikullegowda)**, Thorchakanahalli, Maddur, Mandya.

Finally I express heartfelt thanks to my family members and my villagers. Special thanks to my proud parents **Smt. Jayamma** and **Sri. Jayaramu**, who poured and will be pouring shower of love and affection in addition to proudly sacrificing their entire life to allow me chase my dreams. Your perseverance, desire and blessings have driven me to reach this level with ease. I thank my dear brother **Sri. Shivashankara** for encouraging, providing solid support and standing behind me like a pillar to do everything possible that allows me pursue what I love. I appreciate and thank my sweet sister **Smt. Ranjini J.**, for being beside me always to share my ups and downs and giving advises that make me a good human being. Special thanks to my mama **Sri. Siddegowda C. B.**, who is my backbone and a person behind my all success. I am grateful and proud to have person like him who gave exhaustive support and never ending encouragement throughout my life journey so far. I deeply feel that without family members, surely, this research work would not have been possible. I also thank all my villagers of Arethippuru (Aarathipura), Maddur, Mandya, who directly or indirectly are the reason behind my decision for taking different path rather than agriculture.

Place: Surathkal

Date: September 21, 2018

Raghu J (Mandya)

NITK Surathkal

Abstract

Track breakages are common in target tracking due to highly maneuvering targets, association with false alarms or incorrect target-originated measurements, low detection probability, close target formations, large measurement errors, and long sampling intervals, among other causes. Existing track segment association (TSA) algorithms solve this breakage problem by predicting old track segments and retrodicting young track segments to a common time followed by two-dimensional (2-D) assignment. This approach presents two disadvantages. First, these algorithms predict or retrodict from the actual point of termination or beginning of their respective tracks: that is, they do not check if the cause of a track termination was incorrect association nor do they redress such an erroneous association. Second, these algorithms do not utilize the measurement information during the breakage period. But very often, track terminations occur due to incorrect measurement association.

To solve the first aforementioned problem, a 2-D assignment-based TSA algorithm is proposed which releases incorrectly associated measurements by going backward and forward in time along old and young track segments, respectively, and then performing prediction and retrodiction. Further, to address both these shortcomings in existing TSA algorithms simultaneously, a novel multi-frame assignment-based TSA algorithm is proposed which estimates the track during the breakage period, utilizing both unassociated and released measurements simultaneously.

In addition to the track breakages, other frequently encountering issue in multiple-target tracking is track switching/swapping. Track stitching or TSA algorithms have been proposed to stitch broken track segments deemed to have originated from the same target across time and to improve track continuity. On the other hand, measurements from closely-spaced multiple targets fall within their validation gates causing tracking errors that eventually lead to not just track breakage but also track swapping. Therefore, TSA alone is insufficient to improve the overall tracker performance as it considers only the broken tracks but not the continuous ones that might have swaps among themselves or with other broken tracks.

To address track swapping issue, an algorithm, which detects and breaks possible track swaps before un-swapping using kinematic, classification, and amplitude information, is proposed. Track swap detection involves identifying the most likely instant of track swap without ground truth. Further, the proposed algorithm is extended to stitch broken track segments (as in the standard TSA case) as well as those track segments that are algorithmically broken due to detection of possible swaps.

Moreover, all the proposed algorithms can handle target maneuvers subject to a single turn during the breakage period. In the proposed solution, model parameters such as starting time of the turn, ending time of the turn, and turn rate are obtained by maximizing the likelihood that a given measurement-tuple originated from the track couple under consideration. Simulation results demonstrate that the proposed algorithms are superior to existing ones in terms of improved track continuity and consistency in track identity maintenance.

Keywords: Track segment association, Data association, Multi-frame assignment, Target tracking, Track swaps, Track switches, Track un-switching, Track un-swapping

Contents

Acknowledgment	i
Abstract	iii
List of Figures	ix
List of Tables	xi
Nomenclature	xiii
1 INTRODUCTION	1
1.1 BACKGROUND	1
1.1.1 Estimation and Tracking	1
1.1.2 Some Terminology	1
1.2 MOTION MODELS AND TRACKING SCHEME	2
1.2.1 State and Measurement Models	2
1.2.2 Traditional Target Detection and Tracking	4
1.3 CONTRIBUTION OF THE THESIS	5
1.4 OVERVIEW	5
2 LITERATURE REVIEW	7
2.1 OUTLINE	7
2.2 EXISTING WORK	7
2.3 MOTIVATION	13
2.4 LIST OF PUBLICATIONS	14
3 TRACK STITCHING	15
3.1 OUTLINE	15

3.2	TRACK SEGMENT ASSOCIATION	15
3.2.1	Track Grouping	15
3.2.2	Possible Starting and Ending Times	17
3.2.3	Track Smoothing	20
3.2.4	2-D Assignment for Track Segment Association	21
3.2.5	Multi-frame Assignment for Track Segment association	23
3.3	MODEL PARAMETER ESTIMATION	29
3.3.1	<i>S</i> -D Assignment Case	30
3.3.2	2-D Assignment Case	31
3.4	RESULTS AND DISCUSSIONS	33
3.4.1	Target Simulation	33
3.4.2	TSA Parameters	33
3.4.3	Single Target Scenario	34
3.4.4	Multiple Target Scenario	44
3.5	SUMMARY	50
4	TRACK UN-SWITCHING	51
4.1	OUTLINE	51
4.2	TRACK UN-SWITCHING	51
4.2.1	Track Grouping	51
4.2.2	Track List Updating	52
4.2.3	Track Swap Detection and Track Breaking	54
4.3	ASSOCIATION COST USING KINEMATIC INFORMATION	55
4.3.1	The Likelihood Ratios Using Kinematic Information	55
4.4	ASSOCIATION COST USING CLASSIFICATION INFORMATION	58
4.4.1	Classification Information Modeling	58
4.4.2	The Likelihood Ratios Using Classification Information	59
4.5	ASSOCIATION COST USING AMPLITUDE INFORMATION	61
4.5.1	Amplitude Information Modeling	61
4.5.2	The Likelihood Ratios Using Amplitude Information	62
4.6	RESULTS AND DISCUSSIONS	65
4.6.1	Tracking Filter and Design Parameters	65

4.6.2	Performance Measure	66
4.6.3	Procedure For Automatic Track Swap detection	66
4.6.4	Two Target Case	67
4.6.5	Multiple Target Case	75
4.7	SUMMARY	80
5	CONCLUSIONS AND FUTURE WORK	81
5.1	CONCLUSIONS	81
5.2	FUTURE WORK	82
	Bibliography	83
	List of Publications	88
	About The Author	91

List of Figures

1.1	Traditional detection and tracking scheme	5
2.1	Track swapping after breakage	11
2.2	Track swapping without breakage	12
3.1	Stitching broken tracks	17
3.2	An algorithm for proposed 2-D assignment based TSA	23
3.3	A typical example for S -D assignment	24
3.4	An algorithm for proposed S -D assignment based TSA	28
3.5	Target trajectory	34
3.6	Track stitching	35
3.7	Single target RMSE ($P_D^b = 0.3$, $B_i = 3$, $\lambda = 0\text{m}^{-2}$, $\omega = 4^\circ/\text{s}$)	37
3.8	Single target RMSE ($P_D^b = 0.3$, $B_i = 0$, $\lambda = 1 \times 10^{-6}\text{m}^{-2}$, $\omega = 10^\circ/\text{s}$)	41
3.9	Single target RMSE ($P_D^b = 0.3$, $B_i = 5$, $\lambda = 1 \times 10^{-6}\text{m}^{-2}$, $\omega = 10^\circ/\text{s}$)	42
3.10	Track breakage due to target turn	43
3.11	Track stitching	44
3.12	Track breakage due to false alarms	45
3.13	Results of TSA for multi-target scenario ($\lambda = 1 \times 10^{-4}\text{m}^{-2}$)	46
3.14	Results of TSA for multi-target scenario ($\lambda = 1 \times 10^{-5}\text{m}^{-2}$)	49
4.1	An algorithm for track unswapping	63
4.2	An algorithm to determine the track swap	67
4.3	Automatic track swap detection for two target case	67
4.4	Track un-swapping: Two target case (Scenario 1)	71
4.5	Track un-swapping: Two target case (Scenario 2)	72
4.6	Position RMSE (Scenario 1)	73

4.7	Velocity RMSE (Scenario 1)	73
4.8	Two target case (Scenario 3): track swapping after breakage	74
4.9	Track swapping: Multi-target case	75

List of Tables

3.1	Percentage of Correct Association Decisions ($\omega = 4^\circ/\text{s}$, $\lambda = 0\text{m}^{-2}$) . . .	35
3.2	Number of Continuous Tracks ($\omega = 4^\circ/\text{s}$, $\lambda = 0\text{m}^{-2}$)	36
3.3	Percentage of Correct Association Decisions ($\omega = 10^\circ/\text{s}$, $\lambda = 10^{-6}\text{m}^{-2}$)	39
3.4	Number of Continuous Tracks ($\omega = 10^\circ/\text{s}$, $\lambda = 1 \times 10^{-6}\text{m}^{-2}$)	39
3.5	Percentage of Correct Association Decisions ($\omega = 10^\circ/\text{s}$, $\lambda = 10^{-4}\text{m}^{-2}$)	40
3.6	Number of Continuous Tracks ($\omega = 10^\circ/\text{s}$, $\lambda = 1 \times 10^{-4}\text{m}^{-2}$)	40
3.7	Percentage of Correct Association Decisions ($\lambda = 0\text{m}^{-2}$)	47
3.8	Percentage of Correct Association Decisions ($\lambda = 1 \times 10^{-6}\text{m}^{-2}$) . . .	47
3.9	Percentage of Correct Association Decisions ($\lambda = 1 \times 10^{-4}\text{m}^{-2}$) . . .	48
3.10	Percentage of Correct Association Decisions ($\lambda = 1 \times 10^{-5}\text{m}^{-2}$) . . .	48
4.1	Percentage of Un-swapping and Swapping Introduced	69
4.2	Track Purity Matrices ($B = 10$, $\tau = 4.2677$, $P_{\text{FA}} = 1.1093 \times 10^{-4}$) . .	70
4.3	Track Purity Matrices ($B = 10$, $\tau = 4.3324$, $P_{\text{FA}} = 8.3975 \times 10^{-5}$) . .	74

Nomenclature

Acronyms

2-D	Two-Dimensional
S -D	S -Dimensional
CT	Coordinated turn
CV	Constant velocity
ID	Identity
MSE	Mean-squared-error
NN	Nearest neighbor
RMSE	Root-mean-squared-error
SNR	Signal-to-noise-ratio
T2T	Track-to-track
TSA	Track segment association

Mathematical Notations

$\mathbf{v}(\cdot)$	A zero-mean white Gaussian process noise vector
$(\cdot)'$	Transpose of a vector or matrix
$\alpha(\cdot)$	Amplitude information
$\bar{H}\{\cdot, \cdot\}$	Hypothesis opposite to $H\{\cdot, \cdot\}$
$\beta(\cdot)$	Class information

$\Delta(\cdot)$	Difference between two states
$\Gamma(\cdot)$	Process noise gain
$\mathcal{T}^{\mathcal{O}}(\cdot)$	Old track list
$\mathcal{T}^{\mathcal{Y}}(\cdot)$	Young track list
Π	Track purity matrix
$\Sigma(\cdot)$	Covariance associated with $\Delta(\cdot)$
$\zeta(\cdot)$	Vector of probabilities of class
$C(\cdot)$	Smoother gain
$F(\cdot)$	State transition matrix
$H(\cdot)$	Jacobian matrix
$P(\cdot)$	State covariance matrix
$Q(\cdot)$	Process noise covariance matrix
$R(\cdot)$	Measurement noise covariance matrix
T	A track
$\mathbf{w}(\cdot)$	A zero-mean Gaussian measurement noise vector
$\mathbf{x}(\cdot)$	State vector
$\mathbf{z}(\cdot)$	Measurement vector
$\mathbf{z}^{\kappa\alpha}(\cdot)$	Kinematic and amplitude augmented measurement
$\mathbf{z}^{\kappa\beta}(\cdot)$	Kinematic and class augmented measurement
$\Delta(\cdot)$	Time difference between successive scans
$\delta\omega$	Turn rate step size
$\dot{\eta}(\cdot)$	Velocity along Y coordinate

$\dot{\xi}(\cdot)$	Velocity along X coordinate
\dot{c}	Normalization constant
\emptyset	Spurious source of measurements
$\eta(\cdot)$	Position along Y coordinate
$\eta^p(\cdot)$	Platform position along Y coordinate
$\gamma_{\mathbf{x}}$	Gate threshold corresponding to dimension of vector \mathbf{x}
κ	Kinematic information
λ	False alarm density
$\Lambda(\cdot)$	Likelihood function
\mathbb{C}	Confusion matrix
$\mathbf{Z}^{(\cdot)}$	The measurement set that includes both unassociated and released measurement
\mathbf{X}	Sequence of state vectors
\mathcal{A}	Track from list consisting of old, young and continuous tracks
\mathcal{C}	Continuous track
$\mathcal{L}_{..}$	The likelihood ratio
$\mathcal{M}(\cdot)$	Number of detected measurements
$\mathcal{N}[\cdot, \cdot]$	Gaussian distribution
\mathcal{O}	Old track segment
\mathcal{U}	Un-swapped track
\mathcal{Y}	Young track segment
μ	The spatial density of true and false tracks in the state space

ω	Turning rate
$\phi(\cdot)$	Azimuth
σ_ϕ	Azimuth standard deviation
σ_r	Range standard deviation
τ	Amplitude threshold
$\xi(\cdot)$	Position along X coordinate
$\xi^p(\cdot)$	Platform position along X coordinate
ζ_{ex}	False alarm class probability
$a_{m(\cdot), \dots, m(\cdot)}$	Binary association variable
B	Look-back duration or sliding window size
B_i	Number of scans going backward along an old track
B_j	Number of scans going forward along a young track
$B_{i_{\text{max}}}$	The maximum number of scans possible when going backward along an old track
$B_{j_{\text{max}}}$	The maximum number of scans possible when going forward along a young track
$C_{2\text{-D}}(\cdot)$	Total cost associated with 2-D assignment
$c_{m(\cdot), \dots, m(\cdot)}$	Cost associated with measurement tuple $\mathbf{z}_{m(\cdot), \dots, m(\cdot)}$
$C_{S\text{-D}}(\cdot)$	Total cost associated with S -D assignment
$D(\cdot)$	Squared distance between two measurement vectors
$E[\cdot]$	Expectation operator
$h[\cdot, \cdot]$	Measurement transition model
$H\{\cdot, \cdot\}$	Hypothesis

$I(\cdot)$	An indicator function
j	Possible ending time of a track
k	Scanning time index
$k_{.,e}$	Ending time of a track
$k_{.,s}$	Starting time of a track
k_{t_e}	Turning end time
k_{t_s}	Turning start time
$m(\cdot)$	Measurement detection index
n	Track index variable
N^β	Maximum number of classes
n^β	Class index variable
$N^{\mathcal{O}}(\cdot)$	Number of tracks in old track list
$N^{\mathcal{Y}}(\cdot)$	Number of tracks in young track list
N^M	Number of state transition models
N^S	Maximum number of scans or frames
$p(\cdot)$	Probability density function (pdf)
P_D	Probability of detection
P_{FA}	Probability of false alarm
P_G	Gate probability
$r(\cdot)$	Range
$t(k)$	Actual time at scanning instant k
$\mathcal{T}^c(\cdot)$	Continuous or non-broken track list

$\mathcal{T}^u(\cdot)$	Un-swapped track list
$\Phi^T(\cdot)$	The set of all combinations of candidate track pairs
$\Phi_f^T(\cdot)$	Feasible candidate track pair set
$\Psi^{ij}(\cdot)$	The set of all possible combinations of i 's N^O -tuples and j 's N^Y -tuples
i	Possible starting time of a track
P_D^b	The probability of target detection during the breakage period
V	The volume of the surveillance region

Chapter 1

INTRODUCTION

1.1 BACKGROUND

1.1.1 Estimation and Tracking

Estimation is the process of inferring the value of a quantity of interest from indirect, noisy and uncertain data or observations (Bar-Shalom et al. 2011). That is, estimation can be viewed as the process of selection of a point out of continuous space.

The quantity of interest could be state of dynamic systems which is usually a vector consisting of kinematic and feature related information. Tracking is the estimation of the state of an object in motion. To be precise, tracking is the processing of measurements or observations obtained from targets of interest so as to maintain their present state. This state typically consists of the followings:

- Kinematic components such as position, velocity, acceleration, turn rate, etc.
- Feature components such as radiated signal strength, radar cross-section, target classification, etc.
- Constant or slowly varying parameters such as aerodynamic parameters etc.

Data or measurements are noise-corrupted observations related to the state of a target. These observation could be: range, azimuth and elevation; bearing only from the sensor; range rate (Doppler); time difference of arrival of a signal between two sensors, etc.

1.1.2 Some Terminology

Definition of some of the terminologies that are often used in tracking are as follows:

- **Sensor:** a device that observes the environment by reception of some signals.
- **Frame:** snapshot of the region of the environment obtained by the sensor at a point in time.
- **Signal detection:** thresholding of sensor data to provide measurements.
- **Time stamp:** the time to which a detection pertains.
- **Data association:** processes of establishing which measurement is to be used in a state estimator.

1.2 MOTION MODELS AND TRACKING SCHEME

1.2.1 State and Measurement Models

Let the state transition model (Bar-Shalom et al. 2004) with additive white Gaussian noise that models unpredictable disturbances be defined as

$$\mathbf{x}(k) = \mathbf{F}^i(k)\mathbf{x}(k-1) + \mathbf{\Gamma}(k-1)\mathbf{v}(k-1) \quad i = 1, 2, \dots, N^M \quad (1.1)$$

with four-dimensional state vector

$$\mathbf{x}(k) \triangleq \begin{pmatrix} \xi(k) \\ \dot{\xi}(k) \\ \eta(k) \\ \dot{\eta}(k) \end{pmatrix} \quad (1.2)$$

where k ($k = 1, \dots, N^S$) is scanning instant, N^M is number of state transition models, $\xi(k)$, $\eta(k)$ are the X and Y Cartesian positions, $\dot{\xi}(k)$ and $\dot{\eta}(k)$ are the velocities along these directions and $\mathbf{v}(k)$ is a zero-mean white Gaussian process noise vector (i.e., $\mathbf{v}(k) \sim \mathcal{N}[0, \mathbf{Q}(k)]$) with a 2×2 covariance matrix

$$\mathbf{Q}(k) = E[\mathbf{v}(k)\mathbf{v}(k)']. \quad (1.3)$$

In the above equation $(\cdot)'$ indicates the transpose of a vector or matrix. Also, $\mathbf{F}^i(k)$ is the state transition matrix and could be one of the following. For the constant

velocity (CV) model ($i = 1$)

$$\mathbf{F}^1(k) = \begin{pmatrix} 1 & \Delta(k) & 0 & 0 \\ 0 & 1 & 0 & 0 \\ 0 & 0 & 1 & \Delta(k) \\ 0 & 0 & 0 & 1 \end{pmatrix} \quad (1.4)$$

with $\Delta(k)$ being the sampling interval: that is, the time difference between the present and the previous scans ($\Delta(k) = t(k) - t(k-1)$). For the coordinated turn (CT) model ($i = 2$), with ω being the turn rate,

$$\mathbf{F}^2(k) = \begin{pmatrix} 1 & \frac{\sin(\omega\Delta(k))}{\omega} & 0 & -\frac{1-\cos(\omega\Delta(k))}{\omega} \\ 0 & \cos(\omega\Delta(k)) & 0 & -\sin(\omega\Delta(k)) \\ 0 & \frac{1-\cos(\omega\Delta(k))}{\omega} & 1 & \frac{\sin(\omega\Delta(k))}{\omega} \\ 0 & \sin(\omega\Delta(k)) & 0 & \cos(\omega\Delta(k)) \end{pmatrix} \quad (1.5)$$

and $\mathbf{\Gamma}(k)$ is the noise gain, given by

$$\mathbf{\Gamma}(k) = \begin{pmatrix} \frac{\Delta^2(k)}{2} & 0 \\ \Delta(k) & 0 \\ 0 & \frac{\Delta^2(k)}{2} \\ 0 & \Delta(k) \end{pmatrix}. \quad (1.6)$$

Let the nonlinear measurement model with Gaussian measurement noise that models unpredictable measurement disturbance (Bar-Shalom et al. 2004) be defined as

$$\mathbf{z}(k) = h[k, \mathbf{x}(k)] + \mathbf{w}(k) \quad (1.7)$$

where

$$\mathbf{z}(k) \triangleq \begin{pmatrix} r(k) \\ \phi(k) \end{pmatrix} \quad (1.8)$$

is a two-dimensional measurement vector containing range and azimuth, which are given by

$$r(k) = \sqrt{[\xi(k) - \xi^p(k)]^2 + [\eta(k) - \eta^p(k)]^2}, \quad (1.9)$$

$$\phi(k) = \tan^{-1} \left(\frac{\eta(k) - \eta^p(k)}{\xi(k) - \xi^p(k)} \right), \quad (1.10)$$

respectively, $\xi^p(k)$ and $\eta^p(k)$ are the sensor platform positions along X and Y directions in Cartesian coordinates, respectively, these positions are assumed to be known, and $\mathbf{w}(k)$ is a zero-mean Gaussian measurement noise vector (i.e., $\mathbf{w}(k) \sim \mathcal{N}[0, \mathbf{R}(k)]$) with a 2×2 covariance matrix

$$\begin{aligned} \mathbf{R}(k) &= E[\mathbf{w}(k)\mathbf{w}(k)'] \\ &= \begin{pmatrix} \sigma_r^2 & 0 \\ 0 & \sigma_\phi^2 \end{pmatrix} \end{aligned} \quad (1.11)$$

where σ_r and σ_ϕ denote the range and azimuth standard deviations, respectively. More details on modeling state and measurements can be found in Bar-Shalom et al. 2004, 2011.

1.2.2 Traditional Target Detection and Tracking

The traditional target detection and tracking schemes¹ receive the raw data (observations) from the sensors and apply hard-threshold on every individual frame (scan or ping), i.e., scan-by-scan basis, to extract the plot-list and reduce the data flow to the tracker. Plot-list is also referred as target detections or point measurements. Hard-threshold is determined using a priori information (such as environmental clutter level, detection probability P_D , false alarm probability P_{FA} , etc.). However, threshold decision is made instantaneously, i.e, without using information from recent past frames or scans. Subsequently the tracker is provided with these point measurements to associate them with different frames to arrive at the targets' trajectories as shown in the Figure 1.1. This classical detection and tracking scheme is also called as detect-before-track scheme for obvious reason as it detects first and then tracks.

This traditional detection and tracking scheme can track targets when targets' signal-to-noise-ratio (SNR) and detection probability P_D are high while the false alarm probability P_{FA} is low. However, when the SNR and accuracy are too low it is preferable to use Track-Before-Detect or Track-Before-Declare (McDonald and Balaji 2011, Davey et al. 2012, Davey 2013) schemes which demand higher computational complexity. These Track-Before-Detect methods first track each echo that

¹ In the literature these are also referred to as classical (Grossi et al. 2013) or conventional (Fanaswala and Krishnamurthy 2014) detection and tracking schemes.

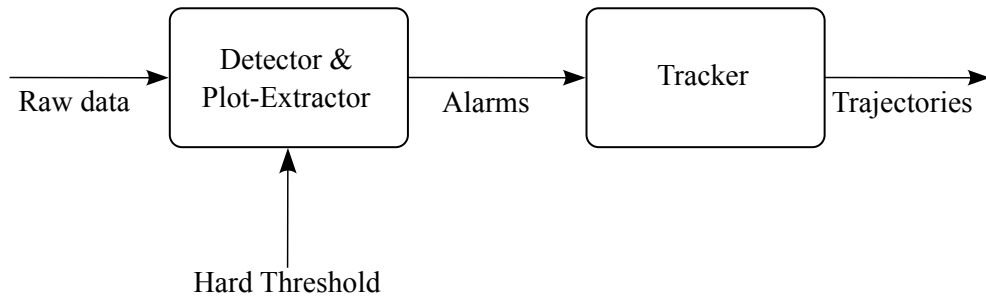


Figure 1.1: Traditional detection and tracking scheme (Grossi et al. 2013) seems to be returned from prospective target before deciding whether the target is present.

1.3 CONTRIBUTION OF THE THESIS

In this thesis, some of the important problems that are associated with track breakages and track switching are identified and to address these issues, multiple solutions are proposed. The key contributions of the thesis are as follows:

- Proposed algorithms to perform TSA even when termination time of old track segment is greater than beginning time of its associated young track segment.
- Presented an algorithm that can utilize all the available data such as unassociated measurements and released measurements to perform TSA comprehensively.
- Proposed algorithms that can integrate kinematic, classification and amplitude information to perform un-swapping and TSA simultaneously to improve the overall tracker performance and
- Developed an algorithm that can automatically determine swapped tracks even when the ground truth is unknown, which is the usual case in practical applications.

1.4 OVERVIEW

Rest of the thesis is structured in the following manner. Existing track segment association and track un-switching/un-swapping approaches along with their disadvantages are discussed in Chapter 2. In Chapter 3, the proposed two-dimensional

and multi-dimensional track segment association approaches are presented in detail to comprehensively utilize all the available data and then to stitch the broken tracks obtained from single and multiple target scenarios for improved track continuity. Different versions of proposed track un-switching/un-swapping algorithms that utilize kinematic as well as non-kinematic information are discussed in detail in Chapter 4. Following this, the concluding remarks and future directions are presented in Chapter 5.

Chapter 2

LITERATURE REVIEW

2.1 OUTLINE

Existing track stitching and track un-switching/un-swapping algorithms along with their disadvantages are presented in Section 2.2. The key points that are motivation for the proposed approaches and the publications out of the thesis work are listed in Sections 2.3 and 2.4, respectively.

2.2 EXISTING WORK

In target tracking systems, track breakage or track segmentation is a major and frequently occurring problem. Track breakage is defined as the total number of track segments less the total number of targets (Yeom et al. 2004). It can easily mislead the tracker in finding the total number of targets present and degrade the overall tracker performance. Track breakage may occur due to highly maneuvering targets, association with incorrect measurement, low detection probability, close target formations, large measurement errors, and long sampling intervals, among other causes. In practical situations, analyzing the history of any particular target (so as to make better tactical decisions) is possible only when consistent track identity (ID) is maintained right from target birth to its death. In real-time target tracking systems, the multi-frame assignment approach can be used for track-to-measurements associations to maintain consistent track ID and to obtain better target state estimates (Popp et al. 2001, Poore 1994). However, these systems face

1. huge computational issues due to the complexity involved in multi-frame assignment; and

2. larger delay in making track-to-measurements associations.

These issues are usually avoided by using either two-dimensional (2-D) or multi-frame assignment approach limited to few scans, but this leads to track breakages and necessitates post-processing — track stitching and hence maintaining consistent track ID throughout. Note that post-processing involves some recursive post-processing latency.

Usually, the track breakage problem is addressed using track segmentation reduction (Song et al. 2013) and track segment association (TSA) approaches. Track segmentation reduction is a track breakage avoidance approach, while TSA is a post-processing technique, in which track segments over time are combined or stitched together to improve track continuity. Track breakage avoidance approach is an approach in which track termination criterion (e.g., M/N logic (Castella 1976, Coraluppi 2005, Dezert and Kirubarajan 1999)) is relaxed so that target and its track association continues. In the literature, TSA is also described as fusing the track segments originating from the same target across two or more sensors (Arnold et al. 1984). A TSA algorithm reduces the number of broken tracks and increases overall tracker performance by maintaining consistent track ID. A graph-based TSA algorithm is given in (Van der Merwe and De Villiers 2013, Mori and Chong 2013, Castñón and Finn 2011), where each track segment is treated as a node and association as an edge. A TSA algorithm for passive target tracking is presented in (Zhu et al. 2015, Mellema 2002). All these algorithms fail to consider the followings: a) a case where track is associated with sequence of false measurements before its termination; b) a case where track is initialized with sequence of false measurements before confirming it, and; c) available information such as kinematic and non-kinematic information during track breakage period.

Track segment association is a 2-D assignment problem performed between two track lists. The first list is a set of all old or terminated track segments and the second list is a set of all new or young track segments that are initialized and have been recently confirmed. Some of the track segment pairs (couples) in the two lists might have originated from the same target over time. For each feasible track segment pair from the two lists, the old track segment is propagated forward (predicted) and

young track segment is propagated backward (retrodicted) to a common time and a hypothesis is formulated to decide whether or not these track segments originated from the same target over time. If the hypothesis is accepted, track fusion is performed the same way as in track-to-track (T2T) association (Bar-Shalom et al. 2011, Mori et al. 2012).

Yeom et al. (2004) and Zhang and Bar-Shalom (2011) presented different TSA algorithms and these algorithms perform forward prediction and backward retrodiction¹ from the actual termination time of the old track segment and starting time of the young track segment, respectively. But, very often, a track may be associated with an incorrect measurement, which eventually leads the track to deviate from its actual path and terminate. Subsequently, a new track is initialized for the same target, possibly, even before the termination of its old track segment. Note that there is also a possibility of initializing this new track from false alarms.

Under the aforementioned circumstances, predicting or retrodicting from the actual time of termination or initialization of respective track segments may not be appropriate for two reasons. First, if the young track segment is initialized before the termination of the old track segment, that is, if the starting time of the young track segment is not equal to or greater than the ending time of the old track segment, then this pair is not a valid candidate for TSA. Second, even if the pair is a valid candidate for TSA, because of possible association of the old track segment with an incorrect measurement before its termination and/or incorrect association at the initialization of the new track segment, there is a strong possibility to make the wrong decision that the given pair of track segments is not from the same target, even if they actually were from the same target. That is, the existing TSA algorithms do not explore possible track termination or initialization due to incorrect association before considering them for TSA. In addition to these factors, current TSA algorithms use a constant velocity (CV) model to bridge the breakage period. Using a CV model alone is not sufficient to track highly maneuvering targets. These concerns provide the motivation for the proposed 2-D assignment-based TSA algorithm. This algorithm first releases incorrectly associated measurements by going backward and forward in time along

¹In the literature, smoothing and retrodication are used alternatively. However, here retrodication means propagating track backward

the old and young track segments, respectively, and then performs the prediction or retrodiction (see Figure 3.1) using the combination of CV and coordinated turn (CT) models (Bar-Shalom et al. 2011).

Zhang et al. (2015) used only the CT model to repair the broken tracks; the turning rate is obtained using unassociated measurements during the breakage period. But the problem with this approach is that standard one-to-one measurement-to-track association criterion is not followed. Utilizing both released and unassociated measurements (as proposed in Chapter 3) to estimate a broken track yields more information for better decision making and improved track accuracy. Released measurements are the measurements that are deemed to have been erroneously associated, hence, removed while going backward and forward along the old and young track segments, respectively. None of the existing TSA algorithms use both released and unassociated measurements simultaneously for estimation during a breakage period. This is the motivation for extending the proposed 2-D TSA algorithm to the proposed multi-frame assignment based TSA algorithm, in which association is performed among terminated tracks, released or unassociated measurements, and newly initialized tracks. The difference between the proposed 2-D TSA and multi-frame TSA algorithms is that the former utilizes no measurements, while the latter utilizes both released and unassociated measurements.

On the other hand, practical multiple-target tracking systems may also suffer from undesirable effect such as track swap. This effect can significantly affect estimation accuracy, track duration, and track continuity, degrading the overall tracker performance. Track swaps occur because of incorrect data association by updating a track using measurements from a different target, incorrect association with clutter measurements and poor track-to-measurement association techniques, among other causes.

Often a track gets terminated or pruned automatically when it is not associated over specified number of consecutive scans (i.e., M/N logic (Castella 1976, Coraluppi 2005, Dezert and Kirubarajan 1999)) or when its track quality (Li and Li 2001, Musicki et al. 1994, Song and Kim 2006, Sinha et al. 2012) falls below a certain threshold. Later, when subsequent measurements from the same target become available, a new track — pertaining to the same target or to a new target — is initialized and sub-

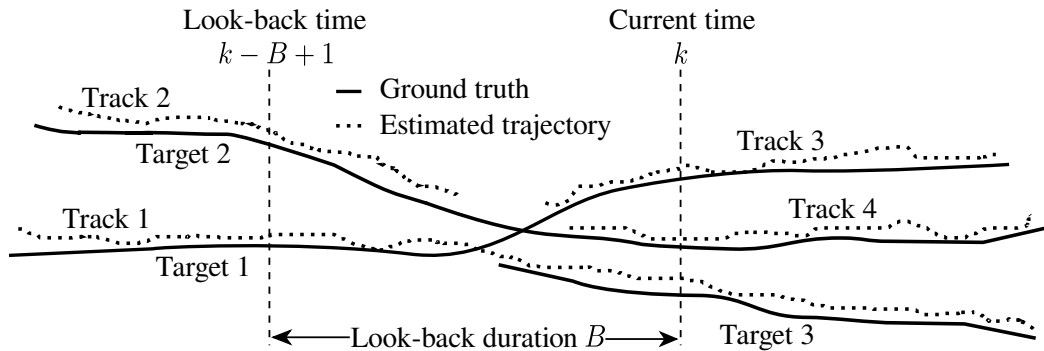


Figure 2.1: Track swapping after breakage

sequently confirmed. In this situation, one side effect of existing algorithms (Yeom et al. 2004, Zhang and Bar-Shalom 2011, Mori and Chong 2013, Castiñón and Finn 2011, Mellema 2002, Van der Merwe and De Villiers 2013, Arnold et al. 1984, Raghu et al. 2018, Zhang et al. 2015, Song et al. 2013) is that they may cause track swaps: that is, they may stitch track segments originated from two different targets, which is undesirable.

To stitch the broken tracks, it is common to use TSA algorithms (Yeom et al. 2004, Zhang and Bar-Shalom 2011, Raghu et al. 2018) without considering any other unbroken (continuous) tracks. But in scenarios with closely spaced targets and high clutter, these unbroken tracks may have been swapped among themselves or with broken track segments. This may happen because of clutter measurements, measurement association ambiguities and target maneuvers. For example, track swaps may occur in a scenario where closely spaced targets are passing through a cluster of windmills. A track swap may happen when a track is associated with a target and after some time the same track is associated with different target while initializing and subsequently confirming a totally new track for first target as shown in Figure 2.1. Similarly, a track swap may also occur with swapping of target identities (IDs) over time as shown in Figure 2.2. Under these situations, it is necessary to first determine track swaps and then break them so that TSA can be performed with the track list consisting of both the regularly broken track segments and the algorithmically broken track segments resulting from track swap detection.

To mitigate the effect of track swap, a particle filter based track probability evaluation approach is presented in (Blom and Bloem 2011) but this approach is limited to two targets. A partially observable Markov decision process (POMDP) based tech-

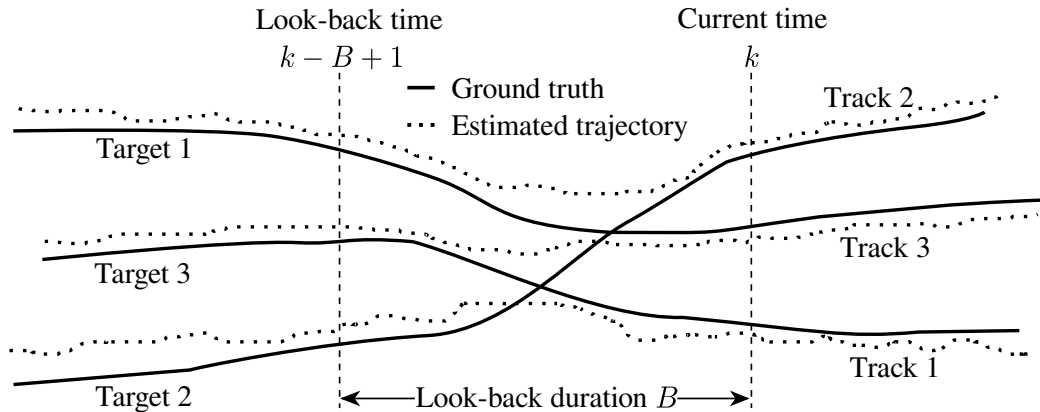


Figure 2.2: Track swapping without breakage

nique is presented in (Ragi and Chong 2012) wherein location of the sensor (mounted on the UAVs) relative to the targets is used to reduce the risk of track swap but this is inapplicable for stationary sensor. In (Shijun et al. 2010), radar and GPS data are fused to avoid track swap. An automated track swap detection technique with known target crossings is presented in (Pulford and Scala 2010). However, a fully automated algorithm to detect track swaps and mitigate the effects of track swaps without apriori information is still lacking. In addition, track swap may result in erroneous calculation of mean-squared-error (MSE). To avoid this, tracks with swaps are excluded in (Pulford and Scala 2010) while computing the MSE, when the correct MSE should be calculated after un-swapping. Flexible ID association-based tracking algorithm is presented in (Sinha and Peters 2009) to avoid the track swaps among the continuous tracks ignoring the broken ones.

Even though approaches (Blom and Bloem 2011, Ragi and Chong 2012, Shijun et al. 2010, Pulford and Scala 2010, Sinha and Peters 2009) deal with track un-swapping, the limitation is that they ignored the fact that there is possibility of track swapping after breakage (see Figure 2.1): that is, they consider only the continuous tracks while ignoring the broken ones. Besides this, approaches in (Yeom et al. 2004, Zhang and Bar-Shalom 2011, Mori and Chong 2013, Castñón and Finn 2011, Mellema 2002, Pannetier and Dezert 2012, Van der Merwe and De Villiers 2013, Arnold et al. 1984, Raghu et al. 2018, Zhang et al. 2015, Song et al. 2013) and (Blom and Bloem 2011, Ragi and Chong 2012, Shijun et al. 2010, Pulford and Scala 2010) use kinematic estimates such as target position and velocity in track stitching and un-swapping, respectively. However, target features such as classification information

(attributes like number of aircraft engines, presence of IFF, type of radar used by target) (Bar-Shalom et al. 2005, Angelova and Mihaylova 2006, Ristic et al. 2004, Mei et al. 2007, Runkle et al. 1999, Bharadwaj et al. 2001, Ji et al. 2005, Zyweck and Bogner 1996) and amplitude information (features like radar cross section (RCS), signal strength, and wing span) (Kirubarajan and Bar-Shalom 1996, Lerro and Bar-Shalom 1993, McAnanama and Kirubarajan 2012) also can help resolve such issues and improve overall tracker performance. Often, class information and/or amplitude information in addition to the kinematic information is available to the tracker. These additional information can be used in post-processing, for example, TSA or un-swapping.

2.3 MOTIVATION

Maneuvering target tracking has been a potential research problem in radar/sonar signal processing with potential civilian and defense applications. The TSA algorithms proposed in the literature by many researchers ignored the followings:

- utilizing the unassociated data (measurements) while performing track stitching
- the case where the young track segment is initialized and confirmed even before the termination of its associated old track segment
- unbroken tracks with which broken tracks have possibility of track swap.

These serve as the strong motivations to propose followings:

- algorithm to perform TSA even when termination time of old track segment is greater than beginning time of its associated young track segment. This is extended to utilizing all the available data such as unassociated measurements and released measurements to perform TSA comprehensively.
- an algorithms that can integrate kinematic, classification and amplitude information to perform un-swapping and TSA simultaneously to improve the overall tracker performance even when the ground truth is unknown, which is the usual case in practical applications.

2.4 LIST OF PUBLICATIONS

The contributions of the thesis resulted in the following publications:

1. **Raghu, J.**, Srihari, P., Tharmarasa, R., Kirubarajan, T. (2018). "Comprehensive Track Segment Association for Improved Track Continuity" *IEEE Transactions on Aerospace and Electronic Systems*, vol. PP, no. 99, pp. 1-1. doi: 10.1109/TAES.2018.2820364
2. **Raghu, J.**, Srihari, P., Tharmarasa, R., Kirubarajan, T., "Classification and Amplitude Aided Track Un-swapping" *to be communicated to IEEE Transactions on Aerospace and Electronic Systems Journal*.

Chapter 3

TRACK STITCHING

3.1 OUTLINE

In this chapter, the problem is formulated to perform track stitching in a systematic way. First step in track stitching is dividing the broken tracks into old track segment list and young track segment list so that track segment association can be carried between the tracks of those two lists. Track segment association can be performed in two possible ways. First is, performing track-to-track association without using any data present within the track stitching duration. Alternatively, second is, performing track-to-track association using data present within the track stitching duration which turns out to be track-to-measurements-to-track association.

3.2 TRACK SEGMENT ASSOCIATION

3.2.1 Track Grouping

When tracking targets in high clutter (i.e., low observable scenarios), track breakage occurs whenever the track is terminated or stops following the target. A new track following the same target is then initialized and subsequently confirmed. This repeats over time, leaving multiple track segments originated from the same target. The ultimate aim of track stitching is to combine all these track segments and maintain a consistent track ID.

Track segment association is performed between the following two track lists at time k (Yeom et al. 2004):

1. Old track segment list ($\mathcal{T}^{\mathcal{O}}(k)$): Let the old track segment list at time k be

$$\mathcal{T}^{\mathcal{O}}(k) = \{\mathbf{T}_{n^{\mathcal{O}}}^{\mathcal{O}}(k)\}_{n^{\mathcal{O}}=1}^{N^{\mathcal{O}}(k)} \quad (3.1)$$

where $N^{\mathcal{O}}(k)$ is the total number of tracks in the old track segment list at time k . This track list consists of tracks that have been terminated recently, due to no association with any measurement, in the time interval $(k - B, k]$, where k is the current time and B is the look-back duration or sliding window size. This look-back time is a design parameter that is decided based on the track breakage rate, false alarm rate, or other factors.

2. Young track segment list ($\mathcal{T}^{\mathcal{Y}}(k)$): Let the young track segment list at time k be

$$\mathcal{T}^{\mathcal{Y}}(k) = \{\mathbf{T}_{n^{\mathcal{Y}}}^{\mathcal{Y}}(k)\}_{n^{\mathcal{Y}}=1}^{N^{\mathcal{Y}}(k)} \quad (3.2)$$

where $N^{\mathcal{Y}}(k)$ is the total number of track segments in the young track segment list at time k . This list consists of tracks that have been started recently in the time interval $(k - B, k)$ provided they attained a certain minimum age. The minimum age of young track is the number of scans during which track should exist within the time interval $(k - B, k)$. This age can be varied, depending upon the track breakage rate. The track segments appear on this list for one of several reasons: it pertains to a track in the old track segment list, a target is newborn, or false alarms result in a track.

The cardinality of these two track lists could be different. As in the standard measurement-to-track 2-D assignment (Bar-Shalom et al. 2011, Blackman and Popoli 1999), dummy tracks are added to both lists to represent no association with a track. A particular track segment from one track list is associated with the dummy track only when it is not assigned to any other track segments of its counterpart list. Updating a track segment list at time $k + 1$ is conducted in the following sequence:

1. Updating the young track segment list $\mathcal{T}^{\mathcal{Y}}(k)$: (a) remove all the tracks that were associated with old track segments at time k ; (b) remove all those tracks with the last updated time $k_{n^{\mathcal{Y}},e}^{\mathcal{Y}} = k + 1$; (c) add all those non-terminated tracks with starting time in the interval $(k - B + 2, k + 1)$ after attaining a certain minimum age.

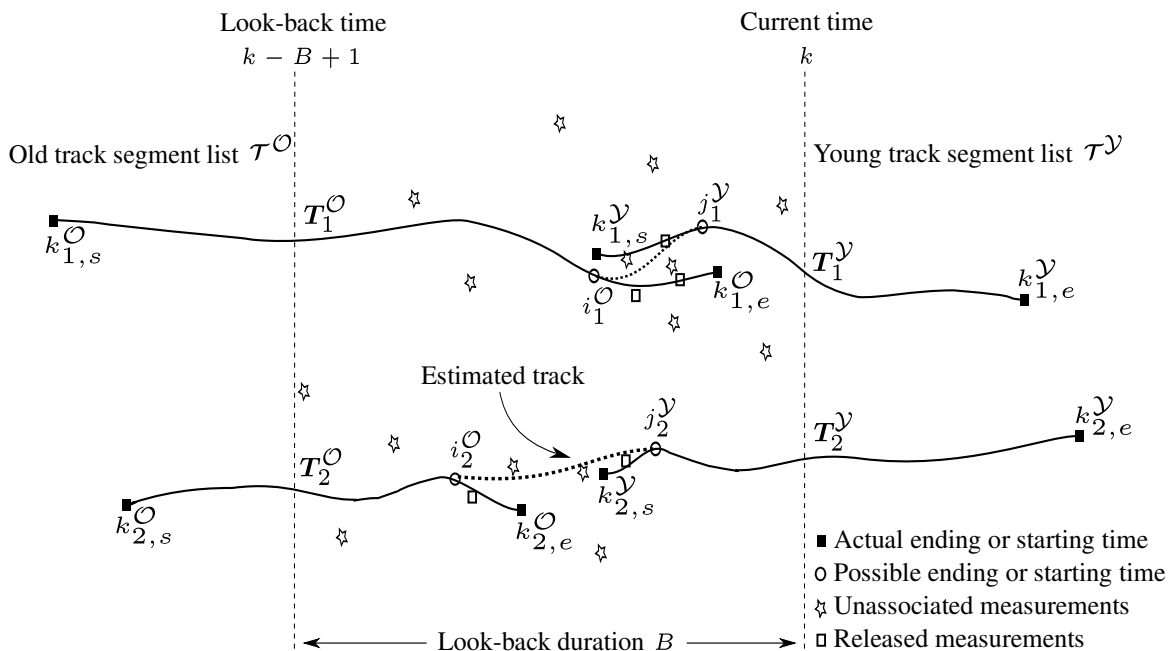


Figure 3.1: Stitching broken tracks

2. Updating the old track segment list $\mathcal{T}^O(k)$: (a) remove all the tracks that were associated with young track segments at time k ; (b) remove all those tracks whose last updated time $k_{n^O,e}^O < k - B + 1$, i.e., tracks that fall out of the sliding window; (c) add all those unassociated but removed tracks of the young track segment list at time $k + 1$.

3.2.2 Possible Starting and Ending Times

Track breakages occur for a variety of reasons. Whenever breakage occurs due to a false (clutter or incorrect) measurement association, it is necessary to start stitching the track not from its original termination time but from its possible termination (ending) time, i_n^O , i.e., searching for possible track termination due to false measurement. Similarly, there is a possibility that some of the track segments from track list $\mathcal{T}^Y(k)$ were initialized with false measurements and subsequently confirmed. This creates the need to consider not the beginning point but rather the possible starting point, j_n^Y , as shown in Figure 3.1. Furthermore, searching for the possible starting and ending times allows us to stitch tracks even if the young track segment started before the termination of its associated old track segment, i.e., when $k_{n^O,e}^O > k_{n^Y,s}^Y$. Note that in (Yeom et al. 2004, Zhang and Bar-Shalom 2011), a track pair is an eligible candidate for stitching only when $k_{n^O,e}^O \leq k_{n^Y,s}^Y$.

At time k , for a given old track segment list $\mathcal{T}^{\mathcal{O}}(k)$ and the young track segment list $\mathcal{T}^{\mathcal{Y}}(k)$, let the set of all combinations of candidate track pairs be

$$\Phi^T(k) = \left\{ \left\{ \mathbf{T}_1^{\mathcal{O}}(k), \mathbf{T}_1^{\mathcal{Y}}(k) \right\}, \left\{ \mathbf{T}_1^{\mathcal{O}}(k), \mathbf{T}_2^{\mathcal{Y}}(k) \right\}, \dots, \left\{ \mathbf{T}_{N^{\mathcal{O}}(k)}^{\mathcal{O}}(k), \mathbf{T}_{N^{\mathcal{Y}}(k)}^{\mathcal{Y}}(k) \right\} \right\}, \quad (3.3)$$

where the old track segment is

$$\mathbf{T}_{n^{\mathcal{O}}}^{\mathcal{O}}(k) = \left\{ \hat{\mathbf{x}}_{n^{\mathcal{O}}}(k|k); k = k_{n^{\mathcal{O}},s}^{\mathcal{O}}, \dots, k_{n^{\mathcal{O}},e}^{\mathcal{O}} \right\}, \quad n^{\mathcal{O}} = 1, \dots, N^{\mathcal{O}}(k) \quad (3.4)$$

and the new (young) track segment is

$$\mathbf{T}_{n^{\mathcal{Y}}}^{\mathcal{Y}}(k) = \left\{ \hat{\mathbf{x}}_{n^{\mathcal{Y}}}(k|k); k = k_{n^{\mathcal{Y}},s}^{\mathcal{Y}}, \dots, k_{n^{\mathcal{Y}},e}^{\mathcal{Y}} \right\}, \quad n^{\mathcal{Y}} = 1, \dots, N^{\mathcal{Y}}(k). \quad (3.5)$$

In (3.4), $k_{n^{\mathcal{O}},s}^{\mathcal{O}}$ and $k_{n^{\mathcal{O}},e}^{\mathcal{O}}$ are the actual beginning and terminating times of the $(n^{\mathcal{O}})^{\text{th}}$ old track segment, respectively. Similarly, in (3.5), $k_{n^{\mathcal{Y}},s}^{\mathcal{Y}}$ and $k_{n^{\mathcal{Y}},e}^{\mathcal{Y}}$ are the actual beginning and terminating times of the $(n^{\mathcal{Y}})^{\text{th}}$ young track segment, respectively.

For each pair of candidates, $\{\mathbf{T}_{n^{\mathcal{O}}}^{\mathcal{O}}(k), \mathbf{T}_{n^{\mathcal{Y}}}^{\mathcal{Y}}(k)\}$, the possible ending and possible starting time pair is $(i_{n^{\mathcal{O}}}^{\mathcal{O}}, j_{n^{\mathcal{Y}}}^{\mathcal{Y}})$. The most likely possible ending time is given by

$$i_{n^{\mathcal{O}}}^{\mathcal{O}} \in \left\{ \max\{k_{n^{\mathcal{O}},e}^{\mathcal{O}} - B_{i_{\max}}, k - B + 1\}, \dots, k_{n^{\mathcal{O}},e}^{\mathcal{O}} \right\} \quad (3.6)$$

where $B_{i_{\max}}$ is the maximum number of scans possible when going backward along an old track segment. Let B_i be a variable indicating the number of scans going backward along old track segment, i.e., $B_i = 0, 1, \dots, B_{i_{\max}}$ and hence for given B_i , the ending time

$$i_{n^{\mathcal{O}}}^{\mathcal{O}} = \max\{k_{n^{\mathcal{O}},e}^{\mathcal{O}} - B_i, k - B + 1\}. \quad (3.7)$$

Similarly, the most likely possible starting time is given by

$$j_{n^{\mathcal{Y}}}^{\mathcal{Y}} \in \left\{ k_{n^{\mathcal{Y}},s}^{\mathcal{Y}}, \dots, \min\{k_{n^{\mathcal{Y}},s}^{\mathcal{Y}} + B_{j_{\max}}, k\} \right\} \quad (3.8)$$

where $B_{j_{\max}}$ is the maximum number of scans possible when going forward along a young track segment. Let B_j be a variable indicating the number of scans going forward along young track segment, i.e., $B_j = 0, 1, \dots, B_{j_{\max}}$ and hence for given B_j , the starting time

$$j_{n^{\mathcal{Y}}}^{\mathcal{Y}} = \min\{k_{n^{\mathcal{Y}},s}^{\mathcal{Y}} + B_j, k\}. \quad (3.9)$$

Track pair $\{\mathbf{T}_{n^{\mathcal{O}}}(k), \mathbf{T}_{n^{\mathcal{Y}}}(k)\}$ is a feasible candidate for an association if and only if track segment $n^{\mathcal{Y}}$ has a possible starting time not less than the possible ending time of track segment $n^{\mathcal{O}}$, i.e.,

$$i_{n^{\mathcal{O}}}^{\mathcal{O}} \leq j_{n^{\mathcal{Y}}}^{\mathcal{Y}}. \quad (3.10)$$

All those track pairs of $\Phi^T(k)$ that do not satisfy the constraint (3.10) are removed to obtain the feasible candidate track pair set

$$\Phi_f^T(k) = \left\{ \left\{ \mathbf{T}_1^{\mathcal{O}}(k), \mathbf{T}_1^{\mathcal{Y}}(k) \right\}, \left\{ \mathbf{T}_1^{\mathcal{O}}(k), \mathbf{T}_2^{\mathcal{Y}}(k) \right\}, \dots, \left\{ \mathbf{T}_{N^{\mathcal{O}}(k)}^{\mathcal{O}}(k), \mathbf{T}_{N^{\mathcal{Y}}(k)}^{\mathcal{Y}}(k) \right\} \right\}. \quad (3.11)$$

Let $\Psi^{ij}(k)$ be the set of all possible combinations of i 's $N^{\mathcal{O}}(k)$ -tuples and j 's $N^{\mathcal{Y}}(k)$ -tuples, as follows:

$$\Psi^{ij}(k) = \{\psi_l^{ij}(k); \quad l = 1, \dots, L(k)\} \quad (3.12)$$

where

$$\psi_l^{ij}(k) = \left(\begin{pmatrix} i_1^{\mathcal{O}}(l) \\ i_2^{\mathcal{O}}(l) \\ \vdots \\ i_N^{\mathcal{O}}(l) \end{pmatrix}, \begin{pmatrix} j_1^{\mathcal{Y}}(l) \\ j_2^{\mathcal{Y}}(l) \\ \vdots \\ j_M^{\mathcal{Y}}(l) \end{pmatrix} \right) \quad (3.13)$$

and $L(k)$ is the total number of possible combinations of i 's $N^{\mathcal{O}}(k)$ -tuples and j 's $N^{\mathcal{Y}}(k)$ -tuples. For a given $\psi_l^{ij}(k)$, track stitching can be done with or without unassociated measurements. If unassociated measurements are not available, or measurements are available but computation is a major issue, then prediction and/or retrodiction can be used to predict the broken track followed by 2-D assignment. Otherwise, unassociated measurements in addition to released measurements are used to formulate the multi-frame assignment problem. These 2-D and multi-frame TSA approaches are discussed in detail in the Sections 3.2.4 and 3.2.5, respectively. In both approaches, while performing association, one of the following decisions is made:

- That the old track segment is dead or due to a false alarm and is thus deleted, i.e., it will not be considered as a valid candidate for association in the future.
- That the old track segment is alive but does not suit any of the young track segments at the current time and, hence, is retained, i.e., it can be a valid candidate for association in the future.

- That an old track segment and a young track segment are indeed from the same target.
- That the young track segment is due to a new target or false alarm and hence is not associated with any of the old track segments at the current time.

3.2.3 Track Smoothing

Usually, smoothing is performed over a complete trajectory, given the available data, to improve the state estimates (Bar-Shalom et al. 2004). In the present study, smoothing is performed over part of the young track segment before it is considered for TSA, and over the stitched duration (breakage period) after TSA is complete. For smoothing, the first few scans are considered to reduce error due to the track initialization method and also to avoid searching for the possible starting time, as it would reduce the computational load significantly. This leads to better decisions while performing TSA.

Smoothing is estimating the state at time $k-1$ within the data interval, i.e., based on data up to $k_1 > k-1$,

$$\hat{\mathbf{x}}(k-1|k_1) = E[\mathbf{x}(k-1)|\{\mathbf{z}(0), \mathbf{z}(1), \dots, \mathbf{z}(k_1)\}], \quad (3.14)$$

where $\{\mathbf{z}(0), \mathbf{z}(1), \dots, \mathbf{z}(k_1)\}$ is data (measurements) up to time k_1 .

More details on smoothing can be found in (Bar-Shalom et al. 2004). Here, the most commonly used fixed interval smoothing process is briefly described. This smoothing technique requires a backward iteration after filtering has been performed and its results, i.e., $\hat{\mathbf{x}}(k-1|k-1)$, $\hat{\mathbf{x}}(k|k-1)$, $\mathbf{P}(k-1|k-1)$, $\mathbf{P}(k|k-1)$ for $k = 1, \dots, k_1-1$ have been stored. The iteration consists of the smoother gain calculation

$$\mathbf{C}(k-1) = [\mathbf{P}(k-1|k-1)]\mathbf{F}(k-1)'[\mathbf{P}(k|k-1)]^{-1} \quad (3.15)$$

followed by the evaluation of smoothed state

$$\hat{\mathbf{x}}(k-1|k_1) = \hat{\mathbf{x}}(k-1|k-1) + \mathbf{C}(k-1)[\hat{\mathbf{x}}(k|k_1) - \hat{\mathbf{x}}(k|k-1)] \quad (3.16)$$

and the covariance of the smoothed state

$$\mathbf{P}(k-1|k_1) = \mathbf{P}(k-1|k-1) + \mathbf{C}(k-1)[\mathbf{P}(k|k_1) - \mathbf{P}(k|k-1)]\mathbf{C}(k-1)' \quad (3.17)$$

for $k = k_1-1, \dots, 2, 1$.

3.2.4 2-D Assignment Approach for Track Segment Association

Since no measurements are used, the track stitching problem becomes easier: that is, it is just a prediction of the old track segment from its possible ending time to the possible starting time of the young track segment. The first step in 2-D assignment (Bar-Shalom et al. 2011, Deb et al. 1997, Pattipati et al. 2000), similar to measurement-to-track association, is deciding whether or not a given pair of track segments is eligible for an association and this process is called gating. This becomes a hypothesis testing problem where the hypotheses are defined as follows:

$$\begin{aligned} H \{ \mathbf{T}_{n^o}^o(k), \mathbf{T}_{n^y}^y(k) \} &: \text{Track segment } \mathbf{T}_{n^o}^o(k) \text{ and track segment } \mathbf{T}_{n^y}^y(k) \text{ are} \\ &\quad \text{from the same target} \\ \bar{H} \{ \mathbf{T}_{n^o}^o(k), \mathbf{T}_{n^y}^y(k) \} &: \text{Track segment } \mathbf{T}_{n^o}^o(k) \text{ and track segment } \mathbf{T}_{n^y}^y(k) \text{ are} \\ &\quad \text{not from the same target.} \end{aligned} \quad (3.18)$$

For a given $\hat{\boldsymbol{\psi}}_l^{ij}$, consider any track segment pair $\{ \mathbf{T}_{n^o}^o(k), \mathbf{T}_{n^y}^y(k) \} \in \Phi_f^T(k)$ and release all the measurements in the interval $(i_{n^o}^o + 1, j_{n^y}^y - 1)$ (for simplicity, i and j are used in this subsection). Propagate the old track segment from its possible ending time (i) to the possible starting time (j) of the young track segment (this is discussed in detail in Section 3.3). This propagated old track segment is represented by its state estimate $\hat{\mathbf{x}}_{n^o}(j|i)$ and the corresponding young track segment at the same time is represented by its state estimate $\hat{\mathbf{x}}_{n^y}(j|j)$. The hypothesis (3.18) testing depends on the difference between these two states, i.e.,

$$\Delta_{n^o n^y}(j|i) = \hat{\mathbf{x}}_{n^o}(j|i) - \hat{\mathbf{x}}_{n^y}(j|j) \quad (3.19)$$

with corresponding covariance

$$\Sigma_{n^o n^y}(j|i) = \mathbf{P}_{n^o}(j|i) + \mathbf{P}_{n^y}(j|j). \quad (3.20)$$

Making use of the chi-square test (Bar-Shalom et al. 2004), hypothesis $H \{ \mathbf{T}_{n^o}^o(k), \mathbf{T}_{n^y}^y(k) \}$ is accepted if

$$[\Delta_{n^o n^y}(j|i)]' [\Sigma_{n^o n^y}(j|i)]^{-1} [\Delta_{n^o n^y}(j|i)] \leq \gamma_{\mathbf{x}} \quad (3.21)$$

is true, where $\gamma_{\mathbf{x}}$ is the gate threshold for state vector dimension — can be obtained using chi-square distribution (Bar-Shalom et al. 2004) — corresponding to a certain gate probability, P_G . Otherwise, $\bar{H} \{ \mathbf{T}_{n^o}^o(k), \mathbf{T}_{n^y}^y(k) \}$ is accepted.

After hypothesis testing, the association between the two track segment lists $\mathcal{T}^{\mathcal{O}}(k)$ and $\mathcal{T}^{\mathcal{Y}}(k)$ is a 2-D assignment problem. Dummy tracks are added to both track lists to represent non-association; this dummy track can be associated with a track declared dead or a track associated with a newborn target. Define an assignment variable, which is binary, as

$$a_{n^{\mathcal{O}}n^{\mathcal{Y}}}^{ij} = \begin{cases} 1 & \text{if track segments } \mathbf{T}_{n^{\mathcal{O}}}^{\mathcal{O}}(k) \text{ and} \\ & \mathbf{T}_{n^{\mathcal{Y}}}^{\mathcal{Y}}(k) \text{ are from the same target} \\ 0 & \text{else.} \end{cases} \quad (3.22)$$

The cost of forward predicted track segment $\mathbf{T}_{n^{\mathcal{O}}}^{\mathcal{O}}(k)$ being associated with track segment $\mathbf{T}_{n^{\mathcal{Y}}}^{\mathcal{Y}}(k)$ is represented by $c_{n^{\mathcal{O}}n^{\mathcal{Y}}}^{ij}$. The ultimate aim is to solve for the optimal set of assignment variables $\{a_{n^{\mathcal{O}}n^{\mathcal{Y}}}^{ij}\}$ such that each old track segment is assigned either to a young track segment or to the dummy track and each young track segment is assigned to an old track segment or to the dummy track. This can be reformulated as

$$\min_{a_{n^{\mathcal{O}}n^{\mathcal{Y}}}^{ij}} \sum_{n^{\mathcal{O}}=0}^{N^{\mathcal{O}}(k)} \sum_{n^{\mathcal{Y}}=0}^{N^{\mathcal{Y}}(k)} a_{n^{\mathcal{O}}n^{\mathcal{Y}}}^{ij} c_{n^{\mathcal{O}}n^{\mathcal{Y}}}^{ij} \quad (3.23)$$

subject to

$$\sum_{n^{\mathcal{O}}=0}^{N^{\mathcal{O}}(k)} a_{n^{\mathcal{O}}n^{\mathcal{Y}}}^{ij} = 1, \quad n^{\mathcal{Y}} = 1, 2, \dots, N^{\mathcal{Y}}(k) \quad (3.24)$$

$$\sum_{n^{\mathcal{Y}}=0}^{N^{\mathcal{Y}}(k)} a_{n^{\mathcal{O}}n^{\mathcal{Y}}}^{ij} = 1, \quad n^{\mathcal{O}} = 1, 2, \dots, N^{\mathcal{O}}(k), \quad (3.25)$$

where $a \in \{0, 1\}$, $n^{\mathcal{O}} = 0$ and $n^{\mathcal{Y}} = 0$ indicate dummy tracks in the old track segment list $\mathcal{T}^{\mathcal{O}}(k)$ and the young track segment list $\mathcal{T}^{\mathcal{Y}}(k)$, respectively, and there are no constraints on these dummy tracks. This 2-D assignment problem can be solved optimally using modified auction algorithm (Pattipati et al. 1992).

Assuming Gaussian innovation is known, the cost $c_{n^{\mathcal{O}}n^{\mathcal{Y}}}^{ij}$, which is the dimensionless negative log-likelihood ratio (Bar-Shalom et al. 2007), is calculated as follows:

$$c_{n^{\mathcal{O}}n^{\mathcal{Y}}}^{ij} = \begin{cases} -\ln \frac{\mathcal{N}(\Delta_{n^{\mathcal{O}}n^{\mathcal{Y}}}(j|i); 0, \Sigma_{n^{\mathcal{O}}n^{\mathcal{Y}}}(j|i))}{\mu} & \text{for } n^{\mathcal{O}} \neq 0 \text{ and } n^{\mathcal{Y}} \neq 0 \\ -\ln(1 - P_D) & \text{for } n^{\mathcal{O}} = 0 \text{ or } n^{\mathcal{Y}} = 0, \end{cases} \quad (3.26)$$

where P_D is the target detection probability and μ is the spatial density of true and false tracks in the state space (Bar-Shalom et al. 2004).

Input: Broken track segments at time k

Output: Stitched tracks at time k

- 1: Group the track segments into old and young track lists (do this only once at the beginning) as discussed in subsection 3.2.1.
- 2: Update old and young track lists as discussed in subsection 3.2.1.
- 3: Perform smoothing on all the tracks of young track list over a fixed period as discussed in subsection 3.2.3.
- 4: Obtain set of all combinations of candidate track pairs $\Phi^T(k)$ as in (3.3).
- 5: Obtain feasible candidate track pair set $\Phi_f^T(k)$ as given in (3.11).
- 6: Obtain the set of all possible combinations of i 's $N^O(k)$ -tuples and j 's $N^Y(k)$ -tuples $\Psi^{ij}(k)$ as given in (3.12).
- 7: Obtain model parameters as discussed in subsection 3.3.2 for each pair of tracks pertaining to $\psi_l^{ij}(k)$.
- 8: For every $\psi_l^{ij}(k)$ obtain corresponding total cost $C_{2-D}(\psi_l^{ij}(k))$ by solving (3.23).
- 9: Obtain $\hat{\psi}_{2-D}^{ij}(k)$ by solving (3.27).
- 10: Perform the track stitching between old and young track segments according to the best solution $\hat{\psi}_{2-D}^{ij}(k)$.
- 11: **return** Stitched tracks.

Figure 3.2: An algorithm for proposed 2-D assignment based TSA

Let $C_{2-D}(\psi_l^{ij}(k))$ represent the total minimum cost corresponding to (3.23) for a given $\psi_l^{ij}(k)$. Now, one needs to solve for a value of $\psi_l^{ij}(k)$ that would minimize the cost $C_{2-D}(\psi_l^{ij}(k))$, as follows:

$$\hat{\psi}_{2-D}^{ij}(k) = \arg \min_{\psi_l^{ij}(k) \in \Psi^{ij}(k)} C_{2-D}(\psi_l^{ij}(k)). \quad (3.27)$$

The solution $\hat{\psi}_{2-D}^{ij}(k)$ is the best combination of possible ending and starting times. The TSA solution corresponding to this $\hat{\psi}_{2-D}^{ij}(k)$ is optimal. Further, the step by step procedure for the implementation of this proposed 2-D assignment based algorithm can be found in Figure 3.2.

3.2.5 Multi-frame Assignment Approach for Track Segment association

In this subsection, the multi-frame assignment (track-to-measurement-to-track) (Deb et al. 1997, Popp et al. 2001) problem to estimate the track during the breakage period is formulated. The multi-frame assignment algorithm can be used for both tracking and post-processing. The difference is that in the former case the assignment is carried-out between the track and a string of detected measurements whereas in

the latter case the assignment is carried between the old track segment, a string of measurements, and the young track segment as shown in Figure 3.3. In the 2-D assignment formulation described above, the old track segments were propagated to the starting point of young track segments. That is, no released or unassociated measurements were used. In contrast, in multi-frame assignment both released and unassociated measurements are used to bridge the old and young track segments. The measurements are released the same way as in the 2-D assignment case. However, both the proposed algorithms have a lag of look-back duration B in making the association decisions (see Figure 3.1).

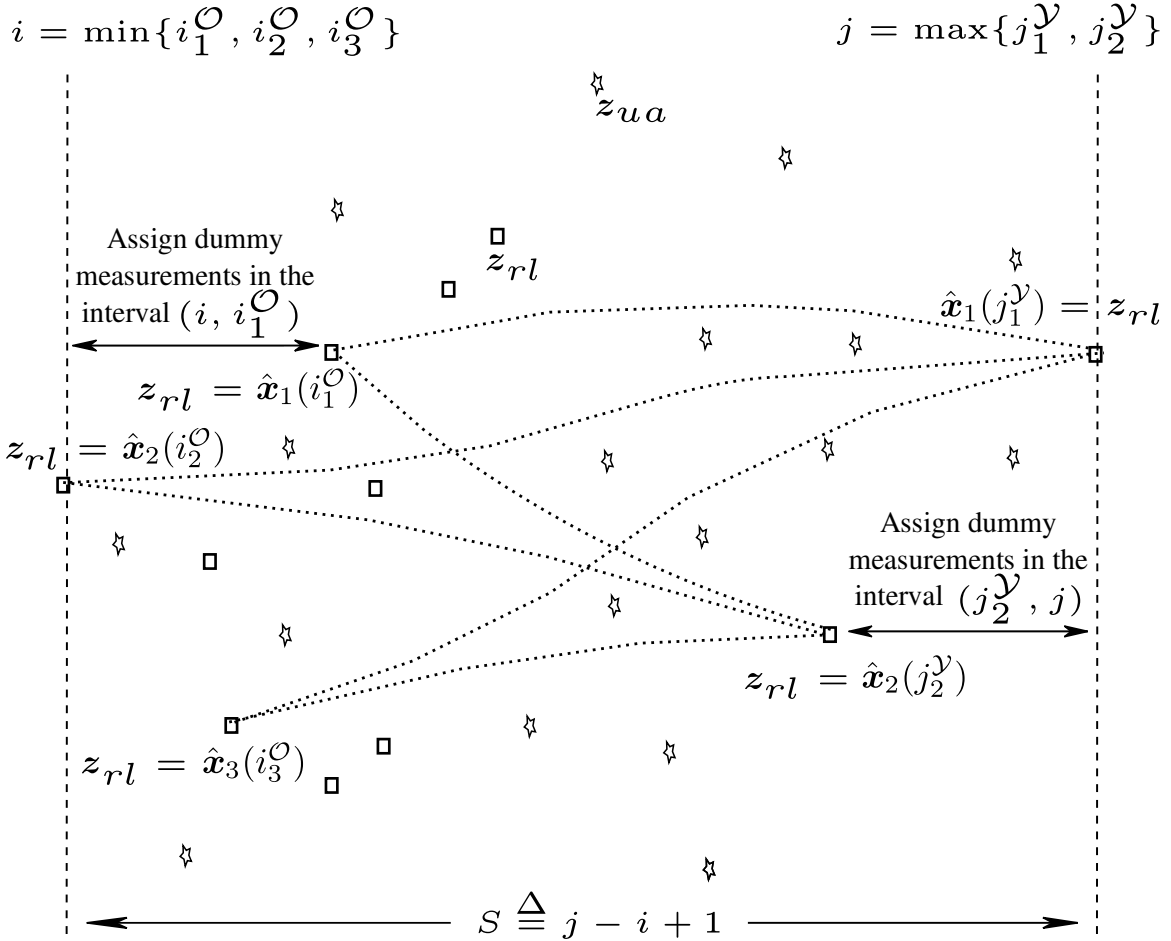


Figure 3.3: A typical example for S -D assignment

The idea behind releasing measurements is to

1. explore the possibility that any measurement is erroneously associated with a track from which it actually did not originate resulting in subsequent track termination; and

2. associate this released measurement to the track that it most likely originated from.

In addition to released measurements, originally unassociated measurements are also used to improve the accuracy of track estimation.

For a given $\psi_l^{ij}(k)$, the track ending time is different for different old track segments; this is the case with the starting time of young track segments, as well. Therefore, to formulate a general multi-frame assignment problem one needs to pick a common i and j . This is accomplished in the following manner:

$$i = \min \left\{ \left\{ \left\{ i_{n^{\mathcal{O}}}^{\mathcal{O}}(l) \right\}_{n^{\mathcal{O}}=1}^{N^{\mathcal{O}}(k)}, \left\{ j_{n^{\mathcal{Y}}}^{\mathcal{Y}}(l) \right\}_{n^{\mathcal{Y}}=1}^{N^{\mathcal{Y}}(k)} \right\}_{l=1}^{L(k)} \right\}, \quad (3.28)$$

$$j = \max \left\{ \left\{ \left\{ i_{n^{\mathcal{O}}}^{\mathcal{O}}(l) \right\}_{n^{\mathcal{O}}=1}^{N^{\mathcal{O}}(k)}, \left\{ j_{n^{\mathcal{Y}}}^{\mathcal{Y}}(l) \right\}_{n^{\mathcal{Y}}=1}^{N^{\mathcal{Y}}(k)} \right\}_{l=1}^{L(k)} \right\}, \quad (3.29)$$

where $N^{\mathcal{O}}(k)$ and $N^{\mathcal{Y}}(k)$ represent the number of old and young track segments, respectively. Similarly, the measurement set, which includes both unassociated and released measurement, is given by

$$\mathbf{Z}^{ij} = \left\{ \mathbf{Z}_{ua}^{ij}, \left\{ \mathbf{Z}_{rl}^{i_{n^{\mathcal{O}}}^{\mathcal{O}}, k_{n^{\mathcal{O}}, e}}^{\mathcal{O}}} \right\}_{n^{\mathcal{O}}=1}^{N^{\mathcal{O}}(k)}, \left\{ \mathbf{Z}_{rl}^{k_{n^{\mathcal{Y}}, s}, j_{n^{\mathcal{Y}}}^{\mathcal{Y}}}^{\mathcal{Y}}} \right\}_{n^{\mathcal{Y}}=1}^{N^{\mathcal{Y}}(k)} \right\}. \quad (3.30)$$

In the present scenario, $S \triangleq j - i + 1$, which may vary with k . Note that the released measurement corresponding to track segment $n^{\mathcal{O}}$ at time $i_{n^{\mathcal{O}}}^{\mathcal{O}}$ is $\hat{\mathbf{x}}_{n^{\mathcal{O}}}(i_{n^{\mathcal{O}}}^{\mathcal{O}})$ and released measurement corresponding to track segment $n^{\mathcal{Y}}$ at time $j_{n^{\mathcal{Y}}}^{\mathcal{Y}}$ is $\hat{\mathbf{x}}_{n^{\mathcal{Y}}}(j_{n^{\mathcal{Y}}}^{\mathcal{Y}})$ (see Figure 3.3). Then, the multi-frame assignment becomes an S -dimensional (S -D) multi-frame assignment problem (Popp et al. 2001, Deb et al. 1997). For each S -D assignment problem, we wish to associate measurements from S lists of $\mathcal{M}(s)$, $s = i, \dots, j$, measurements. Note that S is the same for all $\psi_l^{ij}(k) \in \Psi^{ij}(k)$, which is necessary for dimensionless cost comparison. The measurement $\mathbf{z}_{m(s)}(s)$, $m(s) = 1, \dots, \mathcal{M}(s)$ originated from either a target of $\{\mathbf{T}_{n^{\mathcal{O}}}^{\mathcal{O}}(k), \mathbf{T}_{n^{\mathcal{Y}}}^{\mathcal{Y}}(k)\} \in \Phi_f^T(k)$ or from a spurious source.

To assign a cost to each feasible S -tuple of measurements, a generalized likelihood ratio based on the target state estimates for the measurement candidate associations is used. Then, any of the existing S -D assignment algorithms (Deb et al. 1997, Popp et al. 2001) can be applied to globally minimize the cost. In the track breakage

period, the target may not be detected at every scan. To incorporate this missed detection, add a dummy measurement $\mathbf{z}_0(s)$ to each measurement list. The dummy measurement is assigned to track pair $\{\mathbf{T}_{n^\mathcal{O}}^\mathcal{O}(k), \mathbf{T}_{n^\mathcal{Y}}^\mathcal{Y}(k)\}$, if

- the time s is less than or equal to the actual termination time of the old track segment $n^\mathcal{O}$, i.e., $s \leq i_{n^\mathcal{O}}^\mathcal{O}$
- the time s is greater than the actual starting time of the young track segment $n^\mathcal{Y}$, i.e., $s > j_{n^\mathcal{Y}}^\mathcal{Y}$
- the target is not detected at time s .

These conditions are represented in (3.32) and (3.33).

For a given $\psi_l^{ij}(k)$, the likelihood that an S -tuple of measurements $\mathbf{z}_{m(i),m(i+1),\dots,m(j)}$ originated from the target pertaining to track couple $\{\mathbf{T}_{n^\mathcal{O}}^\mathcal{O}(k), \mathbf{T}_{n^\mathcal{Y}}^\mathcal{Y}(k)\} \in \Phi_f^T(k)$, with the known state $\mathbf{x}_{n^\mathcal{O}n^\mathcal{Y}}(s|s)$ is

$$\Lambda_{n^\mathcal{O}n^\mathcal{Y}}(\mathbf{z}_{m(i),m(i+1),\dots,m(j)}|(n^\mathcal{O}, n^\mathcal{Y})) = \prod_{s=i}^j \left\{ [(1 - P_D)]^{1-I(m(s))} \times [P_D p(\mathbf{z}_{m(s)}(s)|\mathbf{x}_{n^\mathcal{O}n^\mathcal{Y}}(s|s))]^{I(m(s))} \right\} \quad (3.31)$$

where P_D is the target detection probability and $I(m(s))$ is an indicator function, i.e.,

$$I(m(s)) = \begin{cases} 0 & \text{if } m(s) = 0 \\ 1 & \text{else} \end{cases} \quad (3.32)$$

with

$$m(s) = \begin{cases} 0 & \text{if } s \leq i_{n^\mathcal{O}}^\mathcal{O} \\ 0 & \text{elseif } s > j_{n^\mathcal{Y}}^\mathcal{Y} \\ \in \{0, 1, \dots, \mathcal{M}(s)\} & \text{else.} \end{cases} \quad (3.33)$$

The likelihood that the measurements are all spurious or unrelated to $\{\mathbf{T}_{n^\mathcal{O}}^\mathcal{O}(k), \mathbf{T}_{n^\mathcal{Y}}^\mathcal{Y}(k)\}$, i.e., $(n^\mathcal{O}, n^\mathcal{Y}) = \emptyset$, is

$$\Lambda_{n^\mathcal{O}n^\mathcal{Y}}(\mathbf{z}_{m(i),m(i+1),\dots,m(j)}|(n^\mathcal{O}, n^\mathcal{Y}) = \emptyset) = \prod_{s=i}^j \left[\frac{1}{V} \right]^{I(m(s))} \quad (3.34)$$

where V is the volume of the surveillance region. The cost of associating the S -tuple to $\{\mathbf{T}_{n^\mathcal{O}}^\mathcal{O}(k), \mathbf{T}_{n^\mathcal{Y}}^\mathcal{Y}(k)\}$ is given by the negative log-likelihood ratio

$$c_{m(i),m(i+1),\dots,m(j)} = -\ln \mathcal{L}_{n^\mathcal{O}n^\mathcal{Y}:\emptyset} \quad (3.35)$$

where $\mathcal{L}_{n^{\circ}n^{\mathcal{Y}}:\emptyset}$ is the the likelihood ratio given by

$$\begin{aligned}
\mathcal{L}_{n^{\circ}n^{\mathcal{Y}}:\emptyset} &= \frac{\Lambda_{n^{\circ}n^{\mathcal{Y}}}(\mathbf{z}_{m(i),m(i+1),\dots,m(j)}|(n^{\circ}, n^{\mathcal{Y}}))}{\Lambda_{n^{\circ}n^{\mathcal{Y}}}(\mathbf{z}_{m(i),m(i+1),\dots,m(j)}|(n^{\circ}, n^{\mathcal{Y}}) = \emptyset)} \\
&= \frac{\prod_{s=i}^j \left\{ [(1 - P_D)]^{1-I(m(s))} \times [P_D p(\mathbf{z}_{m(s)}(s)|\mathbf{x}_{n^{\circ}n^{\mathcal{Y}}}(s|s))]^{I(m(s))} \right\}}{\prod_{s=i}^j \left[\frac{1}{V} \right]^{I(m(s))}} \\
&= \prod_{s=i}^j \left\{ [(1 - P_D)]^{1-I(m(s))} \times [V P_D p(\mathbf{z}_{m(s)}(s)|\mathbf{x}_{n^{\circ}n^{\mathcal{Y}}}(s|s))]^{I(m(s))} \right\} \quad (3.36)
\end{aligned}$$

Whenever $\mathbf{x}_{n^{\circ}n^{\mathcal{Y}}}(s|s)$ in (3.31) is not known, it can be replaced by its predicted value $\hat{\mathbf{x}}_{n^{\circ}n^{\circ}}(s|s-1)$. Since the multi-frame association is carried out between the old track segment $\mathbf{T}_{n^{\circ}}^{\circ}(k)$, $(S-2)$ -tuple of measurements, and the young track segment $\mathbf{T}_{n^{\mathcal{Y}}}^{\mathcal{Y}}(k)$, $\hat{\mathbf{x}}_{n^{\circ}n^{\mathcal{Y}}}(s-1|s-1)$ represents the estimated state at time $s-1$ given that both old and young track segments are from the same target. At time s , the estimated state $\hat{\mathbf{x}}_{n^{\circ}n^{\mathcal{Y}}}(s-1|s-1)$ is obtained by first updating the old track segment $\mathbf{T}_{n^{\circ}}^{\circ}(k)$ to time $s-1$ using measurement tuple $\mathbf{z}_{m(i),m(i+1),\dots,m(s-1)}$, i.e., estimating $\hat{\mathbf{x}}_{n^{\circ}}(s-1|s-1)$, and then predicting $\hat{\mathbf{x}}_{n^{\circ}}(s-1|s-1)$ to time s , i.e., obtaining $\hat{\mathbf{x}}_{n^{\circ}}(s|s-1)$ which is nothing but $\hat{\mathbf{x}}_{n^{\circ}n^{\mathcal{Y}}}(s|s-1)$.

After simplification the cost (Bar-Shalom et al. 2007) of the candidate association of S -tuple of $\{m(i), m(i+1), \dots, m(j)\}$ measurements to track pair is

$$\begin{aligned}
c_{m(i),m(i+1),\dots,m(j)} &= -\ln \prod_{s=i}^j \left\{ [(1 - P_D)]^{1-I(m(s))} \cdot [V P_D p(\mathbf{z}_{m(s)}(s)|\mathbf{x}_{n^{\circ}n^{\mathcal{Y}}}(s|s))]^{I(m(s))} \right\} \\
&= \sum_{s=i}^j \left\{ [I(m(s)) - 1] \ln(1 - P_D) \right. \\
&\quad \left. - I(m(s)) \ln \frac{V P_D}{|2\pi \Sigma_{n^{\circ}n^{\mathcal{Y}}}(s)|^{\frac{1}{2}}} \right. \\
&\quad \left. + I(m(s)) \left(\frac{1}{2} D_{n^{\circ}n^{\mathcal{Y}}}^{\kappa}(s) \right) \right\} \quad (3.37)
\end{aligned}$$

where $D_{n^{\circ}n^{\mathcal{Y}}}^{\kappa}(s)$ is the squared distance and it is given by

$$D_{n^{\circ}n^{\mathcal{Y}}}(s) = [\Delta_{n^{\circ}n^{\mathcal{Y}}}(s|s-1)]' [\Sigma_{n^{\circ}n^{\mathcal{Y}}}(s)]^{-1} [\Delta_{n^{\circ}n^{\mathcal{Y}}}(s|s-1)]. \quad (3.38)$$

with

$$\Delta_{n^{\circ}n^{\mathcal{Y}}}(s|s-1) = \mathbf{z}_{m(s)}(s) - \hat{\mathbf{z}}_{n^{\circ}n^{\mathcal{Y}}}(s|s-1) \quad (3.39)$$

Input: Broken track segments at time k

Output: Stitched tracks at time k

- 1: Group the track segments into old and young track lists (do this only once at the beginning) as discussed in subsection 3.2.1.
- 2: Update old and young track lists as discussed in subsection 3.2.1.
- 3: Perform smoothing on all the tracks of young track list over a fixed period as discussed in subsection 3.2.3.
- 4: Obtain set of all combinations of candidate track pairs $\Phi^T(k)$ as in (3.3).
- 5: Obtain feasible candidate track pair set $\Phi_f^T(k)$ as given in (3.11).
- 6: Obtain the set of all possible combinations of i 's $N^O(k)$ -tuples and j 's $N^Y(k)$ -tuples $\Psi^{ij}(k)$ as given in (3.12).
- 7: Obtain model parameters as discussed in subsection 3.3.1 for each pair of tracks pertaining to $\psi_l^{ij}(k)$.
- 8: Formulate general multi-frame assignment problem by picking a common i and j using (3.28) and (3.29), respectively.
- 9: Obtain the measurement set \mathbf{Z}^{ij} , which includes both unassociated and released measurement, as given in (3.30).
- 10: For every $\psi_l^{ij}(k)$ obtain corresponding total cost $C_{S-D}(\psi_l^{ij}(k))$ by solving (3.42).
- 11: Obtain $\hat{\psi}_{S-D}^{ij}(k)$ by solving (3.46).
- 12: Perform the track stitching between old and young track segments according to the best solution $\hat{\psi}_{S-D}^{ij}(k)$.
- 13: **return** Stitched tracks.

Figure 3.4: An algorithm for proposed S -D assignment based TSA

and

$$\Sigma_{n^O n^Y}(s) = \mathbf{R}(s) + [\mathbf{H}(s|s-1)]\mathbf{P}_{n^O n^Y}(s|s-1)[\mathbf{H}(s|s-1)]'. \quad (3.40)$$

In the above equation the term $\mathbf{H}(s|s-1)$ is the Jacobian matrix (Bar-Shalom et al. 2004) at $\hat{\mathbf{x}}_{n^O n^Y}(s|s-1)$.

Let us define the binary association variable as

$$a_{m(i),m(i+1),\dots,m(j)} = \begin{cases} 1 & \text{if the } S\text{-tuple } \mathbf{z}_{m(i),m(i+1),\dots,m(j)} \text{ is associated with a} \\ & \text{candidate target} \\ 0 & \text{otherwise.} \end{cases} \quad (3.41)$$

The goal is to find the most likely set of S -tuples such that each track is allocated with at most a measurement from each measurement list and each measurement is assigned to a track or declared as false alarm. This is formulated as a generalized S -D assignment problem:

$$\min_{a_{m(i),m(i+1),\dots,m(j)}} \sum_{m(i)=0}^{\mathcal{M}(i)} \sum_{m(i+1)=0}^{\mathcal{M}(i+1)} \cdots \sum_{m(j)=0}^{\mathcal{M}(j)} a_{m(i),m(i+1),\dots,m(j)} C_{m(i),m(i+1),\dots,m(j)} \quad (3.42)$$

subject to

$$\sum_{m(i+1)=0}^{\mathcal{M}(i+1)} \sum_{m(i+2)=0}^{\mathcal{M}(i+2)} \cdots \sum_{m(j)=0}^{\mathcal{M}(j)} a_{m(i),m(i+1),\dots,m(j)} = 1, \quad m(i) = 1, 2, \dots, \mathcal{M}(i) \quad (3.43)$$

$$\sum_{m(i)=0}^{\mathcal{M}(i)} \sum_{m(i+2)=0}^{\mathcal{M}(i+2)} \cdots \sum_{m(j)=0}^{\mathcal{M}(j)} a_{m(i),m(i+1),\dots,m(j)} = 1, \quad m(i+1) = 1, 2, \dots, \mathcal{M}(i+1) \quad (3.44)$$

$\vdots \qquad \qquad \qquad \vdots \qquad \qquad \qquad \vdots$

$$\sum_{m(i)=0}^{\mathcal{M}(i)} \sum_{m(i+1)=0}^{\mathcal{M}(i+1)} \cdots \sum_{m(j-1)=0}^{\mathcal{M}(j-1)} a_{m(i),m(i+1),\dots,m(j)} = 1, \quad m(j) = 1, 2, \dots, \mathcal{M}(j) \quad (3.45)$$

where a is a binary variable, i.e., $a \in \{0, 1\}$. Note that there are no constraints on the dummy measurements. Using dummy measurements, the association is performed over a complete set of S -tuples for a given $\boldsymbol{\psi}_l^{ij}(k)$. Thus, if a target was missed in the measurement list s , the corresponding S -tuple has $m(s) = 0$.

Let $C_{S-D}(\boldsymbol{\psi}_l^{ij}(k))$ represent the total minimum cost corresponding to (3.42) for a given $\boldsymbol{\psi}_l^{ij}(k)$. Now, one needs to solve for a value of $\boldsymbol{\psi}_l^{ij}(k)$ that would minimize the cost $C_{S-D}(\boldsymbol{\psi}_l^{ij}(k))$ as follows:

$$\hat{\boldsymbol{\psi}}_{S-D}^{ij}(k) = \arg \min_{\boldsymbol{\psi}_l^{ij}(k) \in \boldsymbol{\Psi}^{ij}(k)} C_{S-D}(\boldsymbol{\psi}_l^{ij}(k)). \quad (3.46)$$

The TSA solution S -tuples corresponding to this $\hat{\boldsymbol{\psi}}_{S-D}^{ij}(k)$ would be optimal. Further, the step by step procedure for the implementation of this proposed S -D assignment based algorithm can be found in Figure 3.4.

3.3 MODEL PARAMETER ESTIMATION

It is reasonable to assume that the motion of the target pertaining to a given track couple follows one of the following cases:

1. CV model throughout the breakage period
2. CT model, with turning rate ω , throughout the breakage period
3. Combination of CV model and CT model during breakage period. This combination could be one of the following possibilities
 - (a) CV model followed by CT model

- (b) CV model followed by CT model again followed by CV model
- (c) CT model followed by CV model.

That is, the target can undergo at most one turn during the breakage period, which is a reasonable assumption. We need to estimate the model parameters, i.e., the turning rate ω , as well as the times at which the turn starts and ends. Depending upon the computational requirements, one can decide to go either with first two cases or with all three possible cases. Considering the first two cases is simpler at the expense of tracking accuracy.

3.3.1 S-D Assignment Case

In this case, the goal is to estimate the model parameter ω and the times the turn starts and ends for a given S -tuple of measurements pertaining to the track couple $\{\mathbf{T}_{n^{\mathcal{O}}}(k), \mathbf{T}_{n^{\mathcal{Y}}}(k)\}$ with the corresponding time stamp pair $(i_{n^{\mathcal{O}}}, j_{n^{\mathcal{Y}}})$. The $(i_{n^{\mathcal{O}}} - j_{n^{\mathcal{Y}}})$ -tuple of measurements of this track couple is obtained from the corresponding S -tuple of measurements by retaining the measurements in the interval $(i_{n^{\mathcal{O}}} + 1, j_{n^{\mathcal{Y}}})$. This retained measurement tuple is

$$\mathbf{z}_{m(i_{n^{\mathcal{O}}}+1), m(i_{n^{\mathcal{O}}}+2), \dots, m(j_{n^{\mathcal{Y}}})} = \{\mathbf{z}_{m(i_{n^{\mathcal{O}}}+1)}, \dots, \mathbf{z}_{m(k_{t_s})}, \dots, \mathbf{z}_{m(k_{t_e})}, \dots, \mathbf{z}_{m(j_{n^{\mathcal{Y}}})}\} \quad (3.47)$$

and its corresponding state sequence is

$$\mathbf{X}_{i_{n^{\mathcal{O}}}+1, i_{n^{\mathcal{O}}}+2, \dots, j_{n^{\mathcal{Y}}}} = \{\mathbf{x}_{n^{\mathcal{O}}}(i_{n^{\mathcal{O}}} + 1), \dots, \mathbf{x}_{n^{\mathcal{O}}}(k_{t_s}), \dots, \mathbf{x}_{n^{\mathcal{O}}}(k_{t_e}), \dots, \mathbf{x}_{n^{\mathcal{Y}}}(j_{n^{\mathcal{Y}}})\}, \quad (3.48)$$

where k_{t_s} and k_{t_e} are the turning start and end times, respectively. The likelihood that the measurement tuple $\mathbf{z}_{m(i_{n^{\mathcal{O}}}+1), m(i_{n^{\mathcal{O}}}+2), \dots, m(j_{n^{\mathcal{Y}}})}$ originated from a target whose motion follows one of the three cases discussed above is

$$\begin{aligned} & \Lambda_{n^{\mathcal{O}} n^{\mathcal{Y}}}(\mathbf{z}_{m(i_{n^{\mathcal{O}}}+1), m(i_{n^{\mathcal{O}}}+2), \dots, m(j_{n^{\mathcal{Y}}})} | k_{t_s}, k_{t_e}, \omega, \mathbf{X}_{i_{n^{\mathcal{O}}}+1, i_{n^{\mathcal{O}}}+2, \dots, j_{n^{\mathcal{Y}}}}) \\ &= p\left(k_{t_s}, k_{t_e}, \mathbf{X}_{i_{n^{\mathcal{O}}}+1, i_{n^{\mathcal{O}}}+2, \dots, j_{n^{\mathcal{Y}}}}, \omega, \mathbf{z}_{m(i_{n^{\mathcal{O}}}+1), m(i_{n^{\mathcal{O}}}+2), \dots, m(j_{n^{\mathcal{Y}}})}\right). \end{aligned} \quad (3.49)$$

Using this likelihood function k_{t_s} , k_{t_e} , and ω are estimated by maximizing the log likelihood function, i.e.,

$$\begin{aligned} & (\hat{k}_{t_s}, \hat{k}_{t_e}, \hat{\omega}) = \\ & \arg \max_{\{k_{t_s}, k_{t_e}, \omega\}} \ln \Lambda_{n^{\mathcal{O}} n^{\mathcal{Y}}}(\mathbf{z}_{m(i_{n^{\mathcal{O}}}+1), m(i_{n^{\mathcal{O}}}+2), \dots, m(j_{n^{\mathcal{Y}}})} | k_{t_s}, k_{t_e}, \omega, \mathbf{X}_{i_{n^{\mathcal{O}}}+1, i_{n^{\mathcal{O}}}+2, \dots, j_{n^{\mathcal{Y}}}}), \end{aligned} \quad (3.50)$$

where $|\omega| \leq \omega_{\max}$ and $i_{n^{\mathcal{O}}}^{\mathcal{O}} \leq (k_{t_s} \leq k_{t_e}) \leq j_{n^{\mathcal{Y}}}^{\mathcal{Y}}$. Here, $(k_{t_s} = k_{t_e})$ refers to the first case, $(k_{t_s} = i_{n^{\mathcal{O}}}^{\mathcal{O}}) < (k_{t_e} = j_{n^{\mathcal{Y}}}^{\mathcal{Y}})$ refers to the second case, and the rest refer to the third case. An evaluation of the likelihood function $\Lambda_{n^{\mathcal{O}n^{\mathcal{Y}}}}(\cdot)$ in (3.49) is performed (Zhang et al. 2015) as follows:

$$\begin{aligned}
& \Lambda_{n^{\mathcal{O}n^{\mathcal{Y}}}}(\mathbf{z}_{m(i_{n^{\mathcal{O}}}^{\mathcal{O}}+1), m(i_{n^{\mathcal{O}}}^{\mathcal{O}}+2), \dots, m(j_{n^{\mathcal{Y}}}^{\mathcal{Y}})}) | k_{t_s}, k_{t_e}, \omega, \mathbf{X}_{i_{n^{\mathcal{O}}}^{\mathcal{O}}+1, i_{n^{\mathcal{O}}}^{\mathcal{O}}+2, \dots, j_{n^{\mathcal{Y}}}^{\mathcal{Y}}})} \\
&= p\left(k_{t_s}, k_{t_e}, \mathbf{X}_{i_{n^{\mathcal{O}}}^{\mathcal{O}}+1, i_{n^{\mathcal{O}}}^{\mathcal{O}}+2, \dots, j_{n^{\mathcal{Y}}}^{\mathcal{Y}}}, \omega, \mathbf{z}_{m(i_{n^{\mathcal{O}}}^{\mathcal{O}}+1), m(i_{n^{\mathcal{O}}}^{\mathcal{O}}+2), \dots, m(j_{n^{\mathcal{Y}}}^{\mathcal{Y}})})}\right) \\
&= \prod_{k_1=i_{n^{\mathcal{O}}}^{\mathcal{O}}+1}^{k_{t_s}} \prod_{k_1=k_{t_s}+1}^{k_{t_e}} \prod_{k_1=k_{t_e}+1}^{j_{n^{\mathcal{Y}}}^{\mathcal{Y}}} p_{k_1}\left(k_{t_s}, k_{t_e}, \mathbf{x}_{n^{\mathcal{O}n^{\mathcal{Y}}}}(k_1) | \omega, \mathbf{z}_{m(i_{n^{\mathcal{O}}}^{\mathcal{O}}+1), m(i_{n^{\mathcal{O}}}^{\mathcal{O}}+2), \dots, m(j_{n^{\mathcal{Y}}}^{\mathcal{Y}})})\right) \\
&= \frac{1}{\dot{c}} \exp\left\{-\frac{1}{2}\left(\sum_{k_1=i_{n^{\mathcal{O}}}^{\mathcal{O}}+1}^{k_{t_s}} [\tilde{\mathbf{z}}^{\text{CV}}(k_1|k_1-1)]' [\boldsymbol{\Sigma}^{\text{CV}}(k_1|k_1-1)]^{-1} [\tilde{\mathbf{z}}^{\text{CV}}(k_1|k_1-1)] \right. \right. \\
&\quad + \sum_{k_1=k_{t_s}+1}^{k_{t_e}} [\tilde{\mathbf{z}}^{\text{CT}}(k_1|k_1-1)]' [\boldsymbol{\Sigma}^{\text{CT}}(k_1|k_1-1)]^{-1} [\tilde{\mathbf{z}}^{\text{CT}}(k_1|k_1-1)] \\
&\quad \left. \left. + \sum_{k_1=k_{t_e}+1}^{j_{n^{\mathcal{Y}}}^{\mathcal{Y}}} [\tilde{\mathbf{z}}^{\text{CV}}(k_1|k_1-1)]' [\boldsymbol{\Sigma}^{\text{CV}}(k_1|k_1-1)]^{-1} [\tilde{\mathbf{z}}^{\text{CV}}(k_1|k_1-1)]\right)\right\} \tag{3.51}
\end{aligned}$$

where

$$\tilde{\mathbf{z}}^{\text{CV}}(k_1|k_1-1) = \mathbf{z}(k_1) - h[\hat{\mathbf{x}}^{\text{CV}}(k_1|k_1-1)] \tag{3.52}$$

$$\tilde{\mathbf{z}}^{\text{CT}}(k_1|k_1-1) = \mathbf{z}(k_1) - h[\hat{\mathbf{x}}^{\text{CT}}(k_1|k_1-1)] \tag{3.53}$$

$$\boldsymbol{\Sigma}^{\text{CV}}(k_1|k_1-1) = \mathbf{R}(k_1) + [\mathbf{H}(k_1|k_1-1)] \mathbf{P}^{\text{CV}}(k_1|k_1-1) [\mathbf{H}(k_1|k_1-1)]' \tag{3.54}$$

$$\boldsymbol{\Sigma}^{\text{CT}}(k_1|k_1-1) = \mathbf{R}(k_1) + [\mathbf{H}(k_1|k_1-1)] \mathbf{P}^{\text{CT}}(k_1|k_1-1) [\mathbf{H}(k_1|k_1-1)]'. \tag{3.55}$$

The term $\mathbf{H}(k_1|k_1-1)$ is the Jacobian matrix (Bar-Shalom et al. 2004) at $\hat{\mathbf{x}}(k_1|k_1-1)$ and \dot{c} is a constant, which is irrelevant to the maximization.

3.3.2 2-D Assignment Case

This case is the same as the S -D assignment case except for the fact that no measurement information is used. For a given track pair $\{\mathbf{T}_{n^{\mathcal{O}}}^{\mathcal{O}}(k), \mathbf{T}_{n^{\mathcal{Y}}}^{\mathcal{Y}}(k)\}$, the goal is

to find the turn rate ω , its starting time k_{t_s} , and its ending time k_{t_e} . Similar to the S - D assignment case, here too one can assume that the target motion follows the constant velocity model before and after turning. Let $\hat{\mathbf{x}}_{n^{\mathcal{O}}}(j_{n^{\mathcal{Y}}}^{\mathcal{Y}}|i_{n^{\mathcal{O}}}^{\mathcal{O}}, k_{t_s}, k_{t_e}, \omega)$ and $\mathbf{P}_{n^{\mathcal{O}}}(j_{n^{\mathcal{Y}}}^{\mathcal{Y}}|i_{n^{\mathcal{O}}}^{\mathcal{O}}, k_{t_s}, k_{t_e}, \omega)$ be the predicted state and its covariance of old track segment $n^{\mathcal{O}}$ at time $j_{n^{\mathcal{Y}}}^{\mathcal{Y}}$, respectively; let $\hat{\mathbf{x}}_{n^{\mathcal{Y}}}(j_{n^{\mathcal{Y}}}^{\mathcal{Y}})$ and $\mathbf{P}_{n^{\mathcal{Y}}}(j_{n^{\mathcal{Y}}}^{\mathcal{Y}})$ be the state and its covariance of the young track segment $n^{\mathcal{Y}}$ at the same time $j_{n^{\mathcal{Y}}}^{\mathcal{Y}}$, respectively. The difference between these two estimates is

$$\Delta_{n^{\mathcal{O}}n^{\mathcal{Y}}}(j_{n^{\mathcal{Y}}}^{\mathcal{Y}}|i_{n^{\mathcal{O}}}^{\mathcal{O}}) = \hat{\mathbf{x}}_{n^{\mathcal{O}}}(j_{n^{\mathcal{Y}}}^{\mathcal{Y}}|i_{n^{\mathcal{O}}}^{\mathcal{O}}, k_{t_s}, k_{t_e}, \omega) - \hat{\mathbf{x}}_{n^{\mathcal{Y}}}(j_{n^{\mathcal{Y}}}^{\mathcal{Y}}) \quad (3.56)$$

with corresponding covariance

$$\Sigma_{n^{\mathcal{O}}n^{\mathcal{Y}}}(j_{n^{\mathcal{Y}}}^{\mathcal{Y}}|i_{n^{\mathcal{O}}}^{\mathcal{O}}) = \mathbf{P}_{n^{\mathcal{O}}}(j_{n^{\mathcal{Y}}}^{\mathcal{Y}}|i_{n^{\mathcal{O}}}^{\mathcal{O}}, k_{t_s}, k_{t_e}, \omega) + \mathbf{P}_{n^{\mathcal{Y}}}(j_{n^{\mathcal{Y}}}^{\mathcal{Y}}). \quad (3.57)$$

Now, $(k_{t_s}, k_{t_e}, \omega)$ is estimated as

$$(\hat{k}_{t_s}, \hat{k}_{t_e}, \hat{\omega}) = \arg \min_{\{k_{t_s}, k_{t_e}, \omega\}} [\Delta_{n^{\mathcal{O}}n^{\mathcal{Y}}}(j_{n^{\mathcal{Y}}}^{\mathcal{Y}}|i_{n^{\mathcal{O}}}^{\mathcal{O}})]' [\Sigma_{n^{\mathcal{O}}n^{\mathcal{Y}}}(j_{n^{\mathcal{Y}}}^{\mathcal{Y}}|i_{n^{\mathcal{O}}}^{\mathcal{O}})]^{-1} [\Delta_{n^{\mathcal{O}}n^{\mathcal{Y}}}(j_{n^{\mathcal{Y}}}^{\mathcal{Y}}|i_{n^{\mathcal{O}}}^{\mathcal{O}})]. \quad (3.58)$$

The solution $(\hat{k}_{t_s}, \hat{k}_{t_e}, \hat{\omega})$ is obtained from the following predetermined sets

$$k_{t_s} \in \{i_{n^{\mathcal{O}}}^{\mathcal{O}}, i_{n^{\mathcal{O}}}^{\mathcal{O}} + 1, \dots, j_{n^{\mathcal{Y}}}^{\mathcal{Y}}\} \quad (3.59)$$

$$k_{t_e} \in \{i_{n^{\mathcal{O}}}^{\mathcal{O}}, i_{n^{\mathcal{O}}}^{\mathcal{O}} + 1, \dots, j_{n^{\mathcal{Y}}}^{\mathcal{Y}}\} \quad (3.60)$$

$$\omega \in \{-\omega_{\max}, -\omega_{\max} + \delta\omega, -\omega_{\max} + 2\delta\omega, \dots, \omega_{\max}\} \quad (3.61)$$

subject to $k_{t_s} \leq k_{t_e}$. In (3.61), ω_{\max} and $\delta\omega$ represent the maximum turn rate and the step size, respectively. The predicted state $\hat{\mathbf{x}}_{n^{\mathcal{O}}}(j_{n^{\mathcal{Y}}}^{\mathcal{Y}}|i_{n^{\mathcal{O}}}^{\mathcal{O}}, k_{t_s}, k_{t_e}, \omega)$ is obtained as

$$\hat{\mathbf{x}}_{n^{\mathcal{O}}}(k_1|k_1 - 1, k_{t_s}, k_{t_e}, \omega) = \begin{cases} \mathbf{F}^1(k_1)\hat{\mathbf{x}}_{n^{\mathcal{O}}}(k_1 - 1) & \text{if } k_1 \leq k_{t_s} \text{ or } k_1 > k_{t_e} \\ \mathbf{F}^2(k_1)\hat{\mathbf{x}}_{n^{\mathcal{O}}}(k_1 - 1) & \text{otherwise} \end{cases} \quad (3.62)$$

with the corresponding covariance being

$$\begin{aligned} & \mathbf{P}_{n^{\mathcal{O}}}(k_1|k_1 - 1, k_{t_s}, k_{t_e}, \omega) \\ &= \begin{cases} [\mathbf{F}^1(k_1)]\mathbf{P}_{n^{\mathcal{O}}}(k_1 - 1)[\mathbf{F}^1(k_1)]' + \mathbf{\Gamma}(k_1)\mathbf{Q}(k_1)\mathbf{\Gamma}(k_1)' & \text{if } k_1 \leq k_{t_s} \text{ or } k_1 > k_{t_e} \\ [\mathbf{F}^2(k_1)]\mathbf{P}_{n^{\mathcal{O}}}(k_1 - 1)[\mathbf{F}^2(k_1)]' + \mathbf{\Gamma}(k_1)\mathbf{Q}(k_1)\mathbf{\Gamma}(k_1)' & \text{otherwise} \end{cases} \end{aligned} \quad (3.63)$$

for $k_1 = i_{n^{\mathcal{O}}}^{\mathcal{O}} + 1, i_{n^{\mathcal{O}}}^{\mathcal{O}} + 2, \dots, j_{n^{\mathcal{Y}}}^{\mathcal{Y}}$.

3.4 RESULTS AND DISCUSSIONS

3.4.1 Target Simulation

For the evaluation of the proposed algorithms, targets with the following design parameters being common for all scenarios are considered:

1. sampling interval, $\Delta(k) = 1\text{s}$;
2. process noise covariance matrix, $\mathbf{Q}(k) = \begin{pmatrix} 0.4\text{m}^2 & 0 \\ 0 & 0.4\text{m}^2 \end{pmatrix}$;
3. measurement vector consisting of range and azimuth with standard deviations $\sigma_r = 10\text{m}$ and $\sigma_\phi = 0.01 \text{ rad.}$, respectively.

While tracking, the single point track initialization method (Yeom et al. 2004, Musicki and Song 2013) with maximum velocity, $V_{\max} = 50 \text{ m/s}$ for track initialization and a nearest neighbor (NN) (Bar-Shalom et al. 2011) association filter with constant velocity model for filtering are used.

Simulation is performed using MATLAB R2015a on a computer with 64 GB RAM and Intel (R) Xeon(R) processor.

3.4.2 TSA Parameters

To implement the TSA algorithms, the following conditions are considered:

- Eligibility criteria: At time k , all confirmed tracks are eligible to be considered for association.
- Model parameters: $B_{i_{\max}} = 5$, $B_{j_{\max}} = 0$, $|\omega_{\max}| \leq 15^\circ/\text{s}$, $\delta\omega = 0.1^\circ/\text{s}$.
- Look-back duration: $0 \leq B \leq 30$.
- Smoothing: The young track is smoothed before it is considered for an association. Ten scans from the beginning of the young track segment are considered for smoothing.
- Turning duration: It is assumed that a target turn lasts at least four scans.
- Probability of detection: P_D^b is the probability of target detection during the breakage period (i.e., P_D^b is applicable to the target turning duration).

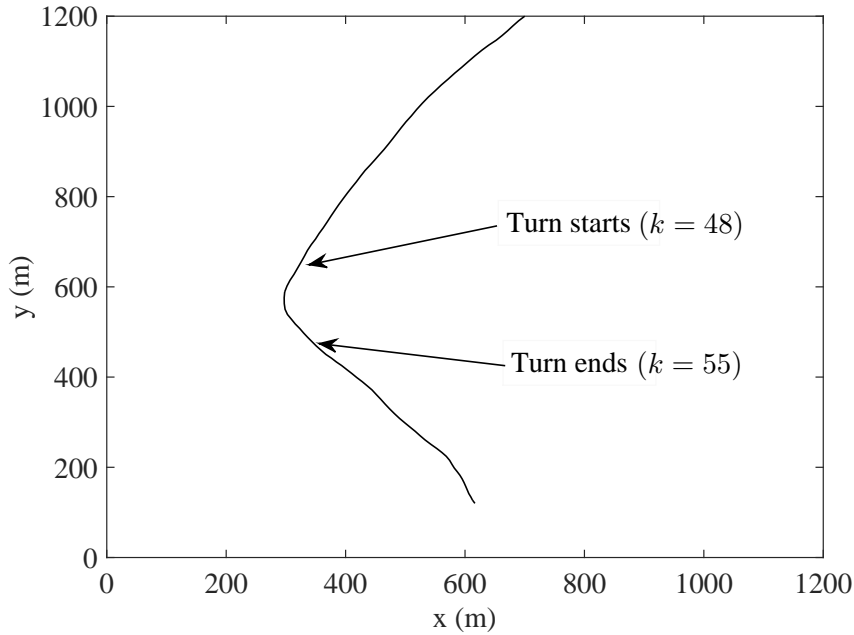


Figure 3.5: Target trajectory ($\omega = 10^\circ/\text{s}$)

- *S-D* assignment: To reduce the computational load, for any given track pair $\{\mathbf{T}_{no}^{\mathcal{O}}(k), \mathbf{T}_{ny}^{\mathcal{Y}}(k)\}$, the optimal model parameters are obtained the same way as in the 2-D case, and then the measurement tuple corresponding to this optimal model parameters is obtained.

3.4.3 Single Target Scenario

In this scenario, a single target with initial state $(700\text{m} \quad -10 \text{ m/s} \quad 1200\text{m} \quad -10 \text{ m/s})'$ taking a turn during the interval 48–55 is generated as shown in Figure 3.5. Since tracking is performed with the constant CV model, track breakages occur around the turning interval. To associate these broken tracks under different clutter and turning rate scenarios, all three TSA algorithms (i.e., existing 2-D TSA (Yeom et al. 2004), proposed 2-D TSA, and proposed *S-D* TSA) are applied. The resulting stitched tracks are associated with the ground truth and the decision is declared as a correct decision if all the broken tracks originating from the same target are stitched (Drummond 1997).

A With no clutter

Figure 3.6 shows the broken tracks and results after stitching by the TSA algorithms. Stitching results are better for the proposed algorithms as they look for a possible target turn during stitching period. Even though the existing TSA algorithm (Yeom

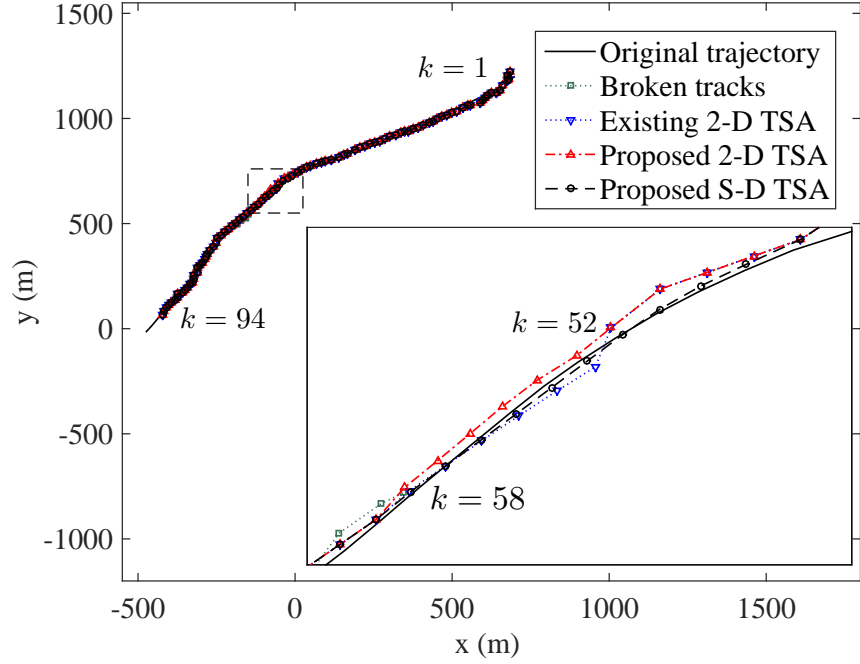


Figure 3.6: Track stitching ($P_D^b = 0.3$, $B_i = 5$, $\lambda = 0\text{m}^{-2}$, $\omega = 4^\circ/\text{s}$, $k_{n\mathcal{O},e}^{\mathcal{O}} < k_{n\mathcal{Y},s}^{\mathcal{Y}}$) et al. 2004) does not look for any possible target turn, it still manages to stitch broken tracks correctly because of the combination of low target turning rate, $\omega = 4^\circ/\text{s}$, and low process noise.

Table 3.1: Percentage of Correct Association Decisions ($B = 15$, $\omega = 4^\circ/\text{s}$, $\lambda = 0\text{m}^{-2}$, 100 Monte Carlo runs)

		% of Correct TSA Decisions												
		Existing 2-D TSA <small>(Yeom et al. 2004)</small>	Proposed 2-D TSA						Proposed S-D TSA					
			B_i (number of frames going backward along old track)											
			0	1	2	3	4	5	0	1	2	3	4	5
P_D^b	0.8	33	47	52	67	81	86	95	48	57	76	96	96	96
	0.6	41	74	74	78	87	91	96	76	78	83	83	92	98
	0.3	57	86	86	88	89	90	93	90	93	94	94	94	94
	0.1	54	86	87	88	90	92	92	86	88	90	92	92	92
	0.0	50	86	86	86	87	87	87	86	86	86	87	87	87
Normalized CPU Time		1	5	10	17	21	31	35	10	17	31	45	61	75

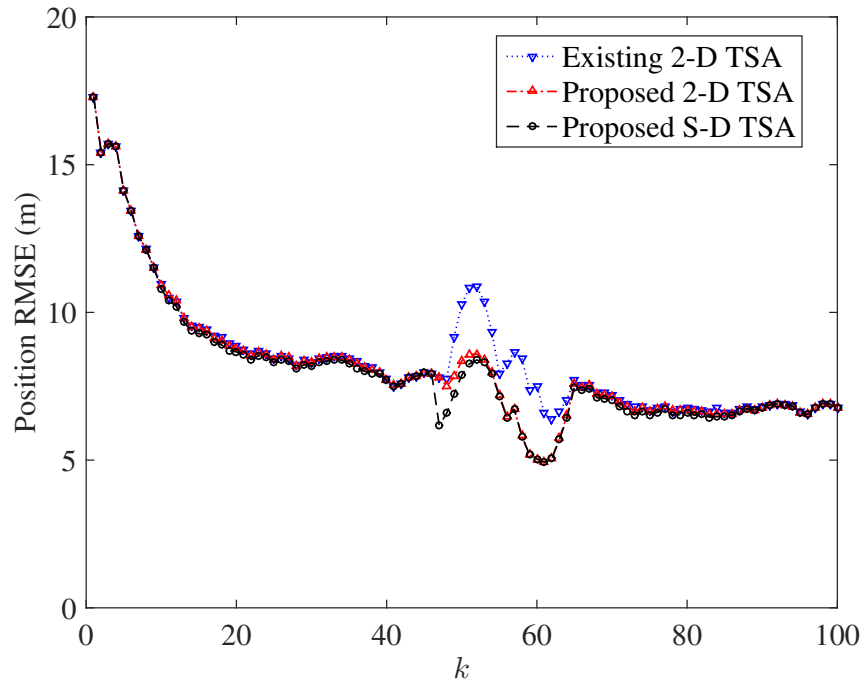
Tables 3.1 and 3.2 show the percentage of correct association decisions and number of continuous tracks, respectively, when there is no clutter. It can be seen that the

Table 3.2: Number of Continuous Tracks
($B = 15$, $\omega = 4^\circ/\text{s}$, $\lambda = 0\text{m}^{-2}$, 100 Monte Carlo runs)

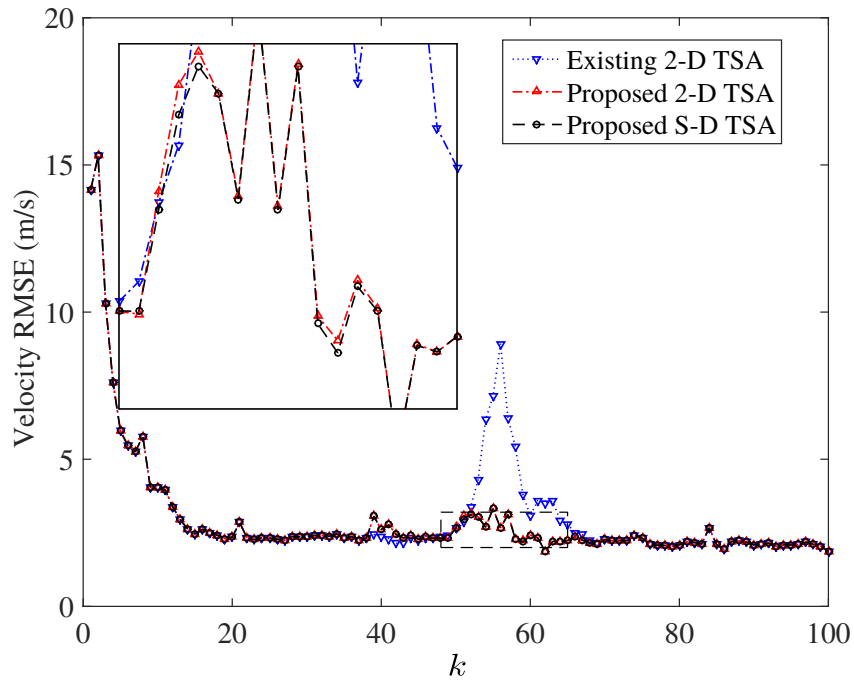
		Number of Continuous Tracks												
		Existing 2-D TSA <small>(Yeom et al. 2004)</small>	Proposed 2-D TSA						Proposed <i>S</i> -D TSA					
			B_i (number of frames going backward along old track)											
			0	1	2	3	4	5	0	1	2	3	4	5
P_D^b	0.8	86	89	90	93	96	97	99	89	91	95	99	99	99
	0.6	73	88	88	90	94	96	98	89	90	92	92	96	99
	0.3	60	87	87	89	90	91	93	90	93	94	94	94	94
	0.1	54	86	87	88	90	92	92	86	88	90	92	92	92
	0.0	50	86	86	86	87	87	87	86	86	86	87	87	87

proposed algorithm performs better compared to the existing ones but with an extra computational cost. Notice that, when P_D^b is 0, 0.1 or 0.3, all the three algorithms — existing TSA algorithm (Yeom et al. 2004), proposed 2-D TSA algorithm, and proposed *S*-D TSA algorithm — show correct association decisions that are even better than higher P_D^b cases. This happens due to the following reason: an increase in the P_D^b reduces the track breakage rate and breaking period.

In the higher P_D^b cases, when a track gets terminated, it is highly likely that its corresponding new track gets initialized within the next few scans or even before the termination of old track segment. The existing TSA algorithm (Yeom et al. 2004) fails to stitch tracks whenever the young track is initialized before the termination of its corresponding old track segment and, in addition, it uses only the CV model to stitch the tracks whenever the young track segment initialization time is greater than or equal to the old track termination. Consequently, the existing TSA algorithm (Yeom et al. 2004) shows results that are inferior to the proposed algorithms as shown in Tables 3.1, 3.3, and 3.5. If the breakage period is less than the assumed minimum turn duration (which is usual in the higher P_D^b cases), the proposed algorithms consider only the CV model to bridge the track segments and hence the percentage of correct association decisions decreases as P_D^b increases. However, the increase in breakage duration is achieved by going backward along old track segment so as to use combination of CV and CT models and hence higher P_D^b cases show rapid increment



(a) Position



(b) Velocity

Figure 3.7: Single target RMSE ($P_D^b = 0.3$, $B_i = 3$, $\lambda = 0\text{m}^{-2}$, $\omega = 4^\circ/\text{s}$) in correct association decision making rate as B_i increases. As a result the proposed algorithms can stitch tracks even if the young track segment is initialized before the termination of its corresponding old track segment.

Position and velocity root-mean-squared-error (RMSE) values are compared in Figure 3.7. The proposed *S-D* TSA algorithm shows improvement over the other two algorithms. This is because of the utilization of available measurement information during breakage period. Even when there are no unassociated measurements during breakage period, the proposed *S-D* TSA algorithm utilizes the released measurements and hence performs better than the proposed 2-D TSA algorithm.

B With low clutter

Figures 3.8 and 3.9 show the RMSE plot corresponding to $B_i = 0$ and $B_i = 5$, respectively, for low clutter $\lambda = 1 \times 10^{-6} \text{m}^{-2}$. The proposed *S-D* TSA algorithm performs better with $B_i = 5$ than with $B_i = 0$. This is because when $B_i = 0$, no measurement is released from the old track segment, i.e., the possibility of a false measurement association, which might have resulted in track termination, is not explored. This results in a large estimation error. When $B_i = 5$, measurements associated during the last 5 scans are released from the old track segment by going backward, and filtering is performed afresh to explore the possibility of a false measurement association. All false measurements were omitted, resulting in improvements in both RMSE and the percentage of correct decisions being made. This is possible because of the known destination (starting point of a young track segment). A sudden decrease in position RMSE is due to the smoothing of the young track segment. Existing 2-D TSA algorithm (Yeom et al. 2004) can rarely make the right decision because of the combination of high turning rate and clutter, as shown in Tables 3.3 and 3.4.

C With high clutter

The increase in the rate of false alarms leads to an increase in the number of broken tracks. For this reason, there is a reduction in performance with the proposed 2-D TSA algorithm. In Tables 3.5 and 3.6 readers can observe that there is significant improvement in the performance of the proposed algorithms, as B_i and P_D^b increase. In particular, the *S-D* TSA algorithm shows greater improvement.

Table 3.3: Percentage of Correct Association Decisions
($B = 15, \omega = 10^\circ/\text{s}, \lambda = 1 \times 10^{-6}\text{m}^{-2}, 100$ Monte Carlo runs)

		% of Correct TSA Decisions												
		Existing 2-D TSA <small>(Yeom et al. 2004)</small>	Proposed 2-D TSA						Proposed <i>S</i> -D TSA					
			B_i (number of frames going backward along old track)											
			0	1	2	3	4	5	0	1	2	3	4	5
P_D^b	0.8	04	55	57	59	62	66	71	59	62	70	76	84	95
	0.6	02	69	72	76	78	78	79	69	74	76	77	84	91
	0.3	00	75	77	78	78	78	78	75	77	79	83	91	93
	0.1	00	77	79	80	80	80	81	77	79	81	83	83	84
	0.0	00	76	78	78	78	79	79	76	79	80	81	81	81
Normalized CPU Time		1	5	8	16	21	30	35	10	18	34	48	69	81

Table 3.4: Number of Continuous Tracks
($B = 15, \omega = 10^\circ/\text{s}, \lambda = 1 \times 10^{-6}\text{m}^{-2}, 100$ Monte Carlo runs)

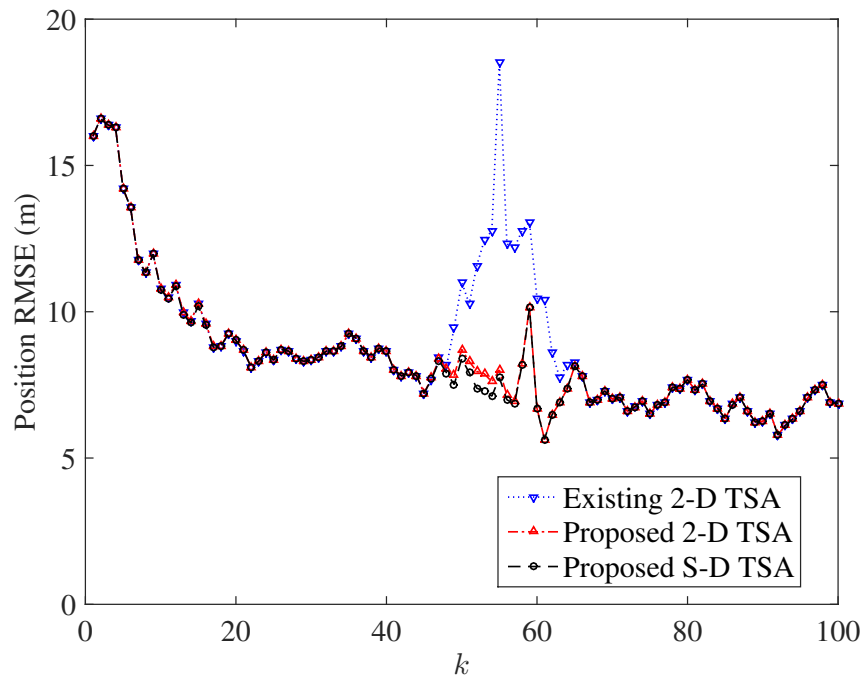
		Number of Continuous Tracks												
		Existing 2-D TSA <small>(Yeom et al. 2004)</small>	Proposed 2-D TSA						Proposed <i>S</i> -D TSA					
			B_i (number of frames going backward along old track)											
			0	1	2	3	4	5	0	1	2	3	4	5
P_D^b	0.8	10	58	60	62	65	68	73	62	65	72	78	85	96
	0.6	03	70	73	77	80	80	81	70	76	78	79	85	92
	0.3	00	75	77	78	78	78	78	75	77	79	83	91	93
	0.1	00	77	79	80	80	80	81	77	79	81	83	83	84
	0.0	00	76	78	78	78	79	79	76	79	80	81	81	81

Table 3.5: Percentage of Correct Association Decisions
($B = 15$, $\omega = 10^\circ/\text{s}$, $\lambda = 1 \times 10^{-4}\text{m}^{-2}$, 100 Monte Carlo runs)

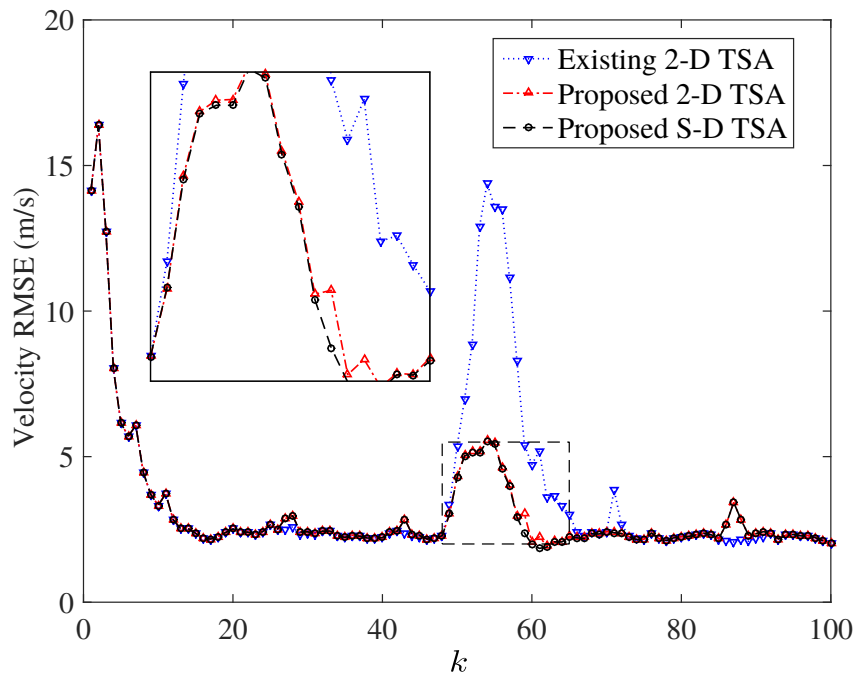
		% of Correct TSA Decisions												
		Existing 2-D TSA <small>(Yeom et al. 2004)</small>	Proposed 2-D TSA						Proposed <i>S</i> -D TSA					
			B_i (number of frames going backward along old track)											
			0	1	2	3	4	5	0	1	2	3	4	5
P_D^b	0.8	02	41	46	49	56	58	62	41	53	64	70	81	95
	0.6	00	57	59	60	61	61	62	57	62	69	71	72	75
	0.3	00	69	71	71	71	71	71	69	71	77	81	81	84
	0.1	00	71	72	72	73	73	75	72	73	73	73	73	73
	0.0	00	68	68	69	69	69	69	68	70	70	70	70	70
Normalized CPU Time		1	5	9	16	22	30	33	14	23	39	52	76	97

Table 3.6: Number of Continuous Tracks
($B = 15$, $\omega = 10^\circ/\text{s}$, $\lambda = 1 \times 10^{-4}\text{m}^{-2}$, 100 Monte Carlo runs)

		Number of Continuous Tracks												
		Existing 2-D TSA <small>(Yeom et al. 2004)</small>	Proposed 2-D TSA						Proposed <i>S</i> -D TSA					
			B_i (number of frames going backward along old track)											
			0	1	2	3	4	5	0	1	2	3	4	5
P_D^b	0.8	09	46	50	53	60	61	65	46	57	67	73	83	96
	0.6	02	58	60	61	62	62	63	58	63	69	70	73	76
	0.3	00	69	71	71	71	71	71	69	71	77	81	81	84
	0.1	00	71	72	72	73	73	75	72	73	73	73	73	73
	0.0	00	68	68	69	69	69	69	68	70	70	70	70	70

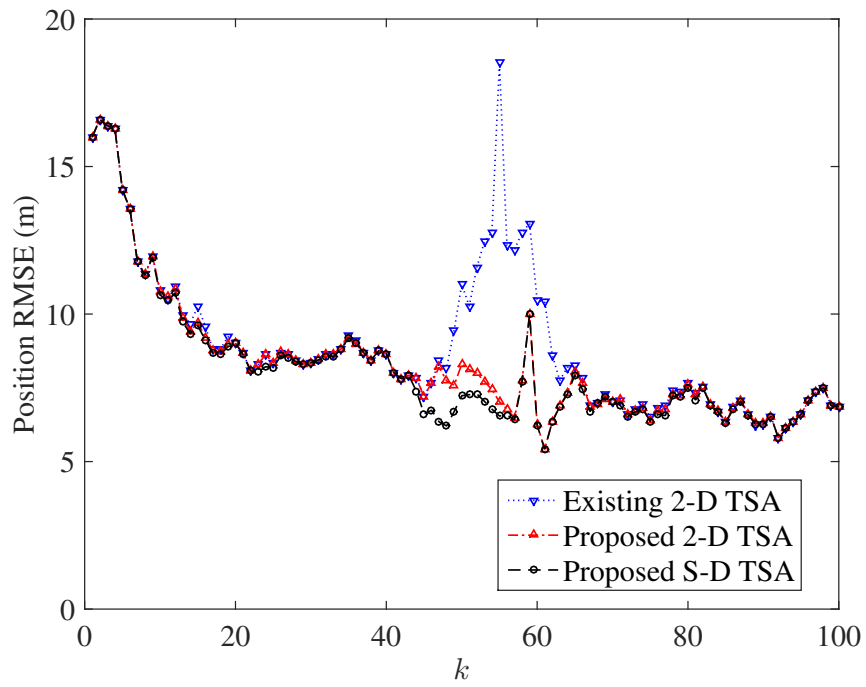


(a) Position

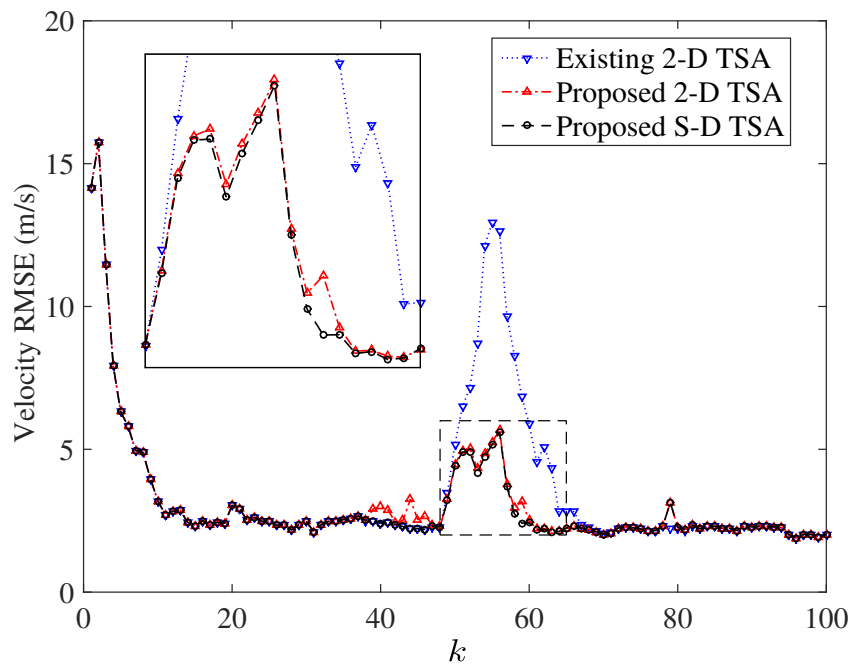


(b) Velocity

Figure 3.8: Single target RMSE ($P_D^b = 0.3$, $B_i = 0$, $\lambda = 1 \times 10^{-6} \text{m}^{-2}$, $\omega = 10^\circ/\text{s}$)



(a) Position



(b) Velocity

Figure 3.9: Single target RMSE ($P_D^b = 0.3$, $B_i = 5$, $\lambda = 1 \times 10^{-6} \text{m}^{-2}$, $\omega = 10^\circ/\text{s}$)

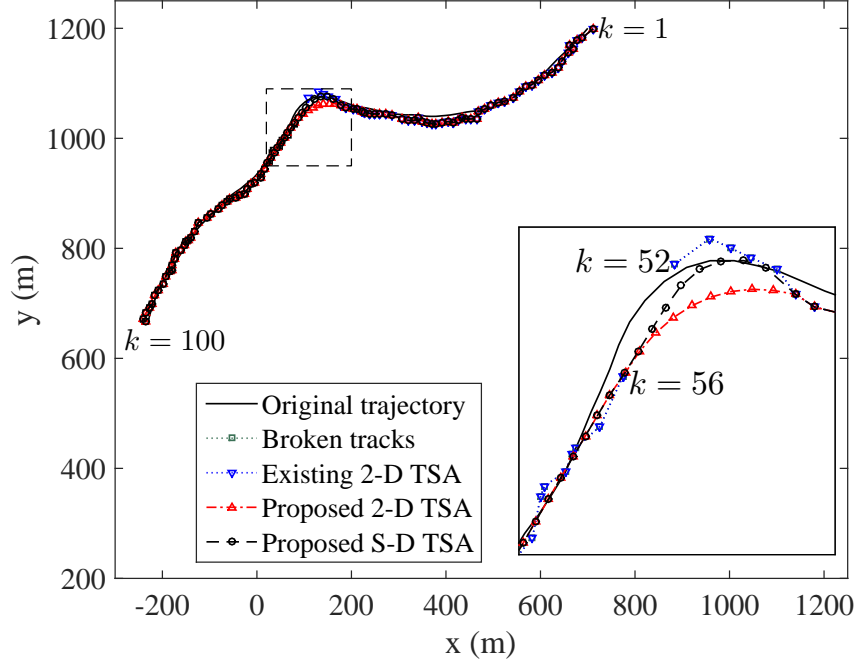


Figure 3.10: Track breakage due to target turn ($P_D^b = 0.2$, $B_i = 5$, $\lambda = 1 \times 10^{-6} \text{m}^{-2}$, $\omega = 10^\circ/\text{s}$)

D Track breakage due to target turn

Figure 3.10 shows that stitched tracks ($k_{n^{\mathcal{O}},e}^{\mathcal{O}} < k_{n^{\mathcal{Y}},s}^{\mathcal{Y}}$) were broken due to a high turn rate. It is observed that only the proposed algorithms are able to stitch a broken track successfully, as they incorporate multiple target motion models (as discussed in Section 3.3) during the breakage period. Because of the utilization of measurement information, the broken path estimated by the proposed S-D TSA algorithm is closer to the original target path than the estimate from the proposed 2-D TSA algorithm.

E Track stitching when $k_{n^{\mathcal{O}},e}^{\mathcal{O}} > k_{n^{\mathcal{Y}},s}^{\mathcal{Y}}$

Figure 3.11 depicts the case of broken tracks where the old track's ending time ($k_{n^{\mathcal{O}},e}^{\mathcal{O}} = 56$) is greater than the young track's starting time ($k_{n^{\mathcal{Y}},s}^{\mathcal{Y}} = 54$). Existing TSA algorithms (Yeom et al. 2004, Zhang and Bar-Shalom 2011) conclude that broken tracks in Figure 3.11 are not eligible for stitching. Since the proposed algorithms go backward in time along an old track segment, for certain values of B_i the ending time of the old track segment becomes less than or equal to the starting time of the young track segment, and hence they become eligible for association. For example, when $B_i \geq 2$, the old track segment ending time ($k_{n^{\mathcal{O}},e}^{\mathcal{O}} \leq 54$) becomes less than or equal to the young track segment starting time ($k_{n^{\mathcal{Y}},s}^{\mathcal{Y}} = 54$); hence they are eligible

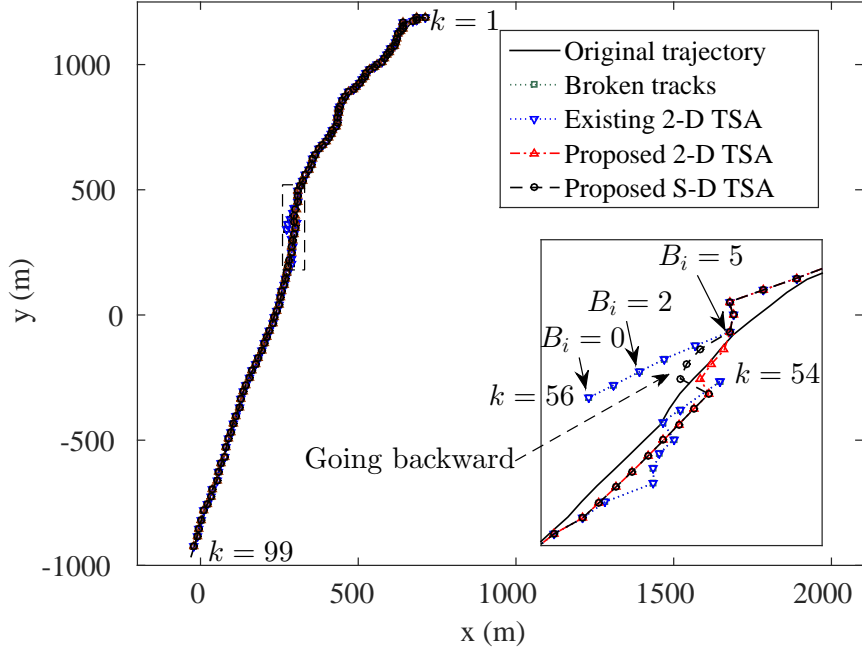


Figure 3.11: Track stitching when $k_{n^O,e}^O > k_{n^Y,s}^Y$

candidates for association. For this reason, we observe an increase in the percentage of correct association decisions by the proposed algorithms as B_i increases, as shown in Tables 3.1, 3.3, and 3.5.

F Track breakage due to false alarm

In Figure 3.12, we can see the stitching of broken tracks that were terminated due to a false measurement association. At time $k \in (51, 52)$, the old track segment is associated with false measurements that ultimately lead to track termination. The proposed TSA algorithms go backward ($B_i = 5$) along the old track segment to successfully explore those two false measurements and omit them from association. This is another reason why we observe an increase in the percentage of correct decisions made by the proposed algorithms as B_i increases, as shown in Tables 3.3 and 3.5.

3.4.4 Multiple Target Scenario

Case 1

In this scenario, multiple targets are simulated, as shown in Figure 3.13(a), and tracked to obtain the broken tracks for $P_D^b = 0.4$ and $\lambda = 1 \times 10^{-4} \text{m}^{-2}$ (as shown in Figure 3.13(b)). All three algorithms are applied to this set of broken tracks to estimate or predict the missing parts. The correct decision is declared if all the existing

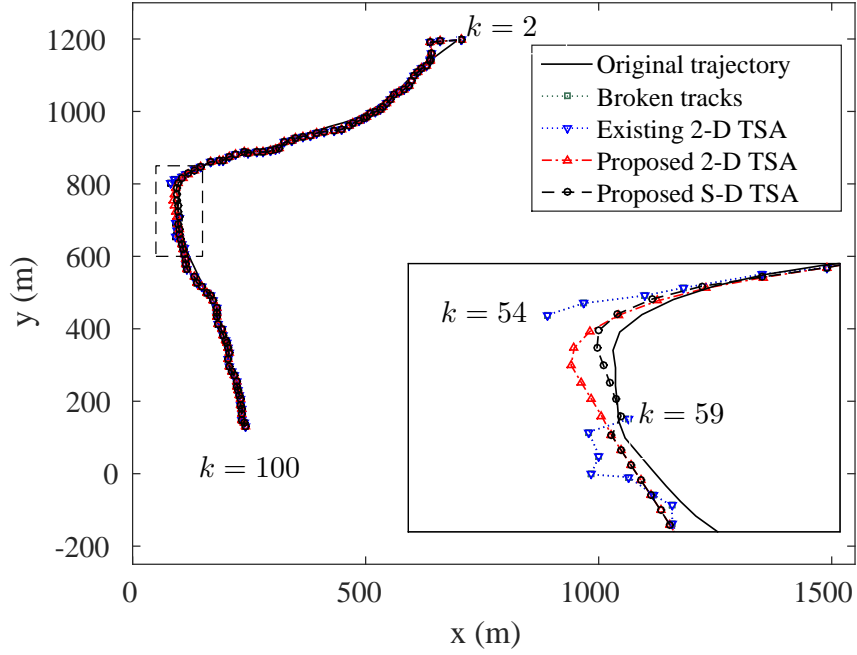
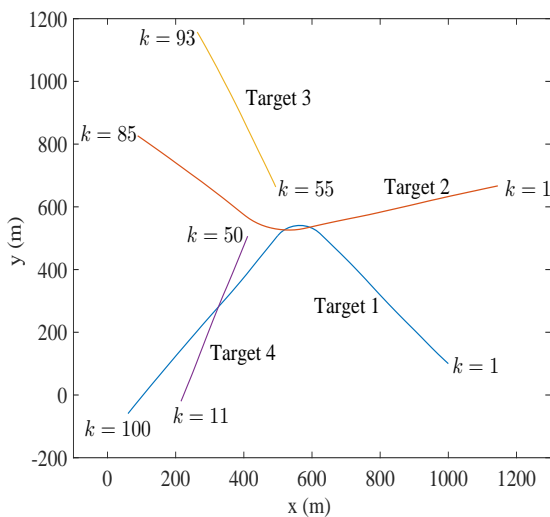


Figure 3.12: Track breakage due to false alarms
 targets are associated with their corresponding broken tracks over time.

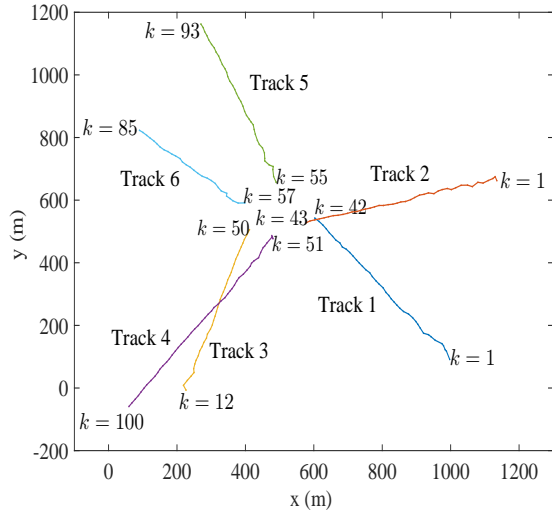
Tables 3.7, 3.8, and 3.9 show the percentage of correct association decisions when there is no clutter, low clutter, and high clutter, respectively. As B_i increases, more measurements are released. These released measurements contain true measurements, false measurements, and measurements with large errors. The proposed 2-D TSA algorithm does not use any measurements; moreover, it releases true measurements and then performs the TSA, resulting in degraded performance. In contrast, the proposed *S*-D TSA algorithm utilizes both the unassociated measurements and the true measurements out of the released measurements. This leads to an increase in performance, even when the clutter density is high and detection probability is low. However, both proposed algorithms show greater improvement in stitching and making right association decisions compared to existing 2-D TSA algorithm (Yeom et al. 2004). Figure 3.13 shows the results of different TSA algorithms.

Case 2

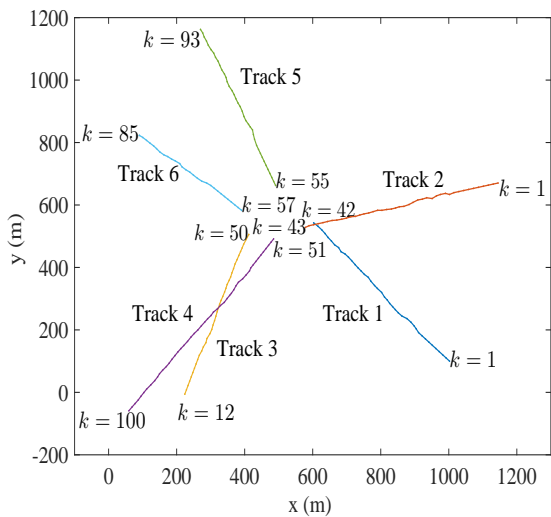
Multiple targets are simulated and tracking is performed to obtain broken tracks, unassociated measurement set for $P_D^b = 0$ and $\lambda = 1 \times 10^{-5} \text{m}^{-2}$. The proposed 2-D TSA and *S*-D TSA algorithms are applied on this set of broken tracks to obtain the results shown in Figures 3.14(c) and 3.14(d), respectively. Further, to show the



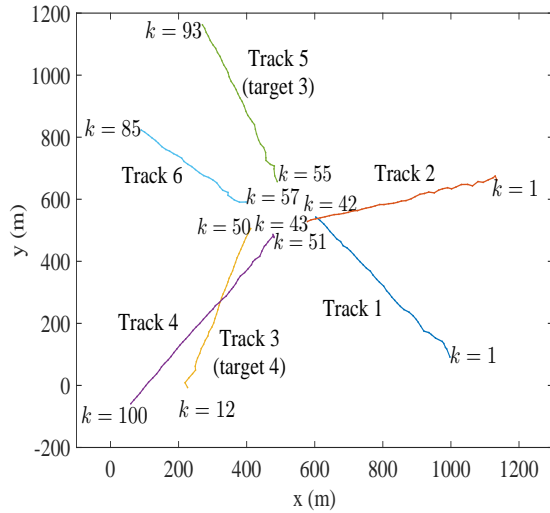
(a) Ground truth



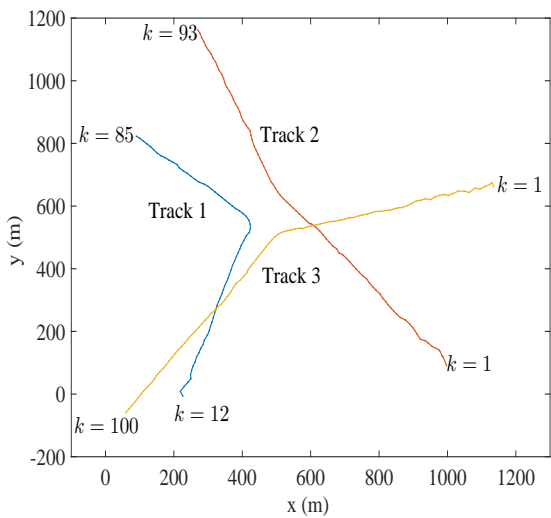
(b) Broken tracks



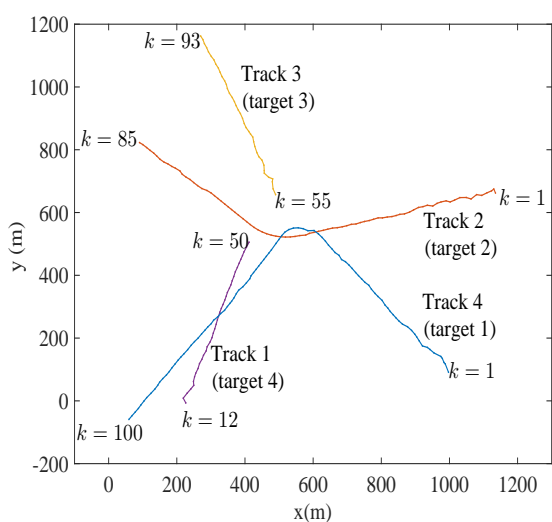
(c) Broken tracks after smoothing



(d) Existing 2-D TSA algorithm



(e) Proposed 2-D TSA algorithm



(f) Proposed S-D TSA algorithm

Figure 3.13: Results of TSA for multi-target scenario ($P_D^b = 0.4$, $\lambda = 1 \times 10^{-4} \text{m}^{-2}$, $B_i = 3$)

Table 3.7: Percentage of Correct Association Decisions
($B = 25$, $\lambda = 0\text{m}^{-2}$, 100 Monte Carlo runs)

		% of Correct TSA Decisions												
		Existing 2-D TSA <small>(Yeom et al. 2004)</small>	Proposed 2-D TSA						Proposed <i>S</i> -D TSA					
			B_i (number of frames going backward along old track)											
			0	1	2	3	4	5	0	1	2	3	4	5
P_D^b	0.5	00	37	33	33	31	32	32	51	53	55	55	56	55
	0.4	00	35	33	29	28	26	26	47	47	47	48	49	49
	0.3	00	31	26	21	20	20	21	41	41	42	42	42	42
	0.2	00	31	31	26	27	22	15	38	38	38	38	38	40
	0.1	00	27	24	20	19	17	14	36	36	36	37	37	37
	0.0	00	29	27	27	25	24	21	29	30	31	30	30	30
Normalized CPU Time		01	05	24	39	40	43	46	15	26	51	68	101	135

Table 3.8: Percentage of Correct Association Decisions
($B = 25$, $\lambda = 1 \times 10^{-6}\text{m}^{-2}$, 100 Monte Carlo runs)

		% of Correct TSA Decisions												
		Existing 2-D TSA <small>(Yeom et al. 2004)</small>	Proposed 2-D TSA						Proposed <i>S</i> -D TSA					
			B_i (number of frames going backward along old track)											
			0	1	2	3	4	5	0	1	2	3	4	5
P_D^b	0.5	00	33	32	31	31	30	29	47	52	52	54	54	54
	0.4	00	31	30	29	25	26	19	41	44	46	47	48	48
	0.3	00	33	31	25	26	21	19	35	39	41	42	42	42
	0.2	00	29	31	24	21	21	23	35	37	38	39	39	41
	0.1	00	27	24	22	18	17	15	32	32	36	36	37	36
	0.0	00	24	25	19	17	17	14	24	25	26	26	26	26
Normalized CPU Time		01	05	24	39	40	43	46	17	29	55	74	121	145

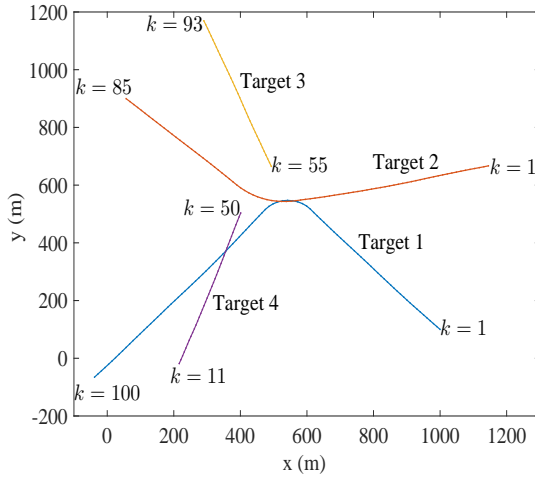
Table 3.9: Percentage of Correct Association Decisions
($B = 25$, $\lambda = 1 \times 10^{-4}\text{m}^{-2}$, 100 Monte Carlo runs)

		% of Correct TSA Decisions												
		Existing 2-D TSA <small>(Yeom et al. 2004)</small>	Proposed 2-D TSA						Proposed S -D TSA					
			B_i (number of frames going backward along old track)											
			0	1	2	3	4	5	0	1	2	3	4	5
P_D^b	0.5	00	33	34	32	31	31	31	43	48	51	54	54	56
	0.4	00	31	29	31	30	30	30	39	44	47	47	48	49
	0.3	00	29	28	28	26	26	26	37	41	41	42	44	46
	0.2	00	29	27	24	21	21	20	35	38	39	39	42	43
	0.1	00	25	24	22	23	22	21	29	32	33	34	34	34
	0.0	00	21	23	22	20	20	20	21	22	24	24	24	24
Normalized CPU Time		01	05	24	39	40	43	46	20	33	61	84	141	162

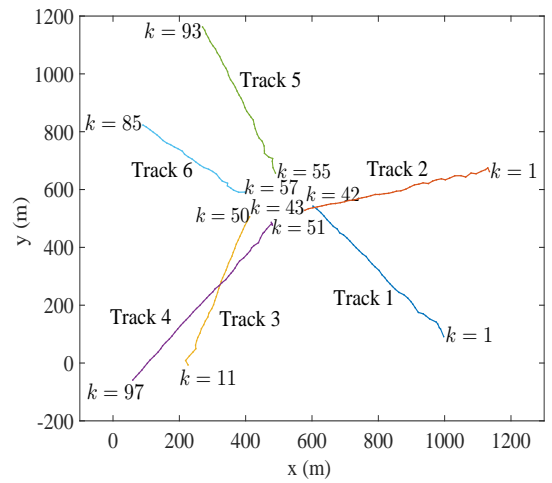
superiority of the latter, unassociated measurement list is updated depending on the chosen P_D^b . Then, the proposed S -D TSA algorithm is applied and resulting decision is tabulated in Table 3.10. Note the effectiveness of the proposed S -D TSA algorithm in turning the completely wrong associations (Figure 3.14(d)) into partially correct associations (Figure 3.14(e)) and correct associations (Figure 3.14(f)) as P_D^b increases. This is obvious because of increase in the available information in updated measurement list.

Table 3.10: Percentage of Correct Association Decisions
($B = 25$, $\lambda = 1 \times 10^{-5}\text{m}^{-2}$, 100 Monte Carlo runs)

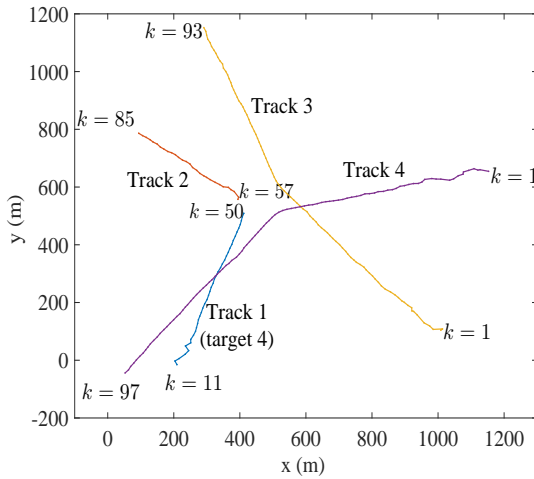
		Existing 2-D TSA <small>(Yeom et al. 2004)</small>		Proposed 2-D TSA		Proposed S -D TSA						
		% of Correct Decision	Normalized CPU Time	% of Correct Decisions	Normalized CPU Time	% of Correct Decisions						Normalized CPU Time
						P_D^b						
						0.0	0.1	0.2	0.3	0.4	0.5	
B_i	0	0	1	28	6	29	34	41	52	54	55	20
	1			21	12	32	36	44	55	57	59	39
	2			22	18	31	37	45	56	58	60	58
	3			22	26	32	38	45	56	58	61	78
	4			18	31	32	40	45	56	58	61	115
	5			17	39	32	40	46	56	58	61	152



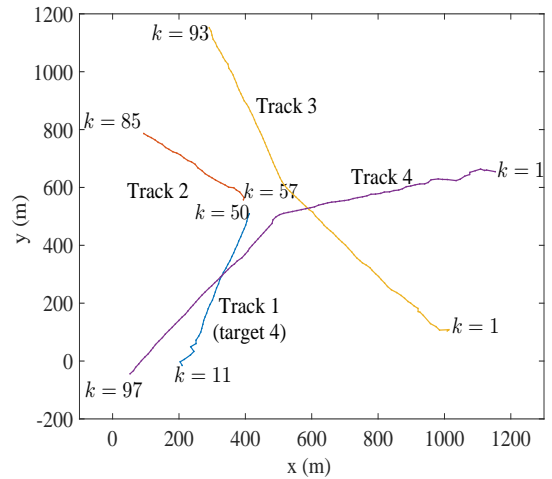
(a) Ground truth



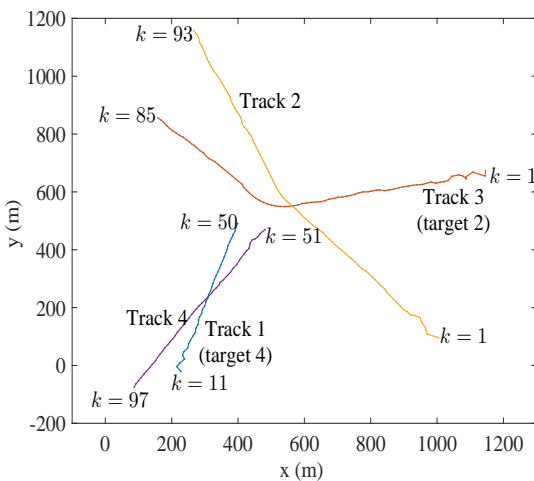
(b) Broken tracks ($P_D^b = 0$)



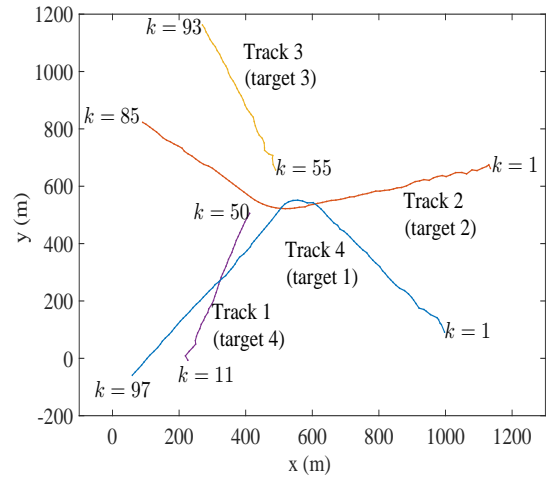
(c) Proposed 2-D TSA algorithm ($P_D^b = 0$, $B_i = 0$)



(d) Proposed S-D TSA algorithm ($P_D^b = 0$, $B_i = 0$)



(e) Proposed S-D TSA algorithm ($P_D^b = 0.1$, $B_i = 0$)



(f) Proposed S-D TSA algorithm ($P_D^b = 0.4$, $B_i = 0$)

Figure 3.14: Results of TSA for multi-target scenario ($\lambda = 1 \times 10^{-5} \text{m}^{-2}$)

3.5 SUMMARY

In Section 3.2, track stitching problem is formulated to: group the broken tracks into two different lists; estimate the possible beginning and termination times of young track segments and old track segments, respectively; use two-dimensional and multi-dimensional assignment techniques for TSA. The model parameters estimation with and without using available data during breakage period followed by the results and comparisons of existing and proposed algorithms are presented and discussed. The following contributing chapter describes the proposed track un-switching and un-swapping algorithms.

Chapter 4

TRACK UN-SWITCHING

4.1 OUTLINE

In this chapter, detailed theoretical and mathematical discussions are presented to perform track stitching considering both the regularly broken track segments (as discussed in Chapter 3) as well as algorithmically broken track segments that are resulting from breaking possible switch/swap detections. Note that, the regularly broken tracks, algorithmically broken tracks, and the possibly available additional information during the time duration of interest are simultaneously considered to perform track track un-swapping (un-switching) comprehensively. In addition to the above, it is also presented how to utilize kinematic data along with non-kinematic data — classification information, amplitude information — so as to achieve further improvements in both track stitching as well as track un-swapping.

4.2 TRACK UN-SWITCHING

4.2.1 Track Grouping

In order to perform un-swapping, it is required to group the tracks into different list as follows:

1. Old track list ($\mathcal{T}^{\mathcal{O}}(k)$): Let the old track list be

$$\mathcal{T}^{\mathcal{O}}(k) = \{\mathbf{T}_{n^{\mathcal{O}}}^{\mathcal{O}}(k)\}_{n^{\mathcal{O}}=1}^{N^{\mathcal{O}}(k)} \quad (4.1)$$

where $N^{\mathcal{O}}(k)$ is the total number of tracks in the old track list at time k . This track list consists of tracks that have been terminated recently — due to no association with any measurement — in the time interval $(k - B + 1, k)$, where

k is the current time and B is the look-back duration or sliding window size. This look-back time is a design parameter that is decided based on the track swapping rate, false alarm rate, or other factors.

2. Young track list ($\mathcal{T}^y(k)$): Let the young track list be

$$\mathcal{T}^y(k) = \{\mathbf{T}_{n^y}^y(k)\}_{n^y=1}^{N^y(k)} \quad (4.2)$$

where $N^y(k)$ is the total number of track segments in the young track list at time k . This list consists of tracks that have been started recently in the time interval $(k - B, k)$ provided they attained a certain minimum age. This age can be varied, depending upon the track breakage rate. The track segments appear on this list for one of several reasons: it pertains to a track in the old track list, a target is newborn, or false alarms result in a track.

3. Continuous track (non-broken) list ($\mathcal{T}^c(k)$): Let the continuous track list be

$$\mathcal{T}^c(k) = \{\mathbf{T}_{n^c}^c(k)\}_{n^c=1}^{N^c(k)} \quad (4.3)$$

where $N^c(k)$ is the total number of tracks in the continuous track list. This track list consists of tracks that are continuous (not broken) in the time duration $(k - B + 1, k)$ and these may have tracks swaps with one or more tracks of old track list and/or young track list.

4. Unswapped track list ($\mathcal{T}^u(k)$): Let the unswapped track list be

$$\mathcal{T}^u(k) = \{\mathbf{T}_{n^u}^u(k)\}_{n^u=1}^{N^u(k)} \quad (4.4)$$

where $N^u(k)$ is the total number of tracks in the unswapped track list at time k . This list will be empty initially and later all those stitched tracks resulting from the track segment association between old track list and young track list will be added to it.

4.2.2 Track List Updating

Once the TSA is performed between old track list $\mathcal{T}^o(k)$ and young track list $\mathcal{T}^y(k)$ that contain broken track segments that exist before post-processing as well as the

track segments that are results of breaking continuous tracks while performing post-processing, all the track lists need to be updated in next time instant. At time $k + 1$, each of the aforementioned track lists is updated in the following enumerated order:

1. Update the unswapped track list $\mathcal{T}^u(k+1)$ in the following sequence: (a) add all the stitched tracks resulting from the TSA between track lists $\mathcal{T}^o(k)$ and $\mathcal{T}^y(k)$: that is, stitched tracks in the previous instant k ; (b) add all those unassociated but removed tracks from list $\mathcal{T}^o(k)$ in the previous instant k ; (c) delete all those tracks which are continuous within the present window $(k - B + 2)$ to $(k + 1)$ — these tracks will be added to continuous track list; and (d) delete all those tracks whose last updated time fall within the present window $(k - B + 2)$ to $(k + 1)$ — these tracks will be added to old track list.
2. Update the continuous track list $\mathcal{T}^c(k + 1)$ in the following sequence: (a) add all those tracks which are continuous within the present window $(k - B + 2)$ to $(k + 1)$; (b) add all those tracks which are continuous in the present window but removed from unswapped track list $\mathcal{T}^u(k + 1)$; (c) add all those tracks of young track list $\mathcal{T}^y(k)$ which are continuous in the present window $(k - B + 2)$ to $(k + 1)$; and (d) delete all those tracks that have gate overlapping (as detailed in subsection 4.2.3) with at least any one of the tracks of $\mathcal{T}^c(k + 1)$ (excluding the one in question) or $\mathcal{T}^o(k)$ or $\mathcal{T}^y(k)$ — these tracks will be broken (by releasing their associated measurements from time $(k - B + 3)$ to k) and added to old and young track lists accordingly.
3. Update the young track list $\mathcal{T}^y(k + 1)$ in the following sequence: (a) delete all the tracks that were associated with old track segments at time k ; (b) delete all those tracks with the last updated time lesser than or equal to k — these tracks will be added to old track list $\mathcal{T}^o(k + 1)$; (c) delete all those tracks which are continuous within the present window $(k - B + 2)$ to $(k + 1)$ — these tracks were added to continuous track list $\mathcal{T}^c(k + 1)$; (d) add all those non-terminated tracks with starting time falling in the interval $(k - B + 3)$ to $(k + 1)$ after attaining certain minimum age; and (e) add all the young tracks which are consequence of breaking overlapping tracks removed from continuous track list $\mathcal{T}^c(k + 1)$ of present stride.

4. Update the old track list $\mathcal{T}^{\mathcal{O}}(k+1)$ in the following sequence: (a) delete all the tracks that were associated with young track segments at time k ; (b) delete all those tracks whose last updated time lesser than or equal to $(k-B+1)$: that is, tracks which are falling out of sliding window — these tracks will be added to unswapped track list at time $k+2$; (c) add all those unassociated but removed tracks (with last updated time lesser than or equal to k) of the young track list $\mathcal{T}^{\mathcal{Y}}(k+1)$; (d) add all those deleted tracks of unswapped track list $\mathcal{T}^{\mathcal{U}}(k+1)$ whose last updated time fall within the present window $(k-B+2)$ to $(k+1)$; and (e) add all the old tracks which are consequence of breaking overlapping tracks removed from continuous track list $\mathcal{T}^{\mathcal{C}}(k+1)$.

4.2.3 Track Swap Detection and Track Breaking

Under the Gaussian assumption of process and measurement noises, track data (state and covariance) at previous scanning time is sufficient statistic to decide whether or not the measurement gates of two different tracks overlap at the present scanning time. If this overlapping persist for longer time then there is highly likely that this would cause undesirable events such as swaps in the forthcoming scans (frames). To overcome this problem, one needs to detect such undesirable events in order to correct them. Therefore, it is required to list the tracks of continuous track list $\mathcal{T}^{\mathcal{C}}(k)$ that have gate overlapping among themselves or with any of the tracks of old track list $\mathcal{T}^{\mathcal{O}}(k)$ and young track list $\mathcal{T}^{\mathcal{Y}}(k)$.

First step is finding whether the following track pair has any possibility of track swaps

$$\{\mathbf{T}_{n^{\mathcal{C}}}^{\mathcal{C}}(k), \mathbf{T}_{n^{\mathcal{A}}}^{\mathcal{A}}(k)\}, \quad n^{\mathcal{C}} = 1, \dots, N^{\mathcal{C}}(k), \quad n^{\mathcal{A}} = 1, \dots, N^{\mathcal{A}}(k) \quad \text{for } n^{\mathcal{C}} \neq n^{\mathcal{A}} \quad (4.5)$$

where $\mathbf{T}_{n^{\mathcal{A}}}^{\mathcal{A}}(k)$ is a track from one of the following lists: continuous track list, old track list, and young track list; $N^{\mathcal{A}}(k)$ represents the number of tracks when all these three lists put together, i.e., $N^{\mathcal{A}}(k) = N^{\mathcal{C}}(k) + N^{\mathcal{O}}(k) + N^{\mathcal{Y}}(k)$. This is basically checking whether or not their predicted measurement gates overlap, i.e.,

$$[\Delta_{n^{\mathcal{C}}n^{\mathcal{A}}}^{\kappa}(k_1)]' [\Sigma_{n^{\mathcal{C}}n^{\mathcal{A}}}^{\kappa}(k_1)]^{-1} [\Delta_{n^{\mathcal{C}}n^{\mathcal{A}}}^{\kappa}(k_1)] \leq \gamma_{z^{\kappa}} \quad k_1 = k - B + 1, \dots, k \quad (4.6)$$

where the difference in the predicted measurement

$$\Delta_{n^c n^A}^\kappa(k) = \hat{\mathbf{z}}_{n^c}^\kappa(k|k-1) - \hat{\mathbf{z}}_{n^A}^\kappa(k|k-1) \quad (4.7)$$

with its corresponding covariance

$$\begin{aligned} \Sigma_{n^c n^A}^\kappa(k) &= E \{ [\Delta_{n^c n^A}^\kappa(k)] [\Delta_{n^c n^A}^\kappa(k)]' \} \\ &= \Sigma_{n^c}^\kappa(k) + \Sigma_{n^A}^\kappa(k) \end{aligned} \quad (4.8)$$

and γ_{z^κ} is the gate threshold for kinematic measurement vector dimension — can be obtained using chi-square distribution (Bar-Shalom et al. 2004) — corresponding to a certain gate probability, P_G . Track overlapping (i.e., track swap) is declared if track pair satisfy (4.6) N^o times within the present window. N^o is chosen depending upon the track swapping rate, false alarm rate, etc. Now, it is required to break all the continuous tracks that involve in overlapping with one or more tracks. Since our main focus is on track un-swapping, breaking process is carried-out by releasing all the measurements within the present window for simplicity. Otherwise, one can adapt the approach similar to the one presented in (Raghu et al. 2018). Resulting broken track segments are added to old and young track lists — these lists already contain regular broken tracks — accordingly so that track un-swapping and TSA can be performed simultaneously.

4.3 ASSOCIATION COST USING KINEMATIC INFORMATION

4.3.1 The Likelihood Ratios Using Kinematic Information

The measurement set, which includes both unassociated and released measurement, through scanning time $k - B + 1$ to k be

$$\begin{aligned} &\mathbf{Z}^{(k-B+1)(k)} \\ &= \left\{ \mathbf{Z}_{ua}^{(k-B+1)(k)}, \left\{ \mathbf{Z}_{rl}^{(k-B+1)(k)} \right\}_{n^o=1}^{N^o(k)}, \left\{ \mathbf{Z}_{rl}^{(k-B+1)(k)} \right\}_{n^y=1}^{N^y(k)}, \left\{ \mathbf{Z}_{rl}^{(k-B+1)(k)} \right\}_{n^c=1}^{N^c(k)} \right\}. \end{aligned} \quad (4.9)$$

and the feasible track-to-measurements-to-track tuple drawn from this measurement set pertaining to pair $\{ \mathbf{T}_{n^o}^o(k), \mathbf{T}_{n^y}^y(k) \}$, $n^o = 1, \dots, N^o(k)$, $n^y = 1, \dots, N^y(k)$,

through scanning time $k - B + 1$ to k is

$$\mathbf{z}_{m(k-B+1),m(k-B+2),\dots,m(k)}^\kappa \quad (4.10)$$

Above tuple $\mathbf{z}_{m(k-B+1),m(k-B+2),\dots,m(k)}^\kappa$ is a sequence consists of the following in order:

1. the old track $\mathbf{T}_{n^\mathcal{O}}^\mathcal{O}(k)$;
2. $(B-2)$ -tuple of kinematic measurements detected during the scanning time $(k - B + 2)$ through $(k - 1)$ — this tuple includes both unassociated measurements and the released measurements (Raghu et al. 2018); and
3. the young track $\mathbf{T}_{n^\mathcal{Y}}^\mathcal{Y}(k)$.

The likelihood that a B -tuple of the sequence of track-to-measurement-to-track kinematic tuple $\mathbf{z}_{m(k-B+1),m(k-B+2),\dots,m(k)}^\kappa$, having originated from target pertaining to track pair $\{\mathbf{T}_{n^\mathcal{O}}^\mathcal{O}(k), \mathbf{T}_{n^\mathcal{Y}}^\mathcal{Y}(k)\}$, with the known state $\mathbf{x}_{n^\mathcal{O}n^\mathcal{Y}}(s|s)$ is

$$\begin{aligned} & \Lambda_{n^\mathcal{O}n^\mathcal{Y}}^\kappa \left(\mathbf{z}_{m(k-B+1),m(k-B+2),\dots,m(k)}^\kappa \mid (n^\mathcal{O}, n^\mathcal{Y}) \right) \\ &= \prod_{s=k-B+1}^k \left\{ [1 - P_D]^{1-I(m(s))} \times [P_D p(\mathbf{z}_{m(s)}^\kappa(s) \mid \hat{\mathbf{x}}_{n^\mathcal{O}n^\mathcal{Y}}(s|s))]^{I(m(s))} \right\} \end{aligned} \quad (4.11)$$

where P_D is target detection probability and $I(m(s))$ is a binary function indicating whether or not measurement is assigned (i.e., target is detected) at time s , that is,

$$I(m(s)) = \begin{cases} 1 & \text{if the measurement is assigned at time } s, \text{ i.e., } m(s) \neq \emptyset \\ 0 & \text{otherwise} \end{cases} \quad (4.12)$$

The likelihood that a B -tuple $\mathbf{z}_{m(k-B+1),m(k-B+2),\dots,m(k)}^\kappa$, is spurious or unrelated to $\{\mathbf{T}_{n^\mathcal{O}}^\mathcal{O}(k), \mathbf{T}_{n^\mathcal{Y}}^\mathcal{Y}(k)\}$, i.e., $(n^\mathcal{O}, n^\mathcal{Y}) = \emptyset$, is

$$\Lambda_\emptyset^\kappa \left(\mathbf{z}_{m(k-B+1),m(k-B+2),\dots,m(k)}^\kappa \mid (n^\mathcal{O}, n^\mathcal{Y}) = \emptyset \right) = \prod_{s=k-B+1}^k \left[\frac{1}{V} \right]^{I(m(s))} \quad (4.13)$$

where V is the volume of the surveillance region.

Therefore the likelihood ratio of each B -tuple of the sequence of kinematic measurements $\mathbf{z}_{m(k-B+1),m(k-B+2),\dots,m(k)}^\kappa$, having originated from target pertaining to track pair $\{\mathbf{T}_{n^\mathcal{O}}^\mathcal{O}(k), \mathbf{T}_{n^\mathcal{Y}}^\mathcal{Y}(k)\}$ versus being extraneous (spurious source) (Popp et al. 2001,

Deb et al. 1997) is

$$\begin{aligned}
\mathcal{L}_{n^{\circ}n^{\mathcal{Y}}:\emptyset}^{\kappa} &= \frac{\Lambda_{n^{\circ}n^{\mathcal{Y}}}^{\kappa}(\mathbf{z}_{m(k-B+1),m(k-B+2),\dots,m(s)}^{\kappa} | (n^{\circ}, n^{\mathcal{Y}}))}{\Lambda_{\emptyset}^{\kappa}(\mathbf{z}_{m(k-B+1),m(k-B+2),\dots,m(k)}^{\kappa} | (n^{\circ}, n^{\mathcal{Y}}) = \emptyset)} \\
&= \frac{\prod_{s=k-B+1}^k \left\{ [1 - P_D]^{1-I(m(s))} \times \left[P_{DP} \left(\mathbf{z}_{m(s)}^{\kappa}(s) | \hat{\mathbf{x}}_{n^{\circ}n^{\mathcal{Y}}}(s|s) \right) \right]^{I(m(s))} \right\}}{\prod_{s=k-B+1}^k \left[\frac{1}{V} \right]^{I(m(s))}} \\
&= \prod_{s=k-B+1}^k \left\{ [1 - P_D]^{1-I(m(s))} \cdot \left[V P_{DP} \left(\mathbf{z}_{m(s)}^{\kappa}(s) | \hat{\mathbf{x}}_{n^{\circ}n^{\mathcal{Y}}}(s|s) \right) \right]^{I(m(s))} \right\} \quad (4.14)
\end{aligned}$$

The cost (Bar-Shalom et al. 2007) associated with tuple $\mathbf{z}_{m(k-B+1),m(k-B+2),\dots,m(k)}^{\kappa}$ is given by the negative log-likelihood ratio, i.e.,

$$\begin{aligned}
c_{\mathbf{z}_{m(k-B+1),m(k-B+2),\dots,m(k)}^{\kappa}}^{\kappa} &= -\ln \mathcal{L}_{n^{\circ}n^{\mathcal{Y}}:\emptyset}^{\kappa} \\
&= \sum_{s=k-B+1}^k \left\{ [I(m(s)) - 1] \ln(1 - P_D) - I(m(s)) \ln \frac{V P_D}{|2\pi \Sigma_{n^{\circ}n^{\mathcal{Y}}}^{\kappa}(s)|^{\frac{1}{2}}} \right. \\
&\quad \left. + \frac{1}{2} I(m(s)) D_{n^{\circ}n^{\mathcal{Y}}}^{\kappa}(s) \right\} \quad (4.15)
\end{aligned}$$

where $D_{n^{\circ}n^{\mathcal{Y}}}^{\kappa}(s)$ is the squared distance and it is given by

$$D_{n^{\circ}n^{\mathcal{Y}}}^{\kappa}(s) = [\Delta_{n^{\circ}n^{\mathcal{Y}}}(s|s-1)]' [\Sigma_{n^{\circ}n^{\mathcal{Y}}}(s)]^{-1} [\Delta_{n^{\circ}n^{\mathcal{Y}}}(s|s-1)]. \quad (4.16)$$

with

$$\Delta_{n^{\circ}n^{\mathcal{Y}}}(s|s-1) = \mathbf{z}_{m(s)}^{\kappa}(s) - \hat{\mathbf{z}}_{n^{\circ}n^{\mathcal{Y}}}(s|s-1) \quad (4.17)$$

and

$$\Sigma_{n^{\circ}n^{\mathcal{Y}}}(s) = \mathbf{R}(s) + [\mathbf{H}(s|s-1)] \mathbf{P}_{n^{\circ}n^{\mathcal{Y}}}(s|s-1) [\mathbf{H}(s|s-1)]' \quad (4.18)$$

In the above equation the term $\mathbf{H}(s|s-1)$ is the Jacobian matrix (Bar-Shalom et al. 2004) at $\hat{\mathbf{x}}_{n^{\circ}n^{\mathcal{Y}}}(s|s-1)$.

To simplify the problem further it is reasonable to assume that target can under go maximum of one turn within the sliding window and the model parameters such as turning rate, its starting and ending times are estimated so as to minimize the association cost $c_{\mathbf{z}_{m(k-B+1),m(k-B+2),\dots,m(k)}^{\kappa}}^{\kappa}$ as detailed in Section 3.3.

4.4 ASSOCIATION COST USING CLASSIFICATION INFORMATION

4.4.1 Classification Information Modeling

Target classes are discrete valued variables that characterize targets and can help distinguish between the measurements that originate from different sources.

Modeling: Let $\beta(k)$ be the discrete-valued class information measurement at scanning time k . The each class information measurement takes value from finite set of N^β classes $\{n^\beta = 1, \dots, N^\beta\}$ (Bar-Shalom et al. 2011). Assuming one has predefined and time independent $N^\beta \times N^\beta$ confusion matrix given by

$$\mathbb{C} = \begin{pmatrix} \mathbb{C}(1, 1) & \dots & \mathbb{C}(1, N^\beta) \\ \vdots & \ddots & \vdots \\ \mathbb{C}(N^\beta, 1) & \dots & \mathbb{C}(N^\beta, N^\beta) \end{pmatrix} \quad (4.19)$$

with each element $\mathbb{C}(i, j)$ is the likelihood of the true class being i when the observed measurement $\beta = j$, i.e.,

$$\mathbb{C}(i, j) = \Pr\{\beta(k) = j | \varsigma = i\} \quad (4.20)$$

where $\Pr\{\cdot\}$ is the probability of occurrence of an event. Therefore the likelihood for selected class j is the j^{th} column of matrix \mathbb{C} .

Probabilities Calculation: The posterior probability of a target being in class i given the class measurement $\beta(k) = j$ can be written (Bar-Shalom et al. 2005) as

$$\begin{aligned} \zeta^i(k) &= \Pr\{\varsigma = i | \beta(k) = j\} \\ &= \frac{\mathbb{C}(i, j)\zeta^i(k-1)}{\sum_{n^\beta=1}^{N^\beta} \mathbb{C}(n^\beta, j)\zeta^{n^\beta}(k-1)} \end{aligned} \quad (4.21)$$

where $\zeta(k-1)$ is the $N^\beta \times 1$ vector consisting of the prior probabilities of class $\{1, \dots, N^\beta\}$ and $\zeta^i(k-1)$ denotes the prior probability of class i .

For track pertaining to $\{\mathbf{T}_{n^o}^O(k), \mathbf{T}_{n^y}^O(k)\}$ the updated (posterior) class probability vector at time k , given the class measurement-tuple $\beta_{m(k-B+1), m(k-B+2), \dots, m(k)}$, is given by (Bar-Shalom et al. 2005)

$$\begin{aligned} \zeta_{n^o n^y}(k) &\triangleq \text{col}[\Pr\{\varsigma = i | \beta(k) = j, \beta_{m(k-B+1), m(k-B+2), \dots, m(k-1)}\}] \\ &= \frac{\mathbb{C}(:, j) \otimes \zeta_{n^o n^y}(k-1)}{[\mathbb{C}(:, j)]' \zeta_{n^o n^y}(k-1)} \end{aligned} \quad (4.22)$$

where $\zeta_{n^{\mathcal{O}}n^{\mathcal{Y}}}(k-1)$ is the prior probability vector, and \otimes is the Schur-Hadamard product, i.e., $\zeta_{n^{\mathcal{O}}}^i(k) = \mathbb{C}(n^{\mathcal{O}}, j) \cdot \zeta_{n^{\mathcal{O}}n^{\mathcal{Y}}}^{\beta}(k-1)$.

4.4.2 The Likelihood Ratios Using Classification Information

Let the augmented measurement vector consisting of kinematic components augmented with the classification component be

$$\mathbf{z}^{\kappa\beta}(k) \triangleq \begin{pmatrix} \mathbf{z}^{\kappa}(k) \\ \beta(k) \end{pmatrix} \quad (4.23)$$

and feasible measurement-tuple similar to (4.10) but includes both kinematic and class information be

$$\mathbf{z}_{m(k-B+1), m(k-B+2), \dots, m(k)}^{\kappa\beta} = \left\{ \mathbf{z}_{m(k-B+1), m(k-B+2), \dots, m(k)}^{\kappa}, \beta_{m(k-B+1), m(k-B+2), \dots, m(k)} \right\}. \quad (4.24)$$

Due to the independent assumption of kinematic and classification information, their combined likelihood ratio $\mathcal{L}_{n^{\mathcal{O}}n^{\mathcal{Y}}:\emptyset}^{\kappa\beta}$ for measurement-tuple $\mathbf{z}_{m(k-B+1), m(k-B+2), \dots, m(k)}^{\kappa\beta}$ originating from a target pertaining to track pair $\{\mathbf{T}_{n^{\mathcal{O}}}^{\mathcal{O}}(k), \mathbf{T}_{n^{\mathcal{Y}}}^{\mathcal{O}}(k)\}$ versus being extraneous, is given by the product of their individual likelihood ratios (Bar-Shalom et al. 2005), i.e.,

$$\mathcal{L}_{n^{\mathcal{O}}n^{\mathcal{Y}}:\emptyset}^{\kappa\beta} = \mathcal{L}_{n^{\mathcal{O}}n^{\mathcal{Y}}:\emptyset}^{\kappa} \cdot \mathcal{L}_{n^{\mathcal{O}}n^{\mathcal{Y}}:\emptyset}^{\beta} \quad (4.25)$$

The likelihood ratio of each B -tuple of the class sequence $\beta_{m(k-B+1), m(k-B+2), \dots, m(k)}$, having originated from target pertaining to $\{\mathbf{T}_{n^{\mathcal{O}}}^{\mathcal{O}}(k), \mathbf{T}_{n^{\mathcal{Y}}}^{\mathcal{O}}(k)\}$ versus being extraneous (spurious source) (Bar-Shalom et al. 2005) is

$$\begin{aligned} \mathcal{L}_{n^{\mathcal{O}}n^{\mathcal{Y}}:\emptyset}^{\beta} &= \frac{\Lambda_{n^{\mathcal{O}}n^{\mathcal{Y}}}^{\beta}(\beta_{m(k-B+1), m(k-B+2), \dots, m(k)} | (n^{\mathcal{O}}, n^{\mathcal{Y}}))}{\Lambda_{\emptyset}^{\beta}(\beta_{m(k-B+1), m(k-B+2), \dots, m(k)} | (n^{\mathcal{O}}, n^{\mathcal{Y}}) = \emptyset)} \\ &= \prod_{s=k-B+1}^k \left[\frac{[\mathbb{C}(:, \beta(s))]'\zeta_{n^{\mathcal{O}}n^{\mathcal{Y}}}(s-1)}{[\mathbb{C}(:, \beta(s))]'\zeta_{\text{ex}}} \right]^{I(m(s))} \end{aligned} \quad (4.26)$$

with the posterior class probability vector

$$\zeta_{n^{\mathcal{O}}n^{\mathcal{Y}}}(s-1) = [\zeta_{n^{\mathcal{O}}n^{\mathcal{Y}}}(s-2)]^{1-I(s-1)} \cdot \left[\frac{\mathbb{C}(:, \beta(s-1)) \otimes \zeta_{n^{\mathcal{O}}n^{\mathcal{Y}}}(s-2)}{[\mathbb{C}(:, \beta(s-1))]'\zeta_{n^{\mathcal{O}}n^{\mathcal{Y}}}(s-2)} \right]^{I(s-1)} \quad (4.27)$$

where ζ_{ex} is a class probability vector corresponding to extraneous target such as new/false target. Note that class probability vector $\zeta_{n^{\mathcal{O}}n^{\mathcal{Y}}}(k-1)$ remains unchanged

through the time $k - 2$ to $k - 1$ if $\mathbf{z}^\kappa(k - 1)$ is a dummy measurement assigned to measurement-tuple $\mathbf{z}_{m(k-B+1),m(k-B+2),\dots,m(k)}^\kappa$ at time $k - 1$.

The cost associated with class-tuple $\beta_{m(k-B+1),m(k-B+2),\dots,m(k)}$ is given by the negative log-likelihood ratio, i.e.,

$$\begin{aligned} c_{\beta_{m(k-B+1),m(k-B+2),\dots,m(k)}}^\beta &= -\ln \mathcal{L}_{n^{\mathcal{O}}n^{\mathcal{Y}}:\emptyset}^\beta \\ &= -\left(\sum_{s=k-B+1}^k I(m(s)) \ln \left(\frac{[\mathbf{C}(:, \beta(s))]'\boldsymbol{\zeta}_{n^{\mathcal{O}}n^{\mathcal{Y}}}(s-1)}{[\mathbf{C}(:, \beta(s))]'\boldsymbol{\zeta}_{\text{ex}}} \right) \right) \end{aligned} \quad (4.28)$$

Therefore when the kinematic and the classification information are integrated, the total cost associated with track-to-measurments-to-track sequence $\mathbf{z}_{m(k-B+1),m(k-B+2),\dots,m(k)}^{\kappa\beta}$ is

$$\begin{aligned} c_{\mathbf{z}_{m(k-B+1),m(k-B+2),\dots,m(k)}^{\kappa\beta}}^{\kappa\beta} &= -\ln \mathcal{L}_{n^{\mathcal{O}}n^{\mathcal{Y}}:\emptyset}^{\kappa\beta} \\ &= c_{\mathbf{z}_{m(k-B+1),m(k-B+2),\dots,m(k)}^\kappa}^\kappa + c_{\beta_{m(k-B+1),m(k-B+2),\dots,m(k)}}^\beta \end{aligned} \quad (4.29)$$

Note that, double counting of target missing information in (4.29) is avoided by considering such missed detections (i.e., when $I(m(s)) = 0$) only while computing kinematic information based cost $c_{\mathbf{z}_{m(k-B+1),m(k-B+2),\dots,m(k)}^\kappa}^\kappa$ but not while computing classification information based cost $c_{\beta_{m(k-B+1),m(k-B+2),\dots,m(k)}}^\beta$. However, to facilitate fair comparison, it is required to consider such missed detections in the latter case as well while performing track-to-measurments-to-track association solely based on classification information. Thus the modified classification information based cost

$c_{\beta_{m(k-B+1),m(k-B+2),\dots,m(k)}}^{\beta*}$ is given by

$$\begin{aligned} c_{\beta_{m(k-B+1),m(k-B+2),\dots,m(k)}}^{\beta*} &= -\ln \mathcal{L}_{n^{\mathcal{O}}n^{\mathcal{Y}}:\emptyset}^{\beta*} \\ &= -\ln \prod_{s=k-B+1}^k \left\{ [1 - P_D]^{1-I(m(s))} \right. \\ &\quad \left. \times \left[\frac{[\mathbf{C}(:, \beta(s))]'\boldsymbol{\zeta}_{n^{\mathcal{O}}n^{\mathcal{Y}}}(s-1)}{[\mathbf{C}(:, \beta(s))]'\boldsymbol{\zeta}_{\text{ex}}} \right]^{I(m(s))} \right\} \\ &= \sum_{s=k-B+1}^k \left\{ [I(m(s)) - 1](1 - P_D) \right. \\ &\quad \left. - I(m(s)) \ln \left(\frac{[\mathbf{C}(:, \beta(s))]'\boldsymbol{\zeta}_{n^{\mathcal{O}}n^{\mathcal{Y}}}(s-1)}{[\mathbf{C}(:, \beta(s))]'\boldsymbol{\zeta}_{\text{ex}}} \right) \right\} \end{aligned} \quad (4.30)$$

4.5 ASSOCIATION COST USING AMPLITUDE INFORMATION

4.5.1 Amplitude Information Modeling

Let $\alpha(k)$ be the continuous-valued amplitude measurement at scanning time k . If the amplitude is target originated then $\alpha(k)$ has an average signal-to-noise-ratio d . Otherwise, i.e., if the measurement is due to noise only then it has unity power. In either case the amplitude measurements are assumed to be Rayleigh distributed (Goldsmith 2005) and hence their pdfs before applying threshold are given by (Kirubarajan and Bar-Shalom 1996)

$$p_1(\alpha(k)) = \frac{\alpha(k)}{1+d} \exp\left(-\frac{\alpha^2(k)}{2(1+d)}\right), \quad \alpha(k) \geq 0 \quad (4.31)$$

and

$$p_0(\alpha(k)) = \alpha(k) \exp\left(-\frac{\alpha^2(k)}{2}\right), \quad \alpha(k) \geq 0 \quad (4.32)$$

respectively. With the known threshold τ — that decides whether the target is detected (Fortmann et al. 1985) — the detection probability of target-originated measurement P_D and the detection probability of clutter or false alarm P_{FA} are respectively defined as follows

$$P_D \triangleq \Pr\{\text{a target-originated measurement exceeds threshold } \tau\} \quad (4.33)$$

$$P_{FA} \triangleq \Pr\{\text{a measurement due to noise only exceeds threshold } \tau\} \quad (4.34)$$

These detection probabilities P_D and P_{FA} are obtained from their respective pdfs as follows

$$P_D = \int_{\tau}^{+\infty} p_1(\alpha(k)) d\alpha(k) = \exp\left(-\frac{\tau^2}{2(1+d)}\right) \quad (4.35)$$

$$P_{FA} = \int_{\tau}^{+\infty} p_0(\alpha(k)) d\alpha(k) = \exp\left(-\frac{\tau^2}{2}\right) \quad (4.36)$$

Now, the density functions corresponding to thresholded measurements are given by

$$\begin{aligned} p_1^\tau(\alpha(k)) &= \frac{p_1(\alpha(k))}{P_D} \\ &= \frac{\alpha(k)}{P_D(1+d)} \exp\left(-\frac{\alpha(k)}{2(1+d)}\right), \quad \alpha(k) \geq \tau \end{aligned} \quad (4.37)$$

$$\begin{aligned}
p_0^\tau(\alpha(k)) &= \frac{p_0(\alpha(k))}{P_{\text{FA}}} \\
&= \frac{\alpha(k)}{P_{\text{FA}}} \exp\left(-\frac{\alpha^2(k)}{2}\right), \quad \alpha(k) \geq \tau
\end{aligned} \tag{4.38}$$

Subsequently, the amplitude likelihood ratio is defined as

$$\rho(k) = \frac{p_1^\tau(\alpha(k))}{p_0^\tau(\alpha(k))}. \tag{4.39}$$

4.5.2 The Likelihood Ratios Using Amplitude Information

Let the augmented measurement vector consisting of kinematic components augmented with the amplitude be

$$\mathbf{z}^{\kappa\alpha}(k) \triangleq \begin{pmatrix} \mathbf{z}^\kappa(k) \\ \alpha(k) \end{pmatrix} \tag{4.40}$$

and feasible measurement-tuple similar to (4.10) but includes both kinematic and amplitude information be

$$\mathbf{z}_{m(k-B+1),m(k-B+2),\dots,m(k)}^{\kappa\alpha} = \left\{ \mathbf{z}_{m(k-B+1),m(k-B+2),\dots,m(k)}^\kappa, \alpha_{m(k-B+1),m(k-B+2),\dots,m(k)} \right\}. \tag{4.41}$$

Usually, one assumes that kinematic and amplitude information are independent of each other. Therefore their combined likelihood ratio $\mathcal{L}_{n^\circ n^\mathcal{Y}:\emptyset}^{\kappa\alpha}$ for measurement-tuple $\mathbf{z}_{m(k-B+1),m(k-B+2),\dots,m(k)}^{\kappa\alpha}$ originating from a target pertaining to track pair $\{\mathbf{T}_{n^\circ}^\circ(k), \mathbf{T}_{n^\mathcal{Y}}^\circ(k)\}$ versus being spurious, is the product of their individual likelihood ratios, i.e.,

$$\mathcal{L}_{n^\circ n^\mathcal{Y}:\emptyset}^{\kappa\alpha} = \mathcal{L}_{n^\circ n^\mathcal{Y}:\emptyset}^\kappa \cdot \mathcal{L}_{n^\circ n^\mathcal{Y}:\emptyset}^\alpha \tag{4.42}$$

The likelihood ratio of each of amplitude-tuple $\alpha_{m(k-B+1),m(k-B+2),\dots,m(k)}$ pertaining to a target of track pair $\{\mathbf{T}_{n^\circ}^\circ(k), \mathbf{T}_{n^\mathcal{Y}}^\circ(k)\}$ versus being extraneous (spurious

Input: Tracks to be unswapped at time k

Output: Unswapped track list at time k

-
- 1: Group the track segments into old, young and continuous track lists (do this only once at the beginning) as discussed in subsection 4.2.1.
 - 2: Detect all those tracks of continuous track list that might have got track swaps with one or more tracks of old and young track lists as discussed in subsection 4.2.3 and break.
 - 3: Update old, young and continuous track lists as discussed in subsection 4.2.2.
 - 4: Perform smoothing on all the tracks of young track list over a fixed period as discussed in subsection 3.2.3.
 - 5: Obtain set of all combinations of candidate track pairs $\Phi^T(k)$ as in (3.3).
 - 6: Obtain feasible candidate track pair set $\Phi_f^T(k)$ as given in (3.11).
 - 7: Release all the measurements pertaining to the broken tracks during the window period $k - B + 1$ to k .
 - 8: Obtain model parameters as discussed in subsection 3.3.1 for each pair of tracks pertaining to $\Phi_f^T(k)$.
 - 9: Obtain the measurement set $\mathbf{Z}^{(k-B+1)(k)}$, which includes both unassociated and released measurement, through scanning time $k - B + 1$ to k , as given in (4.9).
 - 10: Formulate multi-frame assignment problem (during window time $k - B + 1$ to k) and obtain all the possible measurement tuples $\{\mathbf{z}_{m(k-B+1),m(k-B+2),\dots,m(k)}\}$.
 - 11: For every tuple in $\{\mathbf{z}_{m(k-B+1),m(k-B+2),\dots,m(k)}\}$, obtain
 - (a) kinematic cost $c_{\mathbf{z}_{m(k-B+1),m(k-B+2),\dots,m(k)}}^{\kappa}$ as given in (4.15).
 - (b) classification cost $c_{\beta_{m(k-B+1),m(k-B+2),\dots,m(k)}}^{\beta*}$ as given in (4.30).
 - (c) amplitude cost $c_{a_{m(k-B+1),m(k-B+2),\dots,m(k)}}^{\alpha*}$ as given in (4.46).
 - (d) kinematic and classification cost $c_{\mathbf{z}_{m(k-B+1),m(k-B+2),\dots,m(k)}}^{\kappa\beta}$ as given in (4.29).
 - (e) kinematic and amplitude $c_{\mathbf{z}_{m(k-B+1),m(k-B+2),\dots,m(k)}}^{\kappa\alpha}$ as given in (4.45).
 - 12: Obtain the multi-frame assignment solution corresponding to each of cost (a)–(e) in a similar manner to the one discussed in subsection (3.2.5).
 - 13: Perform the track stitching between old and young track segments according to the best solution.
 - 14: Update unswapped track list as discussed in subsection 4.2.2.
 - 15: **return** Unswapped track list.

Figure 4.1: An algorithm for track unswapping

source) is

$$\begin{aligned}
\mathcal{L}_{n^{\mathcal{O}}n^{\mathcal{Y}}:\emptyset}^{\alpha} &= \frac{\Lambda_{n^{\mathcal{O}}n^{\mathcal{Y}}}^{\alpha}(\alpha_{m(k-B+1),m(k-B+2),\dots,m(k)} | (n^{\mathcal{O}}, n^{\mathcal{Y}}))}{\Lambda_{\emptyset}^{\alpha}(\alpha_{m(k-B+1),m(k-B+2),\dots,m(k)} | (n^{\mathcal{O}}, n^{\mathcal{Y}}) = \emptyset)} \\
&= \prod_{s=k-B+1}^k \left[\frac{p_1^{\tau}(\alpha(s))}{\frac{1}{V}p_0^{\tau}(\alpha(s))} \right]^{I(m(s))} \\
&= \prod_{s=k-B+1}^k [V\rho(s)]^{I(m(s))} \\
&= \prod_{s=k-B+1}^k \left[\frac{VP_{\text{FA}}}{P_{\text{D}}(1+d)} \exp\left(\frac{\alpha^2(s)}{2} \frac{d}{1+d}\right) \right]^{I(m(s))} \tag{4.43}
\end{aligned}$$

The cost associated with amplitude-tuple $\alpha_{m(k-B+1),m(k-B+2),\dots,m(k)}$ is given by the negative log-likelihood ratio, i.e.,

$$\begin{aligned}
C_{\alpha_{m(k-B+1),m(k-B+2),\dots,m(k)}}^{\alpha} &= -\ln \mathcal{L}_{n^{\mathcal{O}}n^{\mathcal{Y}}:\emptyset}^{\alpha} \\
&= -\ln \prod_{s=k-B+1}^k \left[\frac{VP_{\text{FA}}}{P_{\text{D}}(1+d)} \exp\left(\frac{\alpha^2(s)}{2} \frac{d}{1+d}\right) \right]^{I(m(s))} \\
&= -\left\{ \sum_{s=k-B+1}^k I(m(s)) \ln\left(\frac{VP_{\text{FA}}}{P_{\text{D}}(1+d)}\right) + I(m(s)) \left(\frac{\alpha^2(s)}{2} \frac{d}{1+d}\right) \right\} \tag{4.44}
\end{aligned}$$

Similar to (4.29), when the kinematic and the amplitude information are integrated, the total cost associated with sequence $\mathbf{z}_{m(k-B+1),m(k-B+2),\dots,m(k)}^{\kappa\alpha}$ is

$$\begin{aligned}
C_{\mathbf{z}_{m(k-B+1),m(k-B+2),\dots,m(k)}^{\kappa\alpha}}^{\kappa\alpha} &= -\ln \mathcal{L}_{n^{\mathcal{O}}n^{\mathcal{Y}}:\emptyset}^{\kappa\alpha} \\
&= C_{\mathbf{z}_{m(k-B+1),m(k-B+2),\dots,m(k)}^{\kappa}}^{\kappa} + C_{\alpha_{m(k-B+1),m(k-B+2),\dots,m(k)}}^{\alpha} \tag{4.45}
\end{aligned}$$

Analogously to (4.30), to perform track-to-measurments-to-track association solely based on amplitude information one should use modified amplitude information based cost $C_{\alpha_{m(k-B+1),m(k-B+2),\dots,m(k)}}^{\alpha*}$ given by

$$\begin{aligned}
C_{\alpha_{m(k-B+1),m(k-B+2),\dots,m(k)}}^{\alpha*} &= -\ln \mathcal{L}_{n^{\mathcal{O}}n^{\mathcal{Y}}:\emptyset}^{\alpha*} \\
&= -\ln \prod_{s=k-B+1}^k \left\{ [(1-P_{\text{D}})]^{1-I(m(s))} \cdot \left[\frac{p_1^{\tau}(\alpha(s))}{\frac{1}{V}p_0^{\tau}(\alpha(s))} \right]^{I(m(s))} \right\} \\
&= \sum_{s=k-B+1}^k \left\{ [I(m(s)) - 1](1 - P_{\text{D}}) - I(m(s)) \ln \frac{VP_{\text{FA}}}{P_{\text{D}}(1+d)} - I(m(s)) \left(\frac{\alpha^2(s) \cdot d}{2(1+d)}\right) \right\}. \tag{4.46}
\end{aligned}$$

Further, the step by step procedure for the implementation of the proposed track un-switching algorithm can be found in Figure 4.1.

4.6 RESULTS AND DISCUSSIONS

4.6.1 Tracking Filter and Design Parameters

The targets are simulated, measurements are generated and tracked using constant velocity based Nearest neighbor (NN) (Bar-Shalom et al. 2011) filter utilizing only the kinematic information to obtain the swapped and un-swapped tracks in two target and multi-target Scenarios. In both the Scenarios the following design parameters are considered:

- Sampling interval, $\Delta(k) = 1\text{s}$;
- One-point initialization method (Yeom et al. 2004, Musicki and Song 2013) with maximum velocity $V_{\max} = 50 \text{ m/s}$ is used for initializing the tracks;
- Process noise covariance matrix, $\mathbf{Q}(k) = \begin{pmatrix} 0.1\text{m}^2 & 0 \\ 0 & 0.1\text{m}^2 \end{pmatrix}$, and;
- Measurement noise covariance matrix, $\mathbf{R}(k) = \begin{pmatrix} 225\text{m}^2 & 0 \\ 0 & 0.0004\text{rad}^2 \end{pmatrix}$.

Similarly, for post-processing the following design parameters are considered:

- It is assumed that classification and amplitude information are available;
- It is assumed that target turn lasts at least 4 scans;
- Minimum number of times two tracks have their predicted measurements gate overlapping within window so as to declare track swap: $N^o = 5$;
- Target will under go at most single turn within the window with maximum turn rate $|\omega_{\max}| \leq 15^\circ/\text{s}$, and;
- Track length needs to be at least 6 scans long to be considered for post-processing;

4.6.2 Performance Measure

Track purity is the primary measure of performance to evaluate the trackers (Kirubaranjan et al. 1999, Schutz et al. 1997) before and after post-processing. Track purity of track is defined as the ratio between the number of measurements from particular target associated with particular track and total number of associated measurements with the same track, i.e.,

$$\begin{aligned} & \text{Track Purity} \\ &= [\Pi_{mn}] \\ &= \frac{\text{number of associated measurements with the target ID } m \text{ in track } n}{\text{total number of associated measurements in the track } n} \end{aligned} \quad (4.47)$$

4.6.3 Procedure For Automatic Track Swap detection

It is relatively straight forward problem to detect the track swap by inspection when the ground truth is known. However, it is still required to understand the exact definition of track swap in order to make swap detection process automated. To accomplish this in two target scenarios, a simple approach (see Figure 4.2) is presented in which the lower inspection time k_L and upper inspection time k_U are computed. The lower inspection time is the time at which both the tracks exist and their respective initialization errors are reasonably minimum (for example, go forward along the tracks by specified number of frames from the scan at which both tracks exist for the first time) that they can be associated with ground truth. Similarly, upper inspection time is one of the following:

1. the time at which both the tracks exist for the last time;
2. the time corresponding to the scan which is prior (for example, go backward along the tracks by specified number of scans) to the scan at which both the tracks exist for the last time — this is to negotiate large tracking errors, if any, prior to track termination.

Therefore lower and higher inspection times are respectively taken as

$$k_L \triangleq \max\{k_{1,s} + N^f, k_{2,s} + N^f\} \quad (4.48)$$

Input: T_n, T_m, k_l, k_u , Ground truth

Output: Decision

-
- 1: Compute k_L and k_U such that $k_L < k_l$ and $k_U > k_u$
 - 2: Compute the distance between ground truth and tracks T_n, T_m
 - 3: **If** distance $>$ threshold
 - 4: reject the association
 - 5: **EndIf**
 - 6: Obtain binary association variables $\{a_{nm}(k_L)\}$ and $\{a_{nm}(k_U)\}$
 - 7: **If** $\{a_{nm}(k_L)\} \neq \{a_{nm}(k_U)\}$
 - 8: Decision = track swapped.
 - 9: **Else**
 - 10: Decision = no track swapping.
 - 11: **EndIf**
 - 12: **return** *Decision*

Figure 4.2: An algorithm to determine the track swap

and

$$k_U \triangleq \min\{k_{1,e} - N^b, k_{2,e} - N^b\} \quad (4.49)$$

where N^f and N^b represent the specified number of scans one has to go forward and backward, respectively. It is always good to keep both the inspection times out of gate overlapping region as shown in Figure 4.3 (i.e., $k_L < k_l$ and $k_U > k_u$) to ensure the better swap detection results.

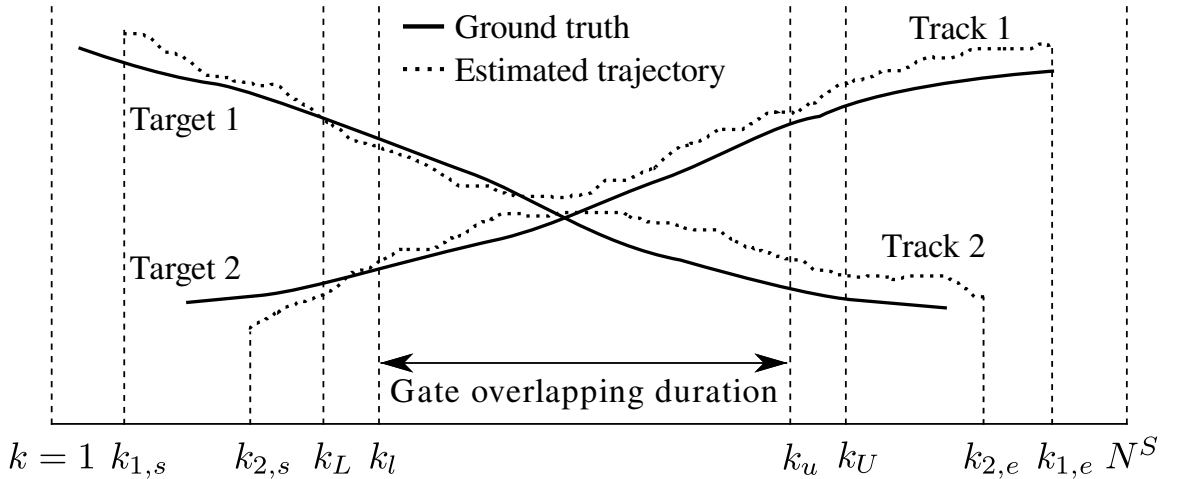


Figure 4.3: Illustration of automatic track swap detection for two target case

4.6.4 Two Target Case

In this section, two targets belonging to different classes and amplitudes are simulated and track using kinematic information to obtain tracks with or without swaps.

Usually, in two target case one can observe the following Scenarios leading to track breakage or/and swaps

A Scenario 1

Targets move towards each other as shown in Figure 4.4(a) before they move away from each other resulting in swapped tracks as shown in Figure 4.4(c)

B Scenario 2

Targets cross each other as shown in Figure 4.5(a) and yield swapped tracks as shown in Figure 4.5(b)

C Scenario 3

Targets move towards each other before they move away and resulting track breakage and track swap as shown in Figure 4.8

Proposed post-processing approach versions — kinematic, classification, kinematic & classification, amplitude, and kinematic & amplitude — are operated on different two target Scenarios mentioned above and the results are tabulated in Tables 4.1–4.3. In Scenario 1 and 2, there are no broken tracks and/or the tracks due to new born tracks and hence the results of proposed algorithm cannot be compared with existing TSA algorithms (Yeom et al. 2004, Raghu et al. 2018). Whereas in Scenario 3, both the algorithms can be operated and their performances can be compared.

In Table 4.1, percentage of successfully un-swapped and swap introduced results of different versions of proposed algorithm for different classifier output accuracy \mathbb{C} and for different SNRs are compared and their corresponding purity matrices are compared in Table 4.2. It can be seen that the kinematic version shows overall improvement of about 19% in un-swapping swapped tracks and avoid introducing any new swap, if there was no swap before, compared to the percentage of correct target-to-track association prior to post-processing. This is due to the use combination of CV and CT models in the former case. Among the different proposed versions, one which utilizes two types of information — kinematic & classification or kinematic & amplitude — shows better un-swapping performance compared to the case where any one type of information is utilized. This is obvious, because, kinematic and class (amplitude)

Table 4.1: Two target case (Scenario 1 & 2): Percentage of Track Un-swapping and Track Swapping Introduced ($B = 10$, $\tau = 4.2677$, $P_{FA} = 1.1093 \times 10^{-4}$, 100 Monte Carlo runs)

Algorithm Used for Post-processing	Parameter			Successfully Un-swapped			Swapping Introduced			Overall Correct T2T Association	
	P_D	\mathbb{C}	d (dB)	Scenario							
				1	2	1 & 2	1	2	1 & 2		
Prior to Post-processing	0.8	–	–	–	–	–	–	–	–	50%	
Version of Proposed Algorithm	Kinematic	0.8	–	–	74%	71%	73%	35%	36%	36%	69%
	Classification	0.8	$\begin{pmatrix} 0.95 & 0.05 \\ 0.05 & 0.95 \end{pmatrix}$	–	82%	81%	82%	24%	25%	25%	79%
		0.8	$\begin{pmatrix} 0.85 & 0.15 \\ 0.15 & 0.85 \end{pmatrix}$	–	79%	77%	78%	26%	27%	27%	76%
		0.8	$\begin{pmatrix} 0.75 & 0.25 \\ 0.25 & 0.75 \end{pmatrix}$	–	75%	73%	74%	27%	27%	27%	74%
	Kinematic and Classification	0.8	$\begin{pmatrix} 0.95 & 0.05 \\ 0.05 & 0.95 \end{pmatrix}$	–	90%	89%	90%	12%	13%	13%	89%
		0.8	$\begin{pmatrix} 0.85 & 0.15 \\ 0.15 & 0.85 \end{pmatrix}$	–	89%	89%	89%	13%	15%	14%	88%
		0.8	$\begin{pmatrix} 0.75 & 0.25 \\ 0.25 & 0.75 \end{pmatrix}$	–	89%	88%	89%	14%	14%	14%	88%
	Amplitude	0.8	–	20 & 16	87%	85%	86%	14%	13%	14%	86%
		0.8	–	18 & 16	78%	79%	79%	20%	22%	21%	79%
		0.8	–	16 & 16	68%	70%	70%	31%	30%	31%	70%
	Kinematic and Amplitude	0.8	–	20 & 16	94%	92%	93%	09%	11%	10%	92%
		0.8	–	18 & 16	82%	85%	84%	17%	15%	16%	84%
		0.8	–	16 & 16	72%	71%	72%	30%	33%	32%	70%

together give more information than kinematic or class or amplitude alone. Among proposed versions classification and amplitude, latter shows better results as there is larger difference in targets' SNR values and therefore when these are clubbed with kinematic information, kinematic & amplitude version shows greater improvement overall. In addition, performances are compared by varying the classifier output accuracy \mathbb{C} and for different SNR values.

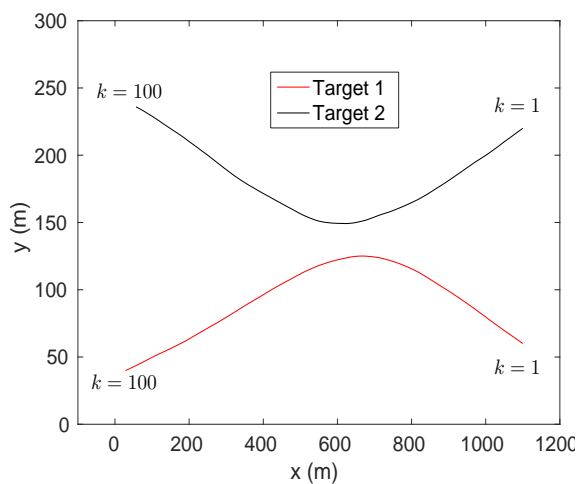
Figures 4.4 and 4.5 show a typical example of Scenario 1 and 2, respectively. Prior to post-processing tracks are swapped as shown in Figures 4.4(c) and 4.5(b)). After applying different versions of proposed algorithm, kinematic version fails to un-

Table 4.2: Two target case (Scenario 1 & 2): Track Purity Matrices $\{\Pi\}$ ($B = 10$, $\tau = 4.2677$, $P_{FA} = 1.1093 \times 10^{-4}$, 100 Monte Carlo runs)

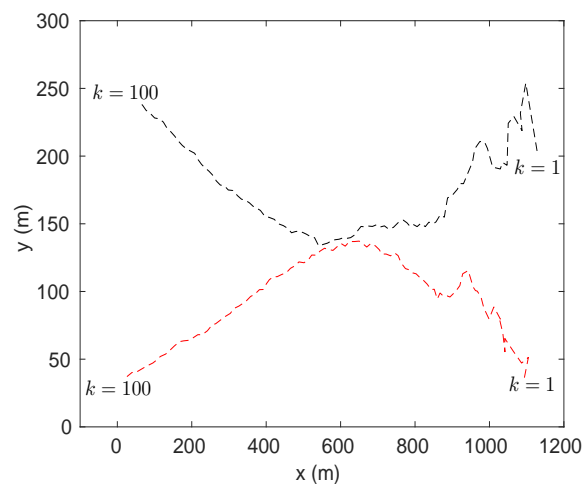
Algorithm Used for Post-processing		Parameter			Track Purity Matrix Π	
		P_D	\mathbb{C}	d (dB)	Successfully Un-swapped (Scenario 1 & 2)	Swapping Introduced (Scenario 1 & 2)
Prior to Post-processing		0.8	-	-	$\begin{pmatrix} 0.4541 & 0.3569 \\ 0.3959 & 0.4331 \end{pmatrix}$	$\begin{pmatrix} 0.7031 & 0.0841 \\ 0.0769 & 0.7258 \end{pmatrix}$
Version of Proposed Algorithm	Kinematic	0.8	-	-	$\begin{pmatrix} 0.6349 & 0.1785 \\ 0.1951 & 0.6115 \end{pmatrix}$	$\begin{pmatrix} 0.6507 & 0.1705 \\ 0.1643 & 0.6544 \end{pmatrix}$
	Classification	0.8	$\begin{pmatrix} 0.95 & 0.05 \\ 0.05 & 0.95 \end{pmatrix}$	-	$\begin{pmatrix} 0.6404 & 0.1473 \\ 0.1408 & 0.6638 \end{pmatrix}$	$\begin{pmatrix} 0.6937 & 0.1417 \\ 0.1380 & 0.6879 \end{pmatrix}$
	Kinematic and Classification	0.8	$\begin{pmatrix} 0.95 & 0.05 \\ 0.05 & 0.95 \end{pmatrix}$	-	$\begin{pmatrix} 0.6683 & 0.1352 \\ 0.1345 & 0.6816 \end{pmatrix}$	$\begin{pmatrix} 0.6741 & 0.1204 \\ 0.1163 & 0.6882 \end{pmatrix}$
	Amplitude	0.8	-	20 & 16	$\begin{pmatrix} 0.6717 & 0.1427 \\ 0.1496 & 0.6884 \end{pmatrix}$	$\begin{pmatrix} 0.6815 & 0.1139 \\ 0.1182 & 0.6992 \end{pmatrix}$
	Kinematic and Amplitude	0.8	-	20 & 16	$\begin{pmatrix} 0.7330 & 0.0972 \\ 0.0881 & 0.7346 \end{pmatrix}$	$\begin{pmatrix} 0.7012 & 0.1007 \\ 0.1040 & 0.7185 \end{pmatrix}$

swap whereas kinematic & classification and kinematic & amplitude version revert the detected swap as shown in Figures 4.4(d) (4.5(c)), 4.4(e) (4.5(d)), and 4.4(f) (4.5(e)), respectively. The position and velocity RMSE values are compared in Figures 4.6 and 4.7, respectively. Similarly to the earlier discussion, it can be clearly seen that versions which use classification or amplitude information in addition to kinematic information perform better by significantly reducing the RMSE errors for each of the target.

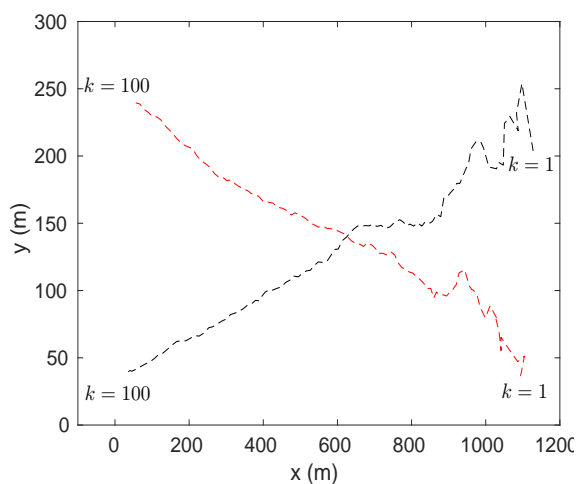
Table 4.3 shows the comparisons of track purity matrices obtained prior to post-processing and after post-processing for Scenario 3 shown in Figure 4.8. As there are broken tracks in this scenario, the existing TSA algorithm (Raghu et al. 2018) can be compared with the proposed algorithm. Since the existing TSA algorithm (Raghu



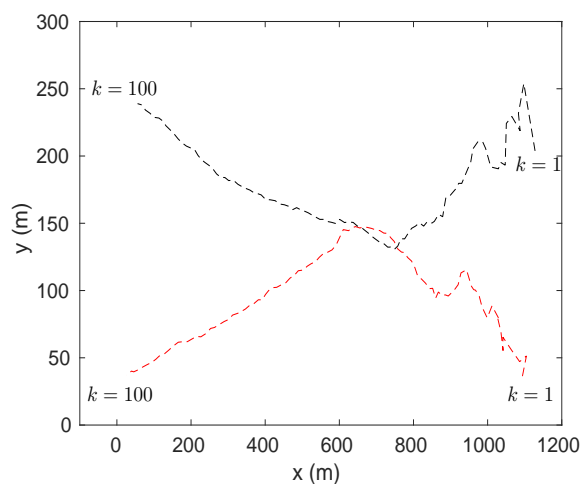
(a) Ground truth



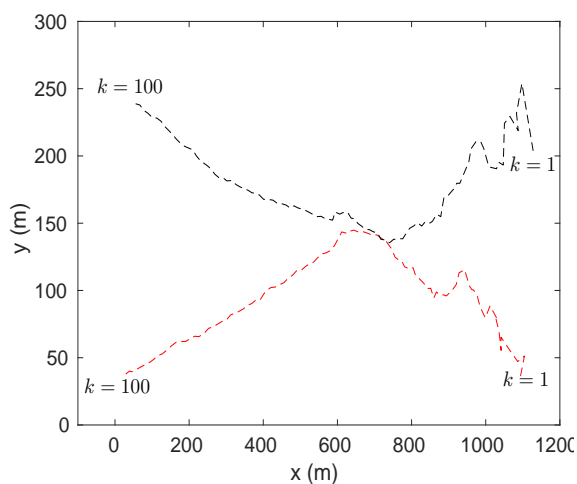
(b) Tracking with known M2T association



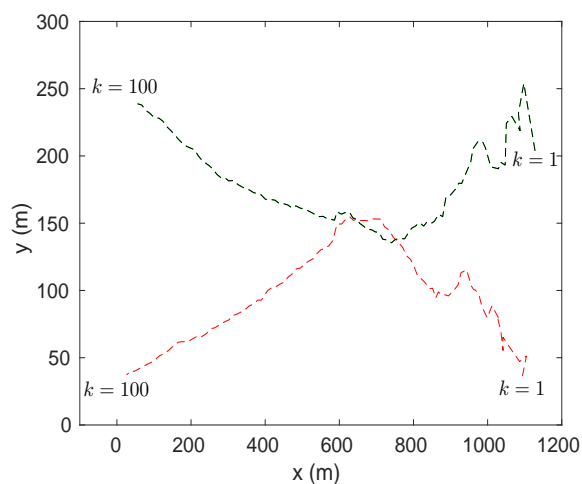
(c) Estimated trajectories prior to post-processing



(d) Post-processing using kinematic information (κ)

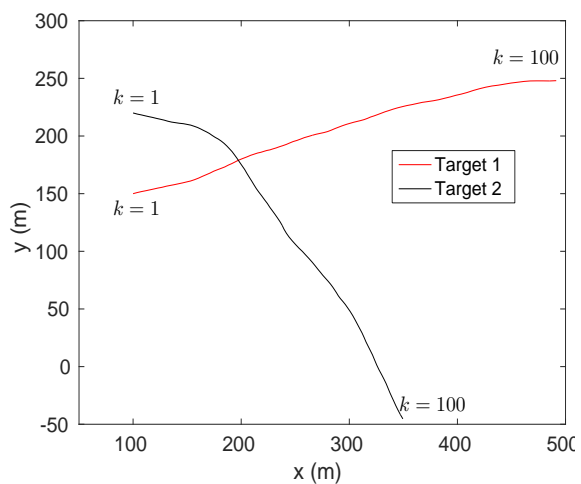


(e) Post-processing using kinematic & classification information ($\kappa + \beta$)

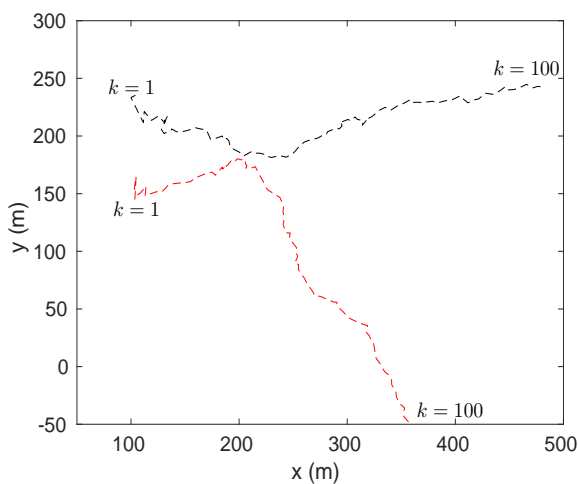


(f) Post-processing using kinematic & amplitude information ($\kappa + \alpha$)

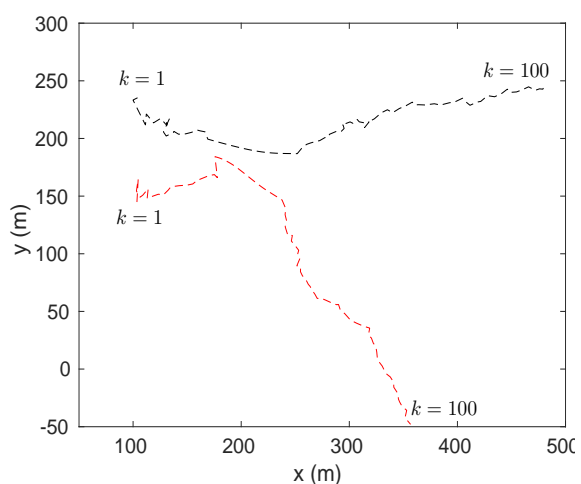
Figure 4.4: Track un-swapping: Two target case (Scenario 1)



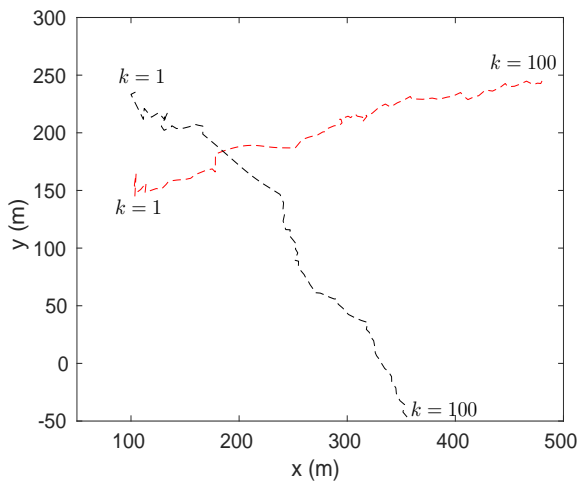
(a) Ground truth



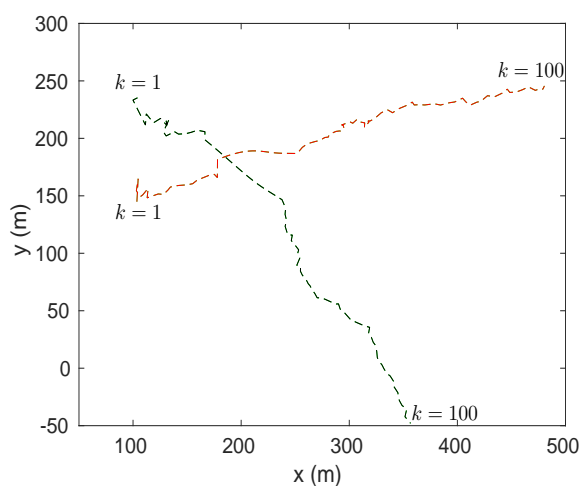
(b) Tracks prior to post-processing



(c) Post-processing using kinematic information (κ)



(d) Post-processing using kinematic & classification information ($\kappa + \beta$)



(e) Post-processing using kinematic & amplitude information ($\kappa + \alpha$)

Figure 4.5: Track un-swapping: Two target case (Scenario 2)

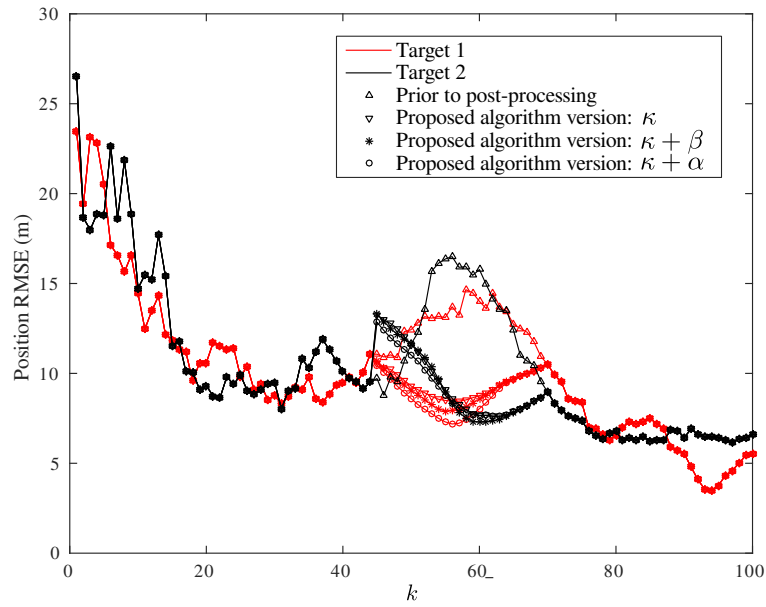


Figure 4.6: Position RMSE (Scenario 1)

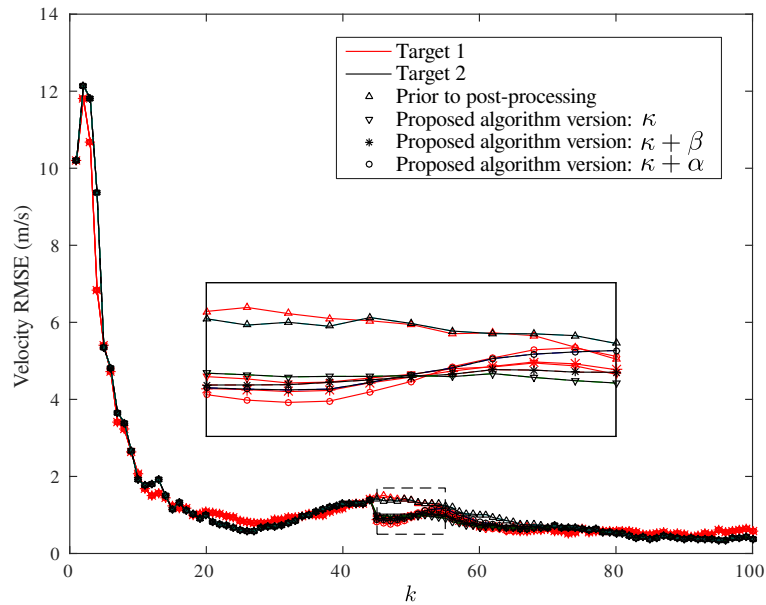


Figure 4.7: Velocity RMSE (Scenario 1)

et al. 2018) always seeks for already broken tracks and it has nothing to do with the non-broken tracks, it will always make a decision that broken track segments (black in color) are from same target and stitch them even though they are actually not form the same target. As a result, it produces poor track purity matrices. Whereas the proposed algorithm considers already broken tracks in addition to broken tracks resulting from the detection of switch/swap simultaneously for TSA and thus it gives better track purity matrices as shown in Table 4.3.

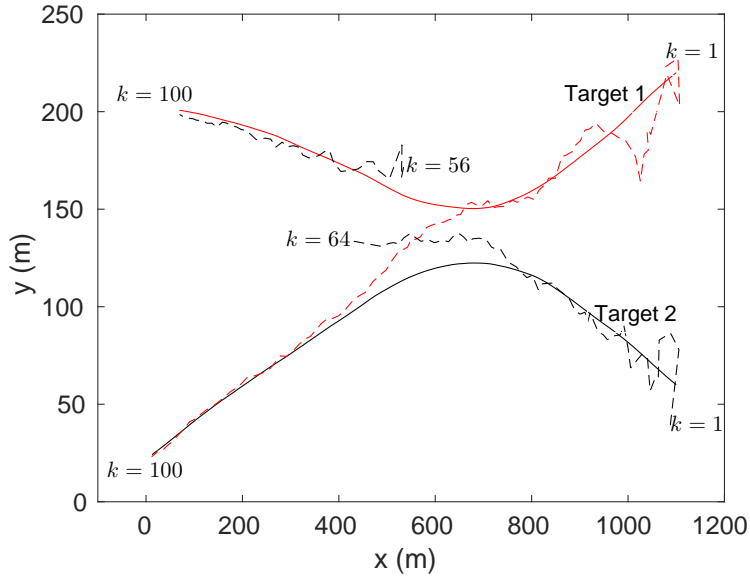


Figure 4.8: Two target case (Scenario 3): track swapping after breakage

Table 4.3: Two target case (Scenario 3): Track Purity Matrices $\{\Pi\}$ ($B = 10$, $\tau = 4.3324$, $P_{FA} = 8.3975 \times 10^{-5}$, 100 Monte Carlo runs)

Algorithm Used for Post-processing		Parameter			Track Purity Matrix Π
		P_D	\mathbb{C}	d (dB)	
Prior to Post-processing		0.8	–	–	$\begin{pmatrix} 0.4540 & 0.3677 & 0.3840 \\ 0.3885 & 0.4441 & 0.3814 \end{pmatrix}$
Existing TSA algorithm (Raghu et al. 2018)		0.8	–	–	$\begin{pmatrix} 0.4432 & 0.3747 \\ 0.3777 & 0.4304 \end{pmatrix}$
Version of Proposed Algorithm	Kinematic	0.8	–	–	$\begin{pmatrix} 0.6665 & 0.1853 \\ 0.1925 & 0.6546 \end{pmatrix}$
	Classification	0.8	$\begin{pmatrix} 0.95 & 0.05 \\ 0.05 & 0.95 \end{pmatrix}$	–	$\begin{pmatrix} 0.6564 & 0.1687 \\ 0.1520 & 0.6601 \end{pmatrix}$
	Kinematic and Classification	0.8	$\begin{pmatrix} 0.95 & 0.05 \\ 0.05 & 0.95 \end{pmatrix}$	–	$\begin{pmatrix} 0.6889 & 0.1526 \\ 0.1531 & 0.6684 \end{pmatrix}$
	Amplitude	0.8	–	20 & 16	$\begin{pmatrix} 0.6370 & 0.1528 \\ 0.1740 & 0.6792 \end{pmatrix}$
	Kinematic and Amplitude	0.8	–	20 & 16	$\begin{pmatrix} 0.7421 & 0.0968 \\ 0.1273 & 0.7518 \end{pmatrix}$

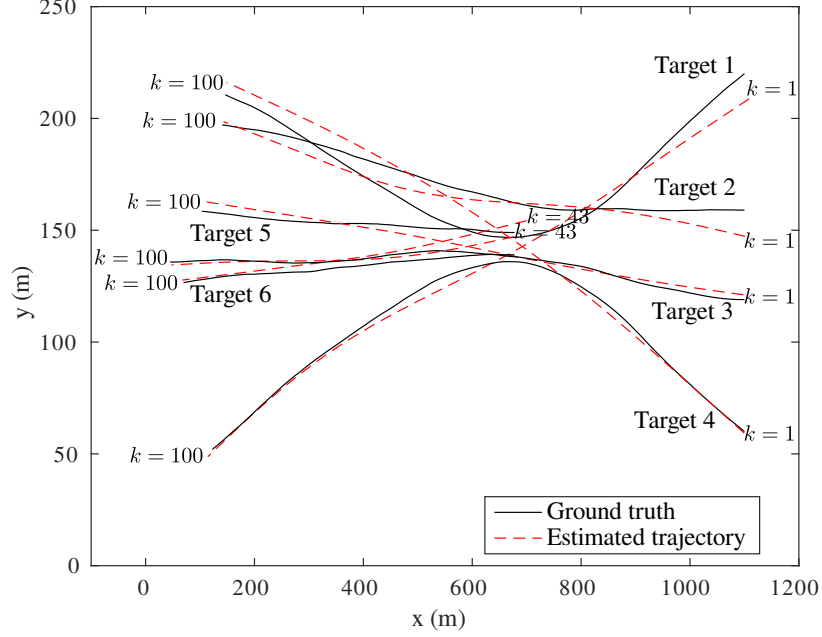


Figure 4.9: Track swapping: Multi-target case

4.6.5 Multiple Target Case

In this section, in order to validate the different versions of proposed algorithm for multiple target case, six targets are simulated and tracks are obtained as shown in the Figure 4.9 and post-processing techniques are applied for different classification and amplitude information cases.

A Scenario 1

Each of the target 1–6 belong to the class 1–6, respectively, with the classifier output accuracy given by the confusion matrix

$$\mathbb{C}_1 = \begin{pmatrix} 0.95 & 0.01 & 0.01 & 0.01 & 0.01 & 0.01 \\ 0.01 & 0.95 & 0.01 & 0.01 & 0.01 & 0.01 \\ 0.01 & 0.01 & 0.95 & 0.01 & 0.01 & 0.01 \\ 0.01 & 0.01 & 0.01 & 0.95 & 0.01 & 0.01 \\ 0.01 & 0.01 & 0.01 & 0.01 & 0.95 & 0.01 \\ 0.01 & 0.01 & 0.01 & 0.01 & 0.01 & 0.95 \end{pmatrix} \quad (4.50)$$

and each of the target 1–6 have SNR given in an order by

$$d_1 = (20\text{dB} \ 19\text{dB} \ 18\text{dB} \ 17\text{dB} \ 16\text{dB} \ 15\text{dB}). \quad (4.51)$$

Off six targets, two targets are born at midway (see Figure 4.9) so as to have swaps while tracking targets real time.

Different versions of post processing algorithms are applied to un-swap the tracks and the resulting track purity matrices are in (4.52)–(4.57). Prior to post-processing, each track purity is in the range of 0.39–0.53 (see the diagonal elements of a matrix). This means that only about 50% of the total measurements associated with a particular track are from the same target and the rest of the measurements are either from other targets or false alarms. Ideally, the track purity should be one, however, due to practical limitations which may not be possible.

Tracks were reconsidered for checking possible track swaps, there is slight improvement and the track purity jumps to the range 0.53–0.59 when only the kinematic information is considered. The track purity further enhances to 0.64–0.68 when only the classification information is considered. This is because, each of the target belongs to a separate class and hence there is less ambiguity in associating two broken track segments. Further, track purity goes to the range 0.70–0.74 when both the kinematic and classification information are used simultaneously and this happens because of obvious reason of more information available.

Similar to the classification and kinematic & classification versions, amplitude and kinematic & amplitude versions show improvement over the kinematic version. However, version with amplitude information is slightly inferior to the version with classification information. This is because, in the former case though each target belongs to different SNR the difference in the SNR value is small (unlike two target case, where difference is 4dB).

$$\begin{aligned}
 & [\mathbf{\Pi}_{mn}]_{\text{Prior to post-processing}} \\
 & = \begin{pmatrix}
 \mathbf{0.4815} & 0.0733 & 0.0730 & 0.0859 & 0.0476 & 0.1390 \\
 0.0538 & \mathbf{0.5354} & 0.1246 & 0.0309 & 0.0780 & 0.0865 \\
 0.0723 & 0.0154 & \mathbf{0.4576} & 0.0692 & 0.0063 & 0.0855 \\
 0.0435 & 0.0718 & 0.0882 & \mathbf{0.4871} & 0.0674 & 0.0572 \\
 0.0706 & 0.0347 & 0.0341 & 0.0466 & \mathbf{0.4970} & 0.0778 \\
 0.0909 & 0.0648 & 0.0402 & 0.0602 & 0.0557 & \mathbf{0.3965}
 \end{pmatrix} \quad (4.52)
 \end{aligned}$$

$$\begin{aligned}
& [\mathbf{\Pi}_{mn}]_{\text{Kinematic } (\kappa)} \\
& = \begin{pmatrix}
\mathbf{0.5548} & 0.0433 & 0.0597 & 0.1384 & 0.0391 & 0.0568 \\
0.0497 & \mathbf{0.5795} & 0.0710 & 0.0787 & 0.0050 & 0.0735 \\
0.0461 & 0.0773 & \mathbf{0.5937} & 0.0253 & 0.0558 & 0.1194 \\
0.0567 & 0.0572 & 0.0079 & \mathbf{0.5128} & 0.0474 & 0.0254 \\
0.0297 & 0.0317 & 0.0599 & 0.0205 & \mathbf{0.5722} & 0.0383 \\
0.0564 & 0.0144 & 0.0271 & 0.0277 & 0.0559 & \mathbf{0.5311}
\end{pmatrix} \quad (4.53)
\end{aligned}$$

$$\begin{aligned}
& [\mathbf{\Pi}_{mn}]_{\text{Classification } (\beta), \mathbb{C}=\mathbb{C}_1} \\
& = \begin{pmatrix}
\mathbf{0.6887} & 0.0253 & 0.0270 & 0.0537 & 0.0330 & 0.0237 \\
0.0148 & \mathbf{0.6668} & 0.0205 & 0.0231 & 0.0418 & 0.0122 \\
0.0293 & 0.0338 & \mathbf{0.6984} & 0.0059 & 0.0025 & 0.0032 \\
0.0063 & 0.0454 & 0.0164 & \mathbf{0.6534} & 0.0396 & 0.0549 \\
0.0090 & 0.0140 & 0.0140 & 0.0374 & \mathbf{0.6419} & 0.0194 \\
0.0263 & 0.0031 & 0.0052 & 0.0332 & 0.0417 & \mathbf{0.6870}
\end{pmatrix} \quad (4.54)
\end{aligned}$$

$$\begin{aligned}
& [\mathbf{\Pi}_{mn}]_{\text{Kinematic and classification } (\kappa + \beta), \mathbb{C}=\mathbb{C}_1} \\
& = \begin{pmatrix}
\mathbf{0.7116} & 0.0154 & 0.0025 & 0.0371 & 0.0037 & 0.0031 \\
0.0046 & \mathbf{0.7226} & 0.0091 & 0.0020 & 0.0174 & 0.0120 \\
0.0319 & 0.0178 & \mathbf{0.7473} & 0.0123 & 0.0277 & 0.0215 \\
0.0279 & 0.0089 & 0.0194 & \mathbf{0.7047} & 0.0158 & 0.0151 \\
0.0096 & 0.0141 & 0.0221 & 0.0373 & \mathbf{0.7116} & 0.0153 \\
0.0197 & 0.0304 & 0.0079 & 0.0169 & 0.0122 & \mathbf{0.7366}
\end{pmatrix} \quad (4.55)
\end{aligned}$$

$$\begin{aligned}
& [\mathbf{\Pi}_{mn}]_{\text{Amplitude } (\alpha), d=d_1} \\
& = \begin{pmatrix}
\mathbf{0.6243} & 0.0007 & 0.0106 & 0.0530 & 0.0282 & 0.0226 \\
0.0170 & \mathbf{0.6399} & 0.0379 & 0.0526 & 0.0173 & 0.0562 \\
0.0243 & 0.0456 & \mathbf{0.6475} & 0.0066 & 0.0367 & 0.0523 \\
0.0365 & 0.0327 & 0.0233 & \mathbf{0.6317} & 0.0281 & 0.0215 \\
0.0494 & 0.0526 & 0.0605 & 0.0287 & \mathbf{0.6435} & 0.0478 \\
0.0463 & 0.0232 & 0.0205 & 0.0132 & 0.0311 & \mathbf{0.6120}
\end{pmatrix} \quad (4.56)
\end{aligned}$$

$$\begin{aligned}
& [\mathbf{\Pi}_{mn}]_{\text{Kinematic and amplitude } (\kappa + \alpha), d=d_1} \\
& = \begin{pmatrix} \mathbf{0.6860} & 0.0351 & 0.0092 & 0.0523 & 0.1725 & 0.0128 \\ 0.0172 & \mathbf{0.6656} & 0.0269 & 0.0171 & 0.0935 & 0.0203 \\ 0.0044 & 0.0380 & \mathbf{0.6591} & 0.0179 & 0.0850 & 0.0510 \\ 0.0169 & 0.0374 & 0.0704 & \mathbf{0.6541} & 0.0820 & 0.0212 \\ 0.0138 & 0.0140 & 0.0335 & 0.0158 & \mathbf{0.6463} & 0.0423 \\ 0.0273 & 0.0138 & 0.0183 & 0.0369 & 0.0552 & \mathbf{0.6531} \end{pmatrix} \quad (4.57)
\end{aligned}$$

B Scenario 2

Each of the target 1–6 belong to the class 1, 2, 3, 4, 5, and 1, respectively, with the classifier output accuracy given by the confusion matrix

$$\mathbb{C}_2 = \begin{pmatrix} 0.96 & 0.01 & 0.01 & 0.01 & 0.01 \\ 0.01 & 0.96 & 0.01 & 0.01 & 0.01 \\ 0.01 & 0.01 & 0.96 & 0.01 & 0.01 \\ 0.01 & 0.01 & 0.01 & 0.96 & 0.01 \\ 0.01 & 0.01 & 0.01 & 0.01 & 0.96 \end{pmatrix} \quad (4.58)$$

and each of the target 1–6 have SNR given in an order by

$$d_2 = (20\text{dB} \ 19\text{dB} \ 18\text{dB} \ 17\text{dB} \ 16\text{dB} \ 20\text{dB}). \quad (4.59)$$

The difference between Scenario 1 and 2 is that in former case all the targets 1–6 belong to separate class and SNR whereas in the latter case targets 1–5 belong to separate class and SNR, and target 6 belongs to same category as that of target 1. Therefore when classification or amplitude information is used to connect that tracks of target 1 and 6, track swapping is introduced by erroneously connecting tracks of different targets and hence reducing the track purity as shown in matrices of (4.60)–(4.65) (see the highlighted diagonal elements). However, this track purity can be maximized by utilizing additional kinematic information. Thus, it is preferable to use proposed classification or amplitude version alone whenever the targets belong to unique category but not otherwise. However, combined versions — kinematic & classification and kinematic & amplitude — work reasonably well in either scenarios.

$$\begin{aligned}
& [\mathbf{\Pi}_{mn}]_{\text{Prior to post-processing}} \\
& = \begin{pmatrix}
\mathbf{0.4691} & 0.1303 & 0.0561 & 0.0238 & 0.0490 & 0.1471 \\
0.0893 & \mathbf{0.4632} & 0.0993 & 0.0895 & 0.1296 & 0.0894 \\
0.0515 & 0.0636 & \mathbf{0.4948} & 0.1219 & 0.1017 & 0.1029 \\
0.0538 & 0.0885 & 0.1029 & \mathbf{0.5133} & 0.0955 & 0.1345 \\
0.0400 & 0.0108 & 0.0799 & 0.0556 & \mathbf{0.3118} & 0.0948 \\
0.1165 & 0.0331 & 0.0871 & 0.0285 & 0.0858 & \mathbf{0.3531}
\end{pmatrix} \quad (4.60)
\end{aligned}$$

$$\begin{aligned}
& [\mathbf{\Pi}_{mn}]_{\text{Kinematic } (\kappa)} \\
& = \begin{pmatrix}
\mathbf{0.5671} & 0.0557 & 0.0568 & 0.0837 & 0.0133 & 0.0979 \\
0.0979 & \mathbf{0.5420} & 0.0432 & 0.0358 & 0.0111 & 0.0589 \\
0.0552 & 0.0352 & \mathbf{0.6064} & 0.0639 & 0.0891 & 0.0412 \\
0.0467 & 0.0405 & 0.1105 & \mathbf{0.5360} & 0.0257 & 0.0471 \\
0.0215 & 0.0920 & 0.0269 & 0.0546 & \mathbf{0.5996} & 0.0942 \\
0.0509 & 0.0114 & 0.0438 & 0.0656 & 0.0734 & \mathbf{0.5422}
\end{pmatrix} \quad (4.61)
\end{aligned}$$

$$\begin{aligned}
& [\mathbf{\Pi}_{mn}]_{\text{Classification } (\beta), \mathbb{C}=\mathbb{C}_2} \\
& = \begin{pmatrix}
\mathbf{0.4176} & 0.0224 & 0.0067 & 0.0224 & 0.0172 & 0.3050 \\
0.0030 & \mathbf{0.7283} & 0.0966 & 0.0377 & 0.0886 & 0.0023 \\
0.0355 & 0.0161 & \mathbf{0.7366} & 0.0074 & 0.1161 & 0.0332 \\
0.0243 & 0.0281 & 0.0117 & \mathbf{0.6944} & 0.1327 & 0.0166 \\
0.0169 & 0.0147 & 0.0265 & 0.0204 & \mathbf{0.7005} & 0.0787 \\
0.3236 & 0.0150 & 0.0062 & 0.0101 & 0.0914 & \mathbf{0.4369}
\end{pmatrix} \quad (4.62)
\end{aligned}$$

$$\begin{aligned}
& [\mathbf{\Pi}_{mn}]_{\text{Kinematic and classification } (\kappa + \beta), \mathbb{C}=\mathbb{C}_2} \\
& = \begin{pmatrix}
\mathbf{0.5288} & 0.0003 & 0.0469 & 0.0207 & 0.0067 & 0.2929 \\
0.0360 & \mathbf{0.7877} & 0.0483 & 0.0078 & 0.0264 & 0.0838 \\
0.0020 & 0.0074 & \mathbf{0.7841} & 0.0113 & 0.0171 & 0.0110 \\
0.0147 & 0.0066 & 0.0179 & \mathbf{0.7554} & 0.0189 & 0.0420 \\
0.0209 & 0.0081 & 0.0154 & 0.0102 & \mathbf{0.7643} & 0.0751 \\
0.2359 & 0.0021 & 0.0207 & 0.0228 & 0.0841 & \mathbf{0.4917}
\end{pmatrix} \quad (4.63)
\end{aligned}$$

$$\begin{aligned}
& [\mathbf{\Pi}_{mn}]_{\text{Amplitude } (\alpha), d=d_2} \\
& = \begin{pmatrix}
\mathbf{0.3889} & 0.0446 & 0.0244 & 0.0258 & 0.0502 & 0.2441 \\
0.0263 & \mathbf{0.6465} & 0.0116 & 0.0390 & 0.0149 & 0.1041 \\
0.0166 & 0.0384 & \mathbf{0.6764} & 0.0053 & 0.0063 & 0.0196 \\
0.0216 & 0.0512 & 0.0129 & \mathbf{0.6966} & 0.0757 & 0.0348 \\
0.0317 & 0.0395 & 0.0458 & 0.0100 & \mathbf{0.6361} & 0.0829 \\
0.3535 & 0.0186 & 0.0217 & 0.0267 & 0.0691 & \mathbf{0.4189}
\end{pmatrix} \quad (4.64)
\end{aligned}$$

$$\begin{aligned}
& [\mathbf{\Pi}_{mn}]_{\text{Kinematic and amplitude } (\kappa + \alpha), d=d_2} \\
& = \begin{pmatrix}
\mathbf{0.4835} & 0.0335 & 0.0261 & 0.0115 & 0.0137 & 0.2160 \\
0.0044 & \mathbf{0.6711} & 0.0190 & 0.0276 & 0.0136 & 0.0179 \\
0.0161 & 0.0264 & \mathbf{0.6900} & 0.0170 & 0.0067 & 0.0453 \\
0.0217 & 0.0189 & 0.0632 & \mathbf{0.7121} & 0.1155 & 0.0503 \\
0.0555 & 0.0341 & 0.0459 & 0.0188 & \mathbf{0.6906} & 0.0897 \\
0.2495 & 0.0233 & 0.0444 & 0.0131 & 0.0324 & \mathbf{0.5184}
\end{pmatrix} \quad (4.65)
\end{aligned}$$

4.7 SUMMARY

Problem is formulated to initially group the tracks into (regular) broken and non-broken tracks (continuous tracks). These continuous tracks might have track swaps among themselves or swaps with one or more regular broken tracks. To address these issues, track swap detection procedure is presented. Eventually, the track stitching is carried-out considering both regular and algorithmically broken tracks due to swap detection simultaneously.

Likelihood ratio and cost calculation associated with track pair is discussed. Similarly, the classification and amplitude information modeling procedures and their associated cost calculation procedures are presented in Section 4.4 and Section 4.5, respectively. Whereas the results and discussions for two target and multiple target scenarios are presented in Section 4.6.

The next chapter presents overall conclusions and future research work that can be carried out for further improvements.

Chapter 5

CONCLUSIONS AND FUTURE WORK

5.1 CONCLUSIONS

Two novel TSA approaches that can successfully stitch broken tracks caused by a highly maneuvering target, association with incorrect measurements, low detection probability, close target formations, large measurement errors, long sampling intervals, and so on, are presented. Both approaches use a combination of CV and CT models subject to a single turn during the breakage period. The first approach bridges the two track segments by forward prediction and backward retrodiction, whereas the second approach estimates the missing part of the track by utilizing both instantly released and unassociated measurements. Fractured tracks can be stitched even if the young track segment is initialized before the termination of its associated old track segment, which is not the case with existing approaches.

It was demonstrated that the proposed approaches outperform existing TSA approaches by exploring the possible false measurement association, which causes track termination, significantly improving track continuity, and maintaining a consistent track ID. It was also shown that the proposed multi-frame TSA approach yields better association results compared to the proposed two-dimensional TSA approach in a multitarget scenario.

In target tracking, very often one encounters mismatch in target-to-track mappings due to updating measurements from a different target, approximation of the true Bayesian update of the target state distribution that the track state represents, incorrect association with successive clutter measurements, and poor track-to-measurement

association techniques, among other causes. In this thesis, different versions of proposed algorithm which utilize one or more of the following information available: kinematic, classification, and amplitude to aid the tracker in un-switching and un-swapping tracks are presented. These techniques improve overall tracker performance by successfully: detecting and reverting the swapped target-to-track mappings; avoiding introducing new track swaps if there is no reversion in target-to-track mappings; and reducing the RMSE errors.

5.2 FUTURE WORK

The proposed algorithms can be extended to consider the case where there exist two or more tracks pertaining to same target at the same time. Presently, each of such track is assumed to be originated from different target. Instead, these kind of tracks need to be detected and fused and then the resulting track can be used for association with another track segment.

Another possible improvement for proposed track un-switching algorithms is to adopt the variable window size so as to gather better information for better association results, particularly, for closely spaced moving targets.

In practical tracking applications, it is always handy to utilize the prior target birth and death rate information in addition to kinematic and non-kinematic information. This additional information can avoid associating tracks which are from two different targets with similar kinematic, classification, and amplitude information. In addition to the above, the varied probability of detection with respect amplitude can also be considered to improve track stitching and unswapping performance further.

In all the proposed approaches model parameters such as turn rate, starting and ending time of turn are obtained subject to a single turn during the breakage period. However, practically target can undergo multiple maneuvers and produce segmented tracks across time and hence in such cases considering more than single turn for estimating parameters is going to be potential future research problem.

Bibliography

- Angelova, D. and Mihaylova, L. (2006). “Joint target tracking and classification with particle filtering and mixture kalman filtering using kinematic radar information.” *Digital Signal Processing*, 16(2), 180 – 204.
- Arnold, J., Bar-Shalom, Y., and Mucci, R. (1984). “Track segment association with a distributed field of sensors.” *American Control Conference, 1984*, IEEE, 605–612.
- Bar-Shalom, Y., Blackman, S. S., and Fitzgerald, R. J. (2007). “Dimensionless score function for multiple hypothesis tracking.” *IEEE Transactions on Aerospace and Electronic Systems*, 43(1), 392–400.
- Bar-Shalom, Y., Kirubarajan, T., and Gokberk, C. (2005). “Tracking with classification-aided multiframe data association.” *IEEE Transactions on Aerospace and Electronic Systems*, 41(3), 868–878.
- Bar-Shalom, Y., Li, X. R., and Kirubarajan, T. (2004). *Estimation with Applications to Tracking and Navigation: Theory Algorithms and Software*. John Wiley & Sons.
- Bar-Shalom, Y., Willett, P. K., and Tian, X. (2011). *Tracking and Data Fusion*. YBS publishing.
- Bharadwaj, P., Runkle, P., Carin, L., Berrie, J. A., and Hughes, J. A. (2001). “Multiaspect classification of airborne targets via physics-based hmms and matching pursuits.” *IEEE Transactions on Aerospace and Electronic Systems*, 37(2), 595–606.
- Blackman, S. and Popoli, R. (1999). *Design and Analysis of Modern Tracking Systems*. Norwood, MA: Artech House.

- Blom, H. A. and Bloem, E. A. (2011). “Decomposed particle filtering and track swap estimation in tracking two closely spaced targets.” *Proceedings of the 14th International Conference on Information Fusion (FUSION)*, ISIF, 1–8.
- Castella, F. R. (1976). “Sliding window detection probabilities.” *IEEE Transactions on Aerospace and Electronic Systems*, AES-12(6), 815–819.
- Castñón, G. and Finn, L. (2011). “Multi-target tracklet stitching through network flows.” *Aerospace Conference*, IEEE, 1–7.
- Coraluppi, S. (2005). “Analysis of tracker performance models for centralized and distributed tracking.” *7th International Conference on Information Fusion (FUSION)*, Vol. 2, 1404–1411 (July).
- Davey, S. J. (2013). “SNR limits on Kalman filter detect-then-track.” *IEEE Signal Processing Letters*, 20(8), 767–770.
- Davey, S. J., Rutten, M. G., and Cheung, B. (2012). “Using phase to improve track-before-detect.” *IEEE Transactions on Aerospace and Electronic Systems*, 48(1), 832–849.
- Deb, S., Yeddanapudi, M., Pattipati, K., and Bar-Shalom, Y. (1997). “A generalized SD assignment algorithm for multisensor-multitarget state estimation.” *IEEE Transactions on Aerospace and Electronic Systems*, 33(2), 523–538.
- Dezert, J. and Kirubarajan, T. (1999). “Performance evaluation of a 2/2 times; m/n logic for track formation in clutter using a bi-band imaging sensor.” *IEE Colloquium on Target Tracking: Algorithms and Applications (Ref. No. 1999/090, 1999/215)*, 15/1–15/4.
- Drummond, O. E. (1997). “Hybrid sensor fusion algorithm architecture and tracklets.” *International Symposium on Optical Science, Engineering, and Instrumentation*, 485–502.
- Fanaswala, M. and Krishnamurthy, V. (2014). “Syntactic models for trajectory constrained track-before-detect.” *IEEE Transactions on Signal Processing*, 62(23), 6130–6142.

- Fortmann, T., Bar-Shalom, Y., Scheffe, M., and Gelfand, S. (1985). “Detection thresholds for tracking in clutter—a connection between estimation and signal processing.” *IEEE Transactions on Automatic Control*, 30(3), 221–229.
- Goldsmith, A. (2005). *Wireless communications*. Cambridge university press.
- Grossi, E., Lops, M., and Venturino, L. (2013). “A novel dynamic programming algorithm for track-before-detect in radar systems.” *IEEE Transactions on Signal Processing*, 61(10), 2608–2619.
- Ji, S., Liao, X., and Carin, L. (2005). “Adaptive multiaspect target classification and detection with hidden markov models.” *IEEE Sensors Journal*, 5(5), 1035–1042.
- Kirubarajan, T. and Bar-Shalom, Y. (1996). “Low observable target motion analysis using amplitude information.” *IEEE Transactions on Aerospace and Electronic Systems*, 32(4), 1367–1384.
- Kirubarajan, T., Bar-Shalom, Y., McAllister, R., Schutz, R., and Engelberg, B. (1999). “Multitarget tracking using an IMM estimator with debiased E-2C measurements for AEW systems.” *Proceedings of the 2nd International Conference on Information Fusion (FUSION)*.
- Lerro, D. and Bar-Shalom, Y. (1993). “Interacting multiple model tracking with target amplitude feature.” *IEEE Transactions on Aerospace and Electronic Systems*, 29(2), 494–509.
- Li, N. and Li, X. R. (2001). “Tracker design based on target perceivability.” *IEEE Transactions on Aerospace and Electronic Systems*, 37(1), 214–225.
- McAnanama, J. and Kirubarajan, T. (2012). “A multiple hypothesis tracker with interacting feature extraction.” *Signal Processing*, 92(12), 2962 – 2974.
- McDonald, M. and Balaji, B. (2011). “Impact of measurement model mismatch on nonlinear track-before-detect performance for maritime radar surveillance.” *IEEE Journal of Oceanic Engineering*, 36(4), 602–614.

- Mei, W., Shan, G., and Li, X. R. (2007). “Simultaneous tracking and classification: a modularized scheme.” *IEEE Transactions on Aerospace and Electronic Systems*, 43(2), 581–599.
- Mellema, G. R. (2002). “An automated approach to passive sonar track segment association.” *Proceedings of the 7th International Command and Control Research and Technology Symposium, Québec City, Canada*.
- Mori, S., Chang, K.-C., and Chong, C.-Y. (2012). “Comparison of track fusion rules and track association metrics.” *15th International Conference on Information Fusion (FUSION)*, ISIF, 1996–2003.
- Mori, S. and Chong, C.-Y. (2013). “Performance analysis of graph-based track stitching.” *16th International Conference on Information Fusion (FUSION)*, ISIF, 196–203.
- Musicki, D., Evans, R., and Stankovic, S. (1994). “Integrated probabilistic data association.” *IEEE Transactions on Automatic Control*, 39(6), 1237–1241.
- Musicki, D. and Song, T. L. (2013). “Track initialization: prior target velocity and acceleration moments.” *IEEE Transactions on Aerospace and Electronic Systems*, 1(49), 665–670.
- Pannetier, B. and Dezert, J. (2012). “Track segment association with classification information.” *Workshop on Sensor Data Fusion: Trends, Solutions, Applications (SDF)*, IEEE, 60–65.
- Pattipati, K., Kirubarajan, T., and Popp, R. (2000). “Survey of assignment techniques for multitarget tracking.” *Multitarget-multisensor Tracking: Applications and Advances*, Vol. 3, 77–159.
- Pattipati, K. R., Deb, S., Bar-Shalom, Y., and Washburn, R. B. (1992). “A new relaxation algorithm and passive sensor data association.” *IEEE Transactions on Automatic Control*, 37(2), 198–213.
- Poore, A. B. (1994). “Multidimensional assignment formulation of data association

- problems arising from multitarget and multisensor tracking.” *Computational Optimization and Applications*, 3(1), 27–57.
- Popp, R. L., Pattipati, K. R., and Bar-Shalom, Y. (2001). “ m -best S -D assignment algorithm with application to multitarget tracking.” *IEEE Transactions on Aerospace and Electronic Systems*, 37(1), 22–39.
- Pulford, G. W. and Scala, B. F. L. (2010). “Multihypothesis viterbi data association: Algorithm development and assessment.” *IEEE Transactions on Aerospace and Electronic Systems*, 46(2), 583–609.
- Raghu, J., Srihari, P., Tharmarasa, R., and Kirubarajan, T. (2018). “Comprehensive track segment association for improved track continuity.” *IEEE Transactions on Aerospace and Electronic Systems*, PP(99), 1–1. doi: 10.1109/TAES.2018.2820364.
- Ragi, S. and Chong, E. K. P. (2012). “Dynamic UAV path planning for multitarget tracking.” *2012 American Control Conference (ACC)*, 3845–3850 (June).
- Ristic, B., Gordon, N., and Bessell, A. (2004). “On target classification using kinematic data.” *ISIF Journal of Advances in Information Fusion*, 5(1), 15 – 21.
- Runkle, P. R., Bharadwaj, P. K., Couchman, L., and Carin, L. (1999). “Hidden markov models for multiaspect target classification.” *IEEE Transactions on Signal Processing*, 47(7), 2035–2040.
- Schutz, R., McAllister, R., Engelberg, B., Maone, V., Helm, R., Kats, V., Dennean, C., Soper, W., and Moran, L. (1997). “Combined Kalman filter (CKF) and JVC algorithms for AEW target tracking applications.” *Proceeding of the SPIE Conference on Signal and Data Processing of Small Targets*, Vol. 3163, 164–176.
- Shijun, Y., Peng, X., Ying, L., and Jinbiao, C. (2010). “An algorithm for reducing the swap of targets during the marine radar tracking.” *2010 IEEE International Conference on Intelligent Computing and Intelligent Systems*, Vol. 3, 760–764 (Oct).
- Sinha, A., Ding, Z., Kirubarajan, T., and Farooq, M. (2012). “Track quality based multitarget tracking approach for global nearest-neighbor association.” *IEEE Transactions on Aerospace and Electronic Systems*, 48(2), 1179–1191.

- Sinha, A. and Peters, D. J. (2009). “Flexible ID association-based tracking algorithm.” *12th International Conference on Information Fusion (FUSION)*, ISIF, 2161–2168.
- Song, T. L. and Kim, D. S. (2006). “Highest probability data association for active sonar tracking.” *9th International Conference on Information Fusion (FUSION)*, 1–8 (July).
- Song, T. L., Musicki, D., and Kim, Y. (2013). “Tracking through occlusions and track segmentation reduction.” *IEEE Transactions on Aerospace and Electronic Systems*, 49(1), 623–631.
- Van der Merwe, L. and De Villiers, J. (2013). “Track-stitching using graphical models and message passing.” *16th International Conference on Information Fusion (FUSION)*, ISIF, 758–765.
- Yeom, S. W., Kirubarajan, T., and Bar-Shalom, Y. (2004). “Track segment association, fine-step IMM and initialization with Doppler for improved track performance.” *IEEE Transactions on Aerospace and Electronic Systems*, 40(1), 293–309.
- Zhang, J., Liang, Y., and Chongyang, H. (2015). “Track segment association based on expectation-maximization algorithm for joint estimate and identification.” *Proceedings of International Conference on Intelligent Unmanned Systems*, Vol. 11.
- Zhang, S. and Bar-Shalom, Y. (2011). “Track segment association for GMTI tracks of evasive move-stop-move maneuvering targets.” *IEEE Transactions on Aerospace and Electronic Systems*, 47(3), 1899–1914.
- Zhu, Y., Zhou, S., Gao, G., and Ji, K. (2015). “Emitter target tracking by tracklet association using affinity propagation.” *IEEE Sensors Journal*, 15(10), 5645–5653.
- Zyweck, A. and Bogner, R. E. (1996). “Radar target classification of commercial aircraft.” *IEEE Transactions on Aerospace and Electronic Systems*, 32(2), 598–606.

List of Publications

1. **Raghu, J.**, Srihari, P., Tharmarasa, R., Kirubarajan, T. (2018). "Comprehensive Track Segment Association for Improved Track Continuity" *IEEE Transactions on Aerospace and Electronic Systems*, vol. PP, no. 99, pp. 1-1. doi: 10.1109/TAES.2018.2820364
2. **Raghu, J.**, Srihari, P., Tharmarasa, R., Kirubarajan, T., "Classification and Amplitude Aided Track Un-swapping" *to be communicated to IEEE Transactions on Aerospace and Electronic Systems Journal*

ABOUT THE AUTHOR

ಡಾ. ರಘು ಜಿ. ಮಂಡ್ಯ

Dr. RAGHU J.



Senior Assistant Professor,
Dept. of E&C Engineering,
Amrita School of Engineering,
Amrita Vishva Vidyapeetham,
Bengaluru, Karnataka – 560035, India.

Mobile: +91 7411574801

Email: raghujmandya@gmail.com

j_raghu@blr.amrita.edu

EMPLOYMENT

Senior Assistant Professor

2018–Present

Department of Electronics and Communication Engineering

Amrita School of Engineering

Amrita Vishva Vidyapeetham, Bengaluru,

Karnataka – 560035, India

Mobile: +91 7411574801

Email: raghujmandya@gmail.com, j_raghu@blr.amrita.edu

QUALIFICATION

Ph.D Radar Target Tracking

2014–2018

National Institute of Technology Karnataka (NITK), Surathkal, India

(Formerly known as Karnataka Regional Engineering College (KREC))

CGPA: 9.32 (Course Work)

Title of the thesis: Track Stitching and Un-switching Algorithms for Multiple Target Tracking

Supervisor: Dr. Pathipati Srihari

Assistant Professor

Department of Electronics and Communication Engineering

National Institute of Technology Karnataka, Surathkal, India

Ph.D (Visiting Scholar) Radar Target Tracking

2016

McMaster University, Hamilton, Ontario, Canada

Supervisor: **Dr. T. Kirubarajan** (<http://www.ece.mcmaster.ca/~kiruba/>)

Distinguished Engineering Professor

Canada Research Chair in Information Fusion

Professor and Associate Chair for Graduate Studies

ECE Department, McMaster University, Canada

M.Tech. Signal Processing

2012–2014

Reva Institute of Technology and Management, Bengaluru
Visvesvaraya Technological University, Belagavi, Karnataka, India

Percentage: 82.25

Supervisor: Dr. Bharathi S. H.

Professor & Deputy Director

School of Electronics and Communication Engineering

Reva University, Bengaluru, India

B.E Electronics and Communication Engineering

2008–2012

Auden Technology and Management Academy, Bengaluru

Visvesvaraya Technological University, Belagavi, Karnataka, India

Percentage: 74.99

Supervisor: Prof. Puttamadegowda J.

Assistant Professor

Department of Electronics and Communication Engineering

Brindavan College of Engineering, Bengaluru, India

PUBLICATIONS

1. **Raghu, J.,** Srihari, P., Tharmarasa, R., Kirubarajan, T. (2018). "Comprehensive Track Segment Association for Improved Track Continuity" *IEEE Transactions on Aerospace and Electronic Systems*, vol. PP, no. 99, pp. 1-1.
doi: 10.1109/TAES.2018.2820364
2. **Raghu, J.,** Srihari, P., Tharmarasa, R., Kirubarajan, T., "Classification and Amplitude Aided Track Un-swapping" *to be communicated to IEEE Transactions on Aerospace and Electronic Systems Journal*.
3. **Raghu, J.,** Srihari, P., Tharmarasa, R., Kirubarajan, T., "Integrating Target Birth and Death Rate Information into Track Stitching and Track-to-Track Fusion" *to be communicated to IEEE Transactions on Aerospace and Electronic Systems Journal*.

EXPERIENCE

Since June 2018 at Amrita School of Engineering, Bengaluru

- Senior Assistant Professor, Department of Electronics and Communication Engineering
- Theory Subject Being Handled
 - Introduction to Radar Systems

1 Year at McMaster University, Canada

- Researcher at McMaster University, Canada during 2016.

4 Years at National Institute of Technology Karnataka, Surathkal

- Researcher at National Institute of Technology Karnataka during 2014–2018.
- Teaching assistant at National Institute of Technology Karnataka (2014–2018).
- Junior Research Fellow (JRF) during 2014–2016
- Senior Research Fellow (SRF) during 2016–2018
- Theory Subjects and LABs assisted are
 - Radar Signal Processing
 - Algorithms for Parameter and State Estimation
 - Multi Target Tracking and Multi Sensor Information Fusion
 - Digital Signal Processing LAB
 - Communication LAB

AREA OF INTEREST

Radar/Sonar Signal Processing, Target Tracking, Track Segment Association (TSA), Track Un-swapping, Data Fusion, Track-Before-Detect (TBD), Bearings Only Target (BOT) Tracking.

MEMBERSHIP OF PROFESSIONAL BODIES

- IEEE — Institute of Electrical and Electronics Engineers Member (Membership Number: 94159096)
- IEEE Aerospace and Electronic Systems Society Member
- IET — The Institution of Engineering and Technology Member (Membership Number: 1100655635)
- ISIF — International Society of Information Fusion Member

COURSE WORK AT MCMASTER UNIVERSITY

I audited the following courses:

- Estimation with application to Tracking and Navigation.
- Multiple Target Tracking.

ACHIEVEMENTS/AWARDS

- Visiting Ph.D scholar at *McMaster University*, Canada, the year 2016.
- Awardee of Ph.D student (2014–2019) fellowship by Ministry of Human Resource and Development (MHRD), Govt. of India.

- Junior Research Fellow (JRF): 2014–2016
- Senior Research Fellow (SRF): 2016–2018
- Awardee of Teaching Assistantship (2014–2019), National Institute of Technology Karnataka, Surathkal, MHRD, Govt. of India.
- Qualified **GATE**-2014 with a percentile of 94.11.
- Earned 24 credits with a CGPA of 9.32 during Ph.D course work at NITK, Surathkal.
- Secured distinction in Bachelor of Engineering (B.E).
- Secured distinction in Master of Technology (M.Tech).
- Carried-out internship at **BOSCH**, Bengaluru, in the year 2011–2012.

ORGANIZED GIAN PROGRAMME

As a co-organizer I have successfully organized the following GIAN courses:

- GIAN Course on ***Estimation, Tracking and Information Fusion*** held on 4–8 December 2017 at National Institute of Technology Karnataka (NITK), Surathkal, India.
 - Foreign Expert: ***Dr. T. Kirubarajn***, Distinguished Engineering Professor, McMaster University, Canada.
- GIAN Course on ***Introduction to Software Defined Networking*** held on 26–30, March 2018 at National Institute of Technology Karnataka (NITK), Surathkal, India.
 - Foreign Expert: ***Dr. Pradeep K. Kondamuri***, Senior Product Architect, Packet Software & Access, Ciena Corp., San Jose, CA, USA.

CONFERENCES/GIAN/WORKSHOPS ATTENDED

- Workshop on ***Research Methodology and Structural Equation Modeling*** held on 16 November 2014 at National Institute of Technology Karnataka (NITK), Surathkal, India.
- ***5th International Symposium on Electronic Systems Design (ISED)*** held on 15–17 December 2014 at National Institute of Technology Karnataka (NITK), Surathkal, India
- Workshop on ***Estimation Theory for Communications and Signal Processing*** held on 21–23 January 2015 at Indian Institute of Technology (IIT), Kanpur, India.
- ***International Radar Symposium India (IRSI-2015)*** held On 15–19 December 2015 at NIMHANS Convention Centre, Bengaluru, India.

- Global Initiative of Academic Network (GIAN) advanced level course on ***Remote Sensing Image Processing and Analysis*** held on 16–20 November 2017 at National Institute of Technology Karnataka (NITK), Surathkal, India
- GIAN Course on ***Estimation, Tracking and Information Fusion*** held on 4–8 December 2017 at National Institute of Technology Karnataka (NITK), Surathkal, India.
- ***International Radar Symposium India (IRSI-2017)*** held on 12–16 December 2017, at NIMHANS Convention Centre Bengaluru, India.
- GIAN Course on ***Advanced Radar System Design and Signal Processing*** held on 18–22 December 2017 at Indian Institute of Technology (IIT), Indore, India.
- GIAN Course on ***Beyond the Kalman Filter: Bayesian Recursive Filtering in Engineering and Finance*** held on 1–5 January 2018 at Indian Institute of Technology (IIT), Patna, India.
- GIAN Course on ***Introduction to Software Defined Networking*** held on 26–30, March 2018 at National Institute of Technology Karnataka (NITK), Surathkal, India.
- GIAN Course on ***Advancement of Radar Systems and Its Applications*** to be held in September/October 2018 at Indian Institute of Technology (IIT), Roorkee, India.

TEACHING INTEREST

I am passionate about teaching and learning while teaching. I adopt myself to make students comfortable in understanding the theoretical as well as practical aspects. Though I can teach number of subjects, following are the some of the courses that appear in my first priority list of teaching:

- Signals and Systems
- Digital Signal Processing
- Radar Signal Processing
- Estimation and Detection Theory
- Algorithms for Parameter and State Estimation
- Multiple Target Tracking and Multiple Sensor Information Fusion
- Radar and Electronic Navigation Systems
- Advanced Digital Signal Processing

RESEARCH INTEREST

Radar or Sonar target tracking is a significant research area, particularly, in defense applications. Processing radar or sonar signals in the presence false alarms and counter measures is a challenging task. In addition, targets employ their own ways of maneuvering strategies to confuse the radars and thereby escape from being detected and tracked. In these type of situations, there is a strong need for novel tracking algorithms even though the existing methodologies solve some of the problems.

I would like to involve myself in contributing to the target tracking area by conducting original research work. I want to establish myself as a young researcher by publishing in high quality peer reviewed journals such as IEEE Transactions. I want to carry-out sponsored research projects in this renowned area of estimation with application to tracking and navigation.

My short-term research goals are as follows:

- Start guiding students to their M.Tech (Research)/Ph.D degrees.
- Applying for sponsored projects from agencies such as DST, SERB and DRDO.
- Writing papers for high quality journals.
- Making collaboration with worldwide well known research group.
- Organizing GIAN programs.

In long-term duration I aim to achieve the followings:

- To have significant number of students successfully guided towards the completion of their M.Tech (Research)/Ph.D degrees.
- To have 5 to 6 sponsored projects completed.
- To have substantial number of published and/or accepted high quality peer reviewed journals.

PERSONAL DETAILS

Name : Mr. Raghu J. (Mandya)
Date of Birth : April 22, 1990
Place of Birth : Arethippuru (ಅರೇತಿಪ್ಪುರು), Maddur, Mandya
Languages Known : ಕನ್ನಡ (Kannada) and English
Permanent Address : S/O Jayaramu, Arethippuru, Koolagere Post,
Maddur Taluk, Mandya, Karnataka - 571433, India.
Mobile : +91 7411574801
Personal Email Address : raghujmandya@gmail.com
Official Email Address : j_raghu@blr.amrita.edu
Sex : Male

REFERENCES

Dr. T. Kirubarajan

Professor and Distinguished Engineering Professor
NSERC/General Dynamics Mission Systems
-Canada Industrial Research Chair in
Target Tracking and Information Fusion
Canada Research Chair in Information Fusion
Electrical and Computer Engineering Department
McMaster University, 1280 Main Street West
Hamilton, Ontario, L8S 4K1 Canada
Email: kiruba@mcmaster.ca
Mobile: +1 416-823-2144

Dr. R. Tharmarasa

Research Associate
Electrical and Computer Engineering Department
McMaster University, 1280 Main Street West
Hamilton, Ontario, L8S 4K1 Canada
Email: tharman@mail.ece.mcmaster.ca
Mobile: +1 647-648-7924

Dr. M. S. Bhat

Professor & Former Head, Dept. of E&C Engg.,
National Institute of Technology Karnataka,
Surathkal, Mangaluru - 575025
Email: msbhat@ieee.org, msb@nitk.ac.in
Telephone: +91-824-2473507
Mobile: +91 9448887426

Dr. Pathipati Srihari

Assistant Professor,
Department of Electronics and
Communication Engineering,
National Institute of Technology Karnataka,
Surathkal, Mangaluru - 575025
Email: srihari.js@gmail.com
Telephone: 0824-2473515
Mobile: +91 9885049285

Dr. U. Shripathi Acharya

Professor & Former Head, Dept. of E&C Engg.,
National Institute of Technology Karnataka,
Surathkal, Mangaluru - 575025
Email: sripati.acharya1@gmail.com
Telephone: +91-824-2473503
Mobile: +91 9845056189

Dr. Muralidhar Kulkarni

Professor & Former Head, Dept. of E&C Engg.,
National Institute of Technology Karnataka,
Surathkal, Mangaluru - 575025
Email: mkulkarni@nitk.ac.in
Telephone: 0824-2473055
Mobile: +91 9480760931

